

Supporting Information

A Mechanistic Continuum of Nucleophilic Aromatic Substitution Reactions with Azole Nucleophiles

Harrison W. Toll[†], Xiaoyi Zhang[†], Tong Gao[†], Guilherme Dal Poggetto[‡], Mikhail Reibarkh[‡], Joshua J. Lee[†], Katherine J. Yang[†], Eugene E. Kwan^{*,¶} and Amanda K. Turek^{*,†}

[†]*Department of Chemistry, Williams College, 47 Lab Campus Drive, Williamstown, MA 01267*

[‡]*Analytical Research and Development, MRL, Merck & Co., Inc., Rahway, New Jersey 07065, United States*

[¶]*Merck & Co. Inc., 33 Avenue Louis Pasteur, Boston, Massachusetts 02115, United States*

Table of Contents

I. General Information	S-2
A. Materials and Instrumentation	S-2
B. Abbreviations	S-3
II. Kinetics Procedures	S-3
A. General Procedure.....	S-3
B. Determination of Response Factors	S-4
C. Saturation Kinetics	S-6
D. Rate Law Derivations.....	S-9
E. LFER Procedures and Data	S-12
F. Eyring Plot.....	S-21
III. Kinetic Isotope Effect Experiments	S-22
A. Overview	S-22
B. Strategy and Pulse Sequence Development	S-22
C. Pulse Sequence Parameters	S-24
D. Pulse Sequence Code	S-24
E. Data Processing	S-29
F. Sample Preparation.....	S-29

G. Results.....	S-30
IV. Computational Methods and Results.....	S-30
A. General Information.....	S-30
B. Grid Calculations.....	S-31
C. Specific and General Base Calculations.....	S-37
D. Calculations using Indole Anion.....	S-39
E. Coordinates for Key Structures	S-42
V. Characterization of S_NAr Products	S-50
VI. Kinetic Data	S-56
VII. ¹H and ¹³C NMR Spectra for New Compounds	S-93

I. General information

A. Materials and Instrumentation

Kinetic aliquots were analyzed using an Agilent 1260 Series HPLC using a ZORBAX Eclipse Plus C18 column (95 Å, 2.1 x 50 mm, 1.8 µm) and data were processed using MassHunter Qualitative Analysis version 10.0. Normal-phase column chromatography was performed with a Biotage Isolera One flash purification system equipped with columns packed with silica gel. NMR spectra (¹H, ¹³C, ¹⁹F) for characterization were acquired on a 500 MHz Bruker Avance spectrometer at ambient temperature, and NMR data were processed using MestReNova (Version 12.0.4). These NMR data were referenced to TMS (for ¹H NMR), solvent (for ¹³C NMR), or CFC1₃ (for ¹⁹F NMR). NMR data for the kinetic isotope effect experiments were acquired on a Bruker Avance NEO NMR spectrometer (additional details in Part III). IR data were acquired on a Perkin Elmer Spectrum 2 FTIR with ATR attachment. High resolution LCMS data were collected on an Agilent 6230B time-of-flight LC/MS or Thermo Scientific Q Exactive HF-X Hybrid Quadrupole-Orbitrap Mass Spectrometer. Anhydrous *N,N*-dimethylacetamide was stored over 4Å molecular sieves in a septum-seal bottle. All reagents were purchased from commercial sources (Oakwood, Millipore Sigma) and used as received unless otherwise noted. Data processing for kinetics experiments was carried out using Microsoft Excel and Origin 2023b.¹

¹ Origin, Version 2023b. OriginLab Corporation, Northampton, MA, USA.

B. Abbreviations

ArF = aryl fluoride

ATR = attenuated total reflectance

DMA = *N,N*-dimethylacetamide

FTIR = Fourier transform infrared

HPLC = high-performance liquid chromatography

IR = infrared

KIE = kinetic isotope effect

LCMS = liquid chromatography–mass spectrometry

LFER = linear free energy relationship

MQF = multiple quantum filtration

PES = potential energy surface

pMODO = permuted MODulated echo

NMR = nuclear magnetic resonance

TMS = tetramethylsilane

II. Kinetics Procedures

A. General Procedure for Kinetics Experiments

Procedure A: For experiments using solid aryl fluorides

An oven-dried large microwave vial equipped with a magnetic stir bar was charged with the base (5 mmol) and the aryl fluoride. The vial was sealed and DMA (9.3 mL) was added under an atmosphere of argon. The vial was then heated in an oil bath that had been pre-heated to the desired temperature, and the contents were pre-mixed for 5 minutes. Separately, a 1 mL solution of indole in DMA was prepared using an oven-dried screw-top volumetric flask. At the conclusion of the pre-mixing period, 0.7 mL of the indole solution was added to the reaction mixture and a timer was started simultaneously. Aliquots were collected at the indicated timepoints for the first ~10% of the reaction as follows: Stirring was briefly stopped (<2 seconds) during aliquot collection to avoid clogging the needle with the solids in the reaction mixture. Approximately 100–150 μ L of the reaction mixture was collected using a 1 mL disposable syringe (which was discarded after the aliquot was collected) and transferred to a vial. A timepoint was recorded at this point. A 50 μ L sample of the collected solution was then transferred to a 1 or 2 mL volumetric flask and was

diluted with methanol.² The diluted sample was filtered through a plug of Kimtech[®] laboratory wipe and was analyzed by HPLC (10% MeCN/H₂O with 0.01% formic acid for 0.5 min at 0.6 mL/min, ramping 10→90% MeCN over 4.5 min at 0.7 mL/min, 90% MeCN for 1 min at 0.7 mL/min, ramping 90→10% MeCN over 0.75 min at 0.6 mL/min, 10% MeCN over 0.75 min at 0.6 mL/min, hold at 10% MeCN for 2.75 min at 0.6 mL/min, 9 min total).

Procedure B: For experiments using liquid aryl fluorides

An oven-dried large microwave vial equipped with a magnetic stir bar was charged with the base (5 mmol). The vial was sealed and DMA (9.3 mL) and the aryl fluoride were added under an atmosphere of argon. The vial was then heated in an oil bath that had been pre-heated to the desired temperature, and the contents were pre-mixed for 5 minutes. Separately, a 1 mL solution of indole in DMA was prepared using an oven-dried screw-top volumetric flask. At the conclusion of the pre-mixing period, 0.7 mL of the indole solution was added to the reaction mixture and a timer was started simultaneously. Aliquots were collected and analyzed as described in Procedure A.

B. Determination of Response Factors

The absorbance data obtained by HPLC were converted to concentration data using a response factor determined from a modified Beer's Law plot shown below (Figure S1). A response factor was determined for each unique product obtained in the course of the kinetics experiments. These data were obtained as follows: A stock solution of the product in acetone was prepared in a 1 mL volumetric flask. Samples of varying concentration were prepared by taking aliquots of the stock solution and diluting to 1 mL with methanol in a volumetric flask. The solutions were analyzed by HPLC using the method described above to determine the absorbance at each concentration. The chromatograms corresponding to a specific wavelength (indicated below for each product) were extracted, the peaks corresponding to the product were integrated, and the resulting areas from both runs were simultaneously plotted against the absolute concentration of each sample. The data were fit to a linear equation (1), and the slope obtained is the response factor. All data have been obtained on a single HPLC instrument; therefore, the path length is assumed to be constant for the calibration plot and kinetics data collection.

$$\text{Area} = \text{response factor} \times [P] \quad (1)$$

² The 50 μ L sample could not be collected directly from the reaction mixture due to clogging issues with the gastight syringe needle.

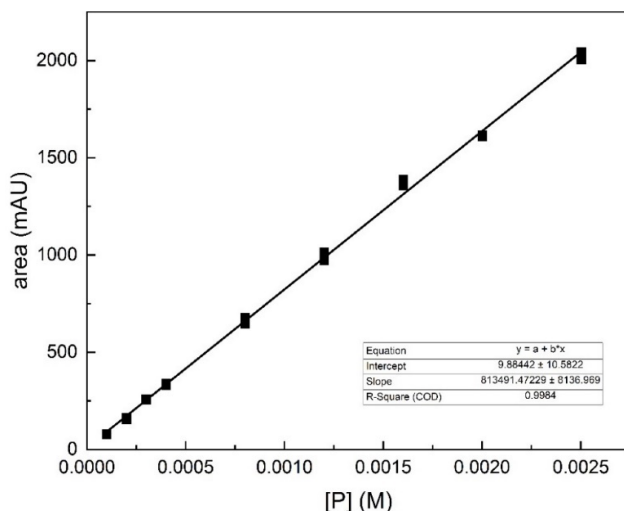
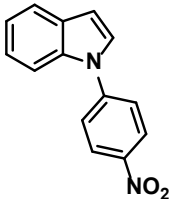
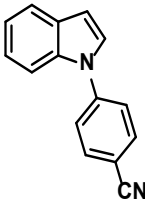
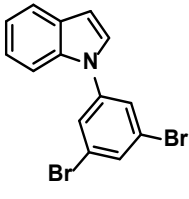
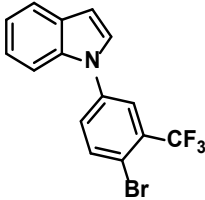
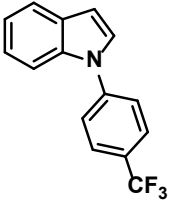
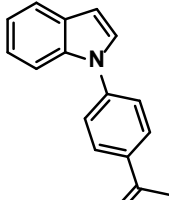
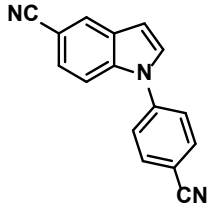
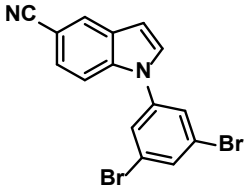
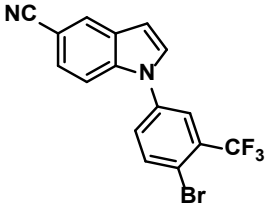
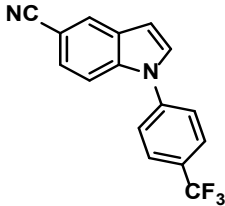
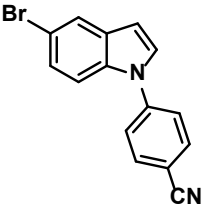
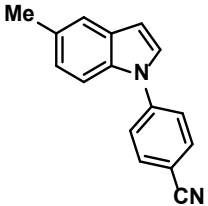
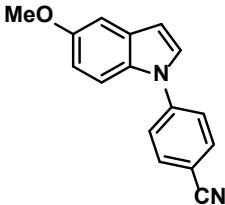


Figure S1. Calibration plot to determine response factor for 1-(4-nitrophenyl)-1*H*-indole. All plots are shown in Section VI.

All response factors obtained in the course of this study are tabulated below (Table S1), along with the wavelengths and bandwidths at which the response factors were determined. The retention times for each compound for the HPLC method described above are also included.

Table S1. Tabulated response factors (M^{-1}) for S_NAr products

 813491 (at 363±20 nm)	 1257250 (at 315±10 nm)	 771985 (at 265±15 nm)
 903319 (at 265±15 nm)	 1026280 (at 265±15 nm)	 1113670 (at 325±30 nm)

 <p>1550040 (at 280±20 nm)</p>	 <p>1677540 (at 265±10 nm)</p>	 <p>1343100 (at 270±20 nm)</p>
 <p>1539570 (at 265±20 nm)</p>	 <p>949327 (at 315±15 nm)</p>	 <p>1005420 (at 320±25 nm)</p>
 <p>910388 (at 325±25 nm)</p>		

C. Kinetic analysis

The kinetic order in both aryl fluoride and indole was evaluated using the general procedure for kinetics experiments, using 4-fluorobenzonitrile and indole. A representative plot of the initial rate data is shown (Figure S2). The specific concentrations used and rate constants obtained for both sets of experiments are listed in Table S2 and Table S3.

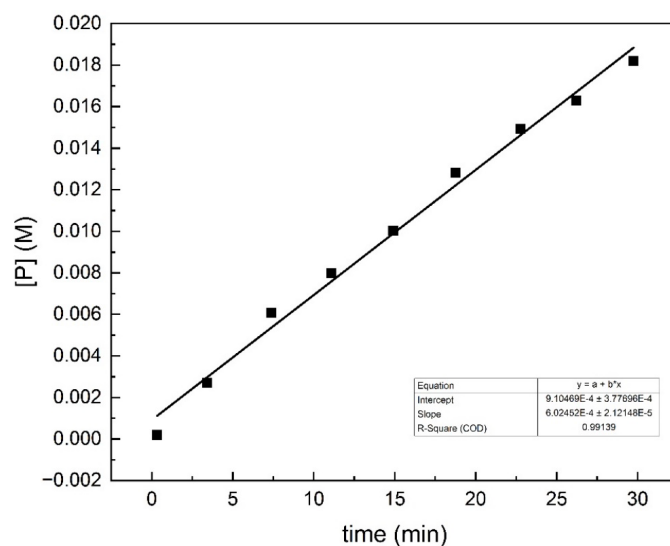


Figure S2. Representative initial rates data. Obtained with 4-fluorobenzonitrile (0.5 M) and indole (0.25 M), with K_3PO_4 as the base. All kinetic data are shown in Section VI.

Table S2. Rate constants obtained from initial rates experiments varying aryl fluoride concentration.

c1ccc2c(c1)c(c[nH]2) + Fc1ccc(C#N)cc1 >> c1ccc2c(c1)c(c[nH]2)c3ccc(C#N)cc3

0.25 M x M K_3PO_4 / DMA, 80 °C

[ArF] ₀ (M)	k_{obs} ($\times 10^{-6}$) (M s^{-1})		
	Run 1	Run 2	Average
0.5	10.0	9.67	9.86
0.25	10.2	9.23	9.72
0.1	8.87	10.1	9.46
0.05	6.01	8.23	7.95
0.025	6.43	6.39	6.41

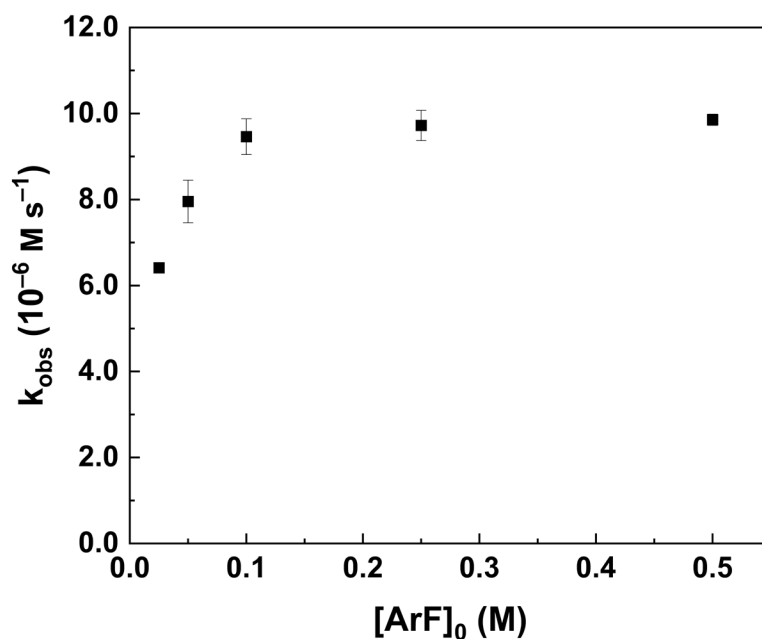
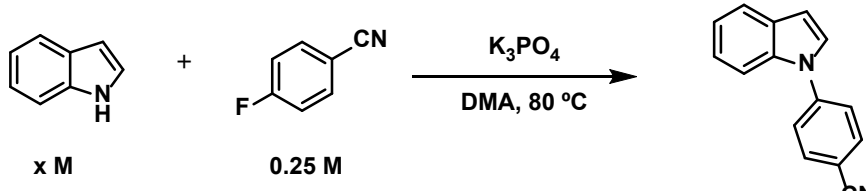


Figure S3. Initial rates as a function of increasing [ArF]₀. Saturation behavior is observed at ~0.1 M [ArF]₀. Rate constants are listed in Table S2. Error bars indicate the range of rate constants observed for two runs.

Table S3. Rate constants obtained from initial rates experiments varying indole concentration.

			
k_{obs} (x10⁻⁶) (M s⁻¹)			
[Indole] ₀ (M)	Run 1	Run 2	Average
0.25	10.02	9.23	9.72
0.175	9.83	--	--
0.1	8.51	10.02	9.34
0.05	8.00	8.73	8.37
0.025	5.93	6.69	6.82
0.01	5.11	4.86	4.99

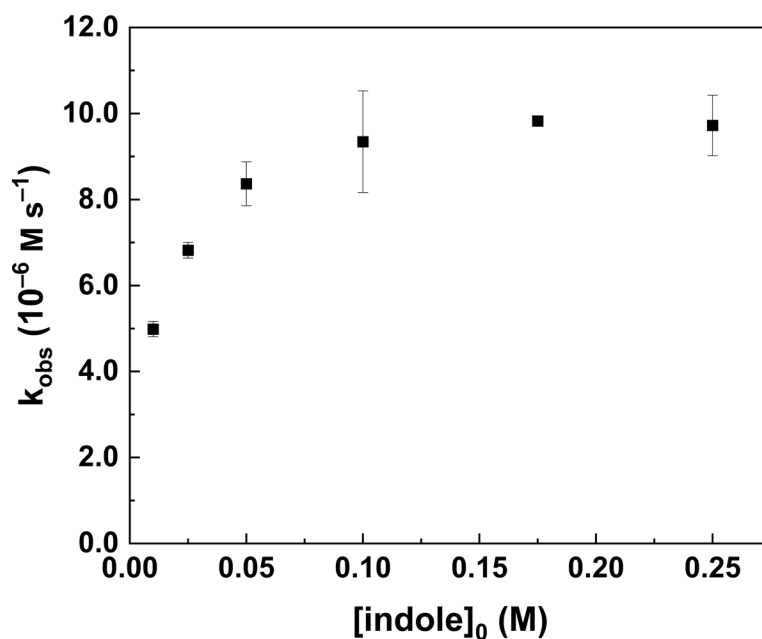
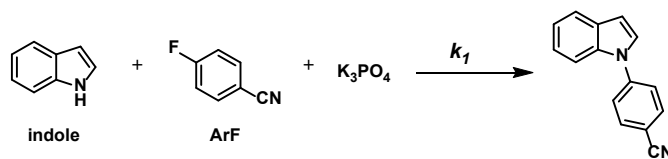


Figure S4. Initial rates as a function of increasing [indole]₀. Saturation behavior is observed at ~0.1 M [indole]₀. Rate constants are listed in Table S3. Error bars indicate the range of rate constants observed for two runs.

D. Rate Law Derivations

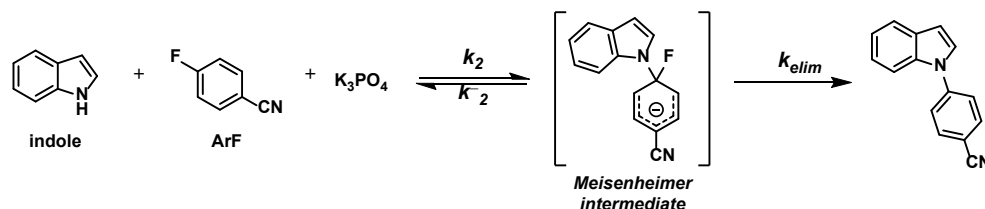
In the following derivations, **MC** refers to the Meisenheimer complex (intermediate).

i. General-base-catalyzed concerted or borderline mechanism



$$rate = k_1[\text{ArF}][\text{indole}][\text{K}_3\text{PO}_4]$$

ii. General-base-catalyzed stepwise mechanism



$$\text{rate} = k_{\text{elim}}[\text{MC}]$$

$$k_2[\text{ArF}][\text{indole}][\text{K}_3\text{PO}_4] = k_{-2}[\text{MC}] + k_{\text{elim}}[\text{MC}]$$

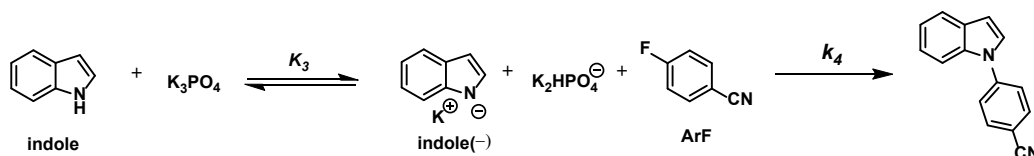
$$[\text{MC}] = \frac{k_2[\text{ArF}][\text{indole}][\text{K}_3\text{PO}_4]}{(k_{-2} + k_{\text{elim}})}$$

$$\text{rate} = \frac{k_2 k_{\text{elim}}[\text{ArF}][\text{indole}][\text{K}_3\text{PO}_4]}{(k_{-2} + k_{\text{elim}})}$$

$$\text{rate} = k_{\text{obs}}[\text{ArF}][\text{indole}][\text{K}_3\text{PO}_4],$$

$$\text{in which } k_{\text{obs}} = \frac{k_2 k_{\text{elim}}}{(k_{-2} + k_{\text{elim}})}$$

iii. Specific-base-catalyzed concerted or borderline mechanism



$$\text{rate} = k_4[\text{ArF}][\text{indole}^-]$$

$$K_3 = \frac{[\text{indole}^-][\text{K}_2\text{HPO}_4]}{([\text{indole}][\text{K}_3\text{PO}_4])}$$

$$[\text{indole}^-] = \frac{K_3[\text{indole}][\text{K}_3\text{PO}_4]}{[\text{K}_2\text{HPO}_4]}$$

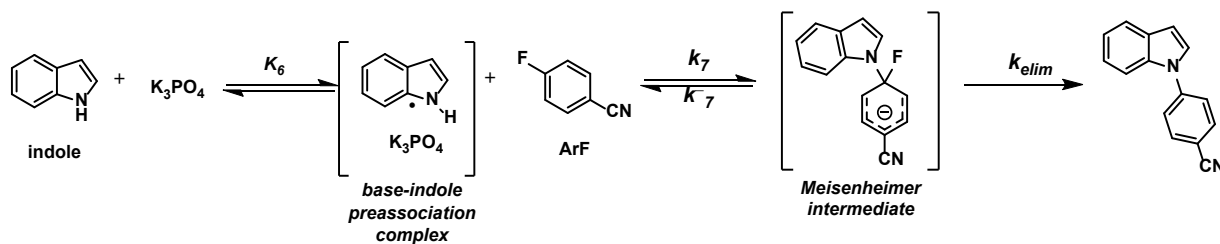
$$\text{rate} = \frac{K_3 k_4[\text{ArF}][\text{indole}][\text{K}_3\text{PO}_4]}{[\text{K}_2\text{HPO}_4]}$$

$$\frac{1}{K_a} = \frac{[\text{K}_3\text{PO}_4]}{[\text{K}_2\text{HPO}_4]}$$

$$\text{rate} = k_{\text{obs}}[\text{ArF}][\text{indole}],$$

$$\text{in which } k_{\text{obs}} = \frac{K_3 k_4}{K_a}$$

v. General-base-catalyzed stepwise mechanism with pre-association of base and indole



$$rate = k_{elim}[\text{MC}]$$

$$k_7[\text{ArF}][\text{K}_3\text{PO}_4 \bullet \text{indole}] = k_{-7}[\text{MC}] + k_{elim}[\text{MC}]$$

$$[\text{MC}] = \frac{k_7[\text{ArF}][\text{K}_3\text{PO}_4 \bullet \text{indole}]}{(k_{-7} + k_{elim})}$$

$$rate = \frac{k_7 k_{elim} [\text{ArF}][\text{K}_3\text{PO}_4 \bullet \text{indole}]}{(k_{-7} + k_{elim})}$$

$$K_6 = \frac{[\text{K}_3\text{PO}_4 \bullet \text{indole}]}{([\text{indole}][\text{K}_3\text{PO}_4])}$$

$$[\text{K}_3\text{PO}_4 \bullet \text{indole}] = K_6[\text{indole}][\text{K}_3\text{PO}_4]$$

$$rate = \frac{K_6 k_7 k_{elim} [\text{ArF}][\text{indole}][\text{K}_3\text{PO}_4]}{(k_{-7} + k_{elim})}$$

$$rate = k_{obs}[\text{ArF}][\text{indole}][\text{K}_3\text{PO}_4],$$

$$\text{in which } k_{obs} = \frac{K_6 k_7 k_{elim}}{(k_{-7} + k_{elim})}$$

E. LFER Procedures and Data

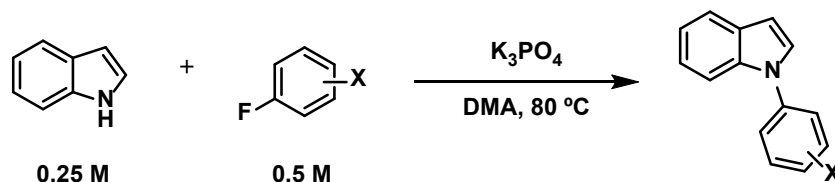
The data for the LFERs were collected using the general procedure for kinetics experiments. The specific indoles, aryl fluorides, and bases used are indicated in each table below. The σ / σ^- values used are also summarized in Table S4. For the multi-substituted aryl fluorides, additivity of σ values was assumed.³

³ Rincón, L. Almeida, R. Is the Hammett's Constant Free of Steric Effects? *J. Phys. Chem. A* **2012**, *116*, 7523–7530.

Table S4. Substituent constants

Substituent	$\sigma^{4,5}$	σ^{-45}
–NO ₂	0.78	1.24
–CN	0.66	0.9
–3,5-Br	0.78 ^a	--
–3-CF ₃ ,4-Br	0.66 ^b	--
–CF ₃	0.54	0.65
–COMe	0.5	0.84
–Br	0.23	0.25
–H	0	0
–Me	–0.17	
–OMe	–0.27	–0.26

^aCalculated by adding two σ_m values (0.39) for –Br. ^bCalculated by adding σ_m for –CF₃ (0.43) and σ_p for –Br (0.23).

Table S5. Initial rate constants for LFER varying aryl fluoride substituent.

–X	$k_{\text{obs}} (\times 10^{-6}) (\text{M s}^{-1})$	
	Run 1	Run 2
–NO ₂	28.4	32.4
–CN	10.0	9.67
–3,5-Br	7.02	7.26
–3-CF ₃ ,4-Br	4.37	4.38
–CF ₃	3.55	3.14
–COMe	4.93	4.07

⁴ Ritchie, C. D.; Sager, W. F. An Examination of Structure-Reactivity Relationships. *Prog. Phys. Org. Chem.* **1964**, 2, 323–400.

⁵ Hansch, C.; Leo, A.; Taft, R. W. A Survey of Hammett Substituent Constants and Resonance and Field Parameters. *Chem. Rev.* **1991**, 91, 165–195.

When σ or σ^- are used for all substituents, the Hammett plots are scattered (Figure S5 and Figure S6).

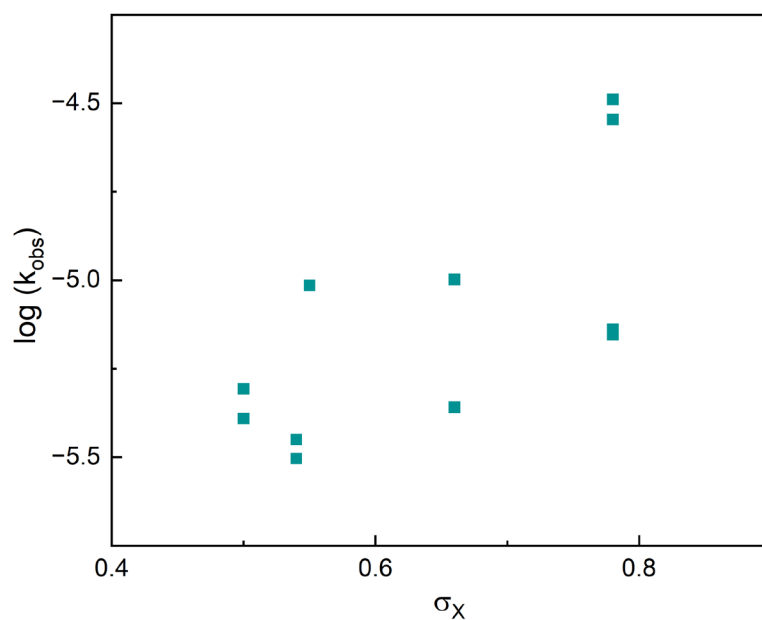


Figure S5. Scattered Hammett plot using σ for all substituents (data in Table S5).

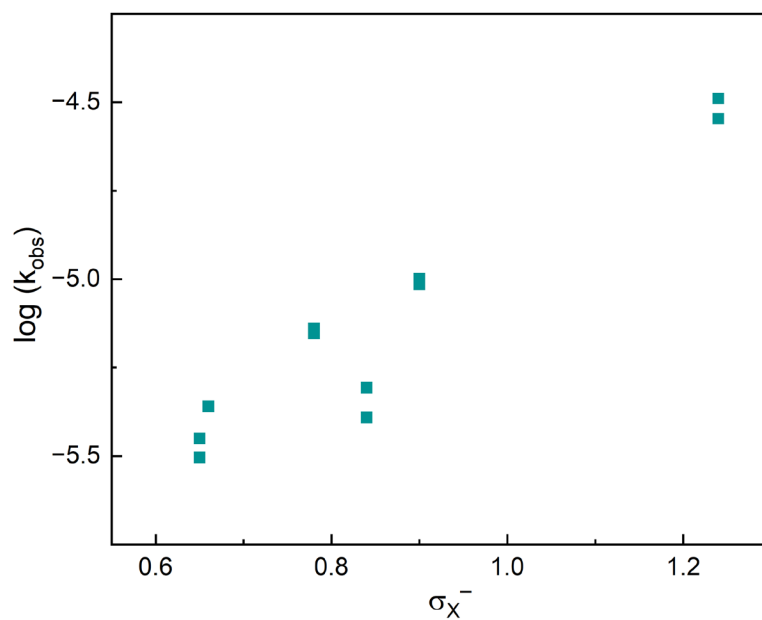


Figure S6. Scattered Hammett plot using σ^- for all substituents (data in Table S5).

The plot is more linear when σ^- is used for more electrophilic aryl fluorides, and σ is used for less electrophilic aryl fluorides (Figure S7).

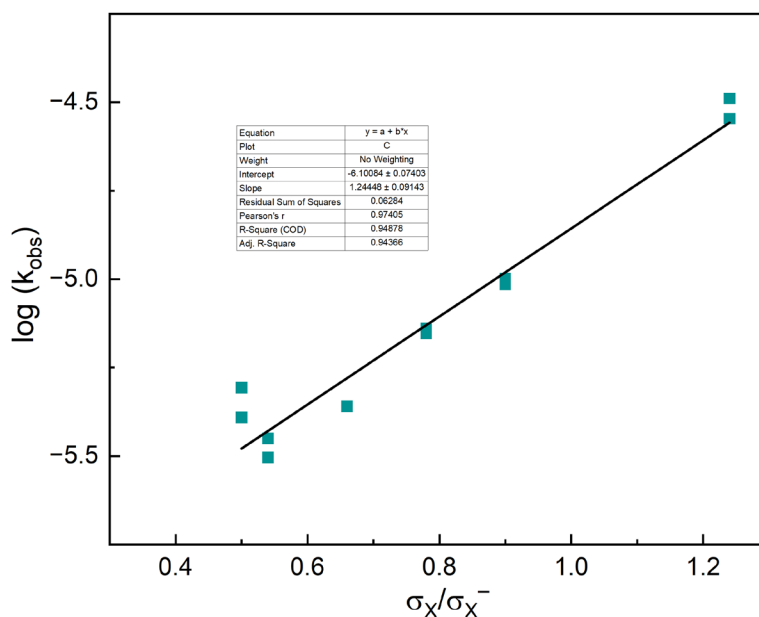
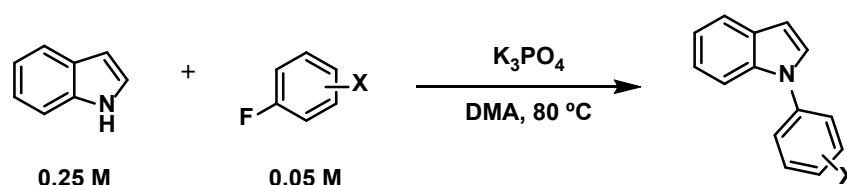


Figure S7. Hammett plot using a mix of σ and σ^- (data in Table S5).

Since all of the LFER data reported here were collected at concentrations within the saturation regime, the same data were also collected using a lower concentration of aryl fluoride to verify that the same behavior would be observed (Table S6). The slope of the plot changes marginally ($\rho = 1.50$ compared with $\rho = 1.24$ at $[\text{ArF}] = 0.5 \text{ M}$) but does not change our interpretation of the data (Figure S8).

Table S6. Initial rate constants for LFER varying aryl fluoride substituent at low concentration.



-X	$k_{\text{obs}} (\times 10^{-6}) (\text{M s}^{-1})$	
	Run 1	Run 2
-NO ₂	17.9	21.3
-CN	6.01	8.56
-3,5-Br	4.96	3.77
-3-CF ₃ ,4-Br	3.62	2.58
-CF ₃	1.62	1.68

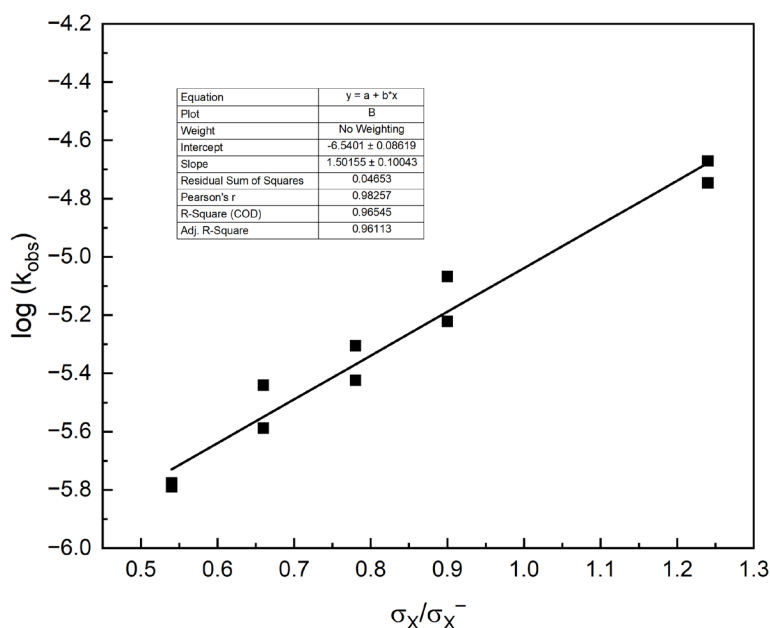


Figure S8. Hammett plot at low concentrations of aryl fluoride (data in Table S6).

For the LFER using 4-cyanoindole, the data point using 4-fluoronitrobenzene was excluded due to the insolubility of the product and resulting inability to determine a response factor (Table S7). These experiments had a slight induction period, but the difference in k_{obs} was negligible whether the induction period was included vs. excluded. The reported k_{obs} were determined without excluding the induction period.

Table S7. Initial rate constants for LFER varying aryl fluoride substituent, using 5-cyanoindole.

	$k_{\text{obs}} (\times 10^{-6}) (\text{M s}^{-1})$		
-X	Run 1	Run 2	
-CN	29.3	29.5	
-3,5-Br	20.7	21.0	
-3-CF ₃ ,4-Br	12.9	13.0	
-CF ₃	7.50	8.66	

Similarly, when a mix of σ and σ^- is used for the reaction using 5-cyanoindole, the correlation becomes more linear and we can approximate a ρ value of 1.58(7) (Figure S9).

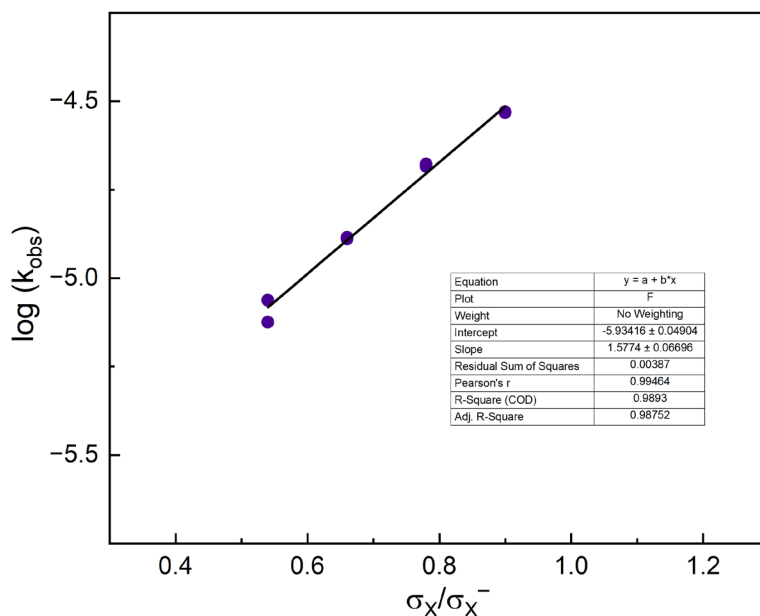
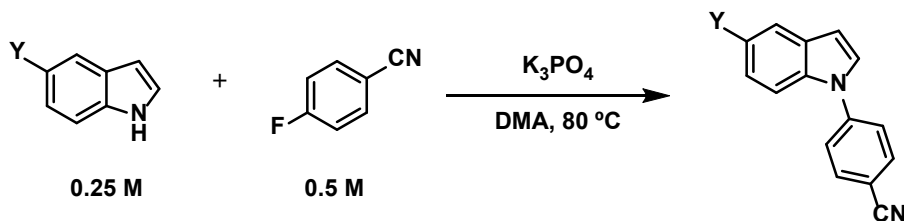


Figure S9. Hammett plot using 5-cyanoindole (data in Table S7).

The reaction was also studied varying the substituents on the indole (Table S8).

Table S8. Initial rate constants for LFER varying indole substituent, using 4-fluorobenzonitrile.



-Y	$k_{obs} (x10^{-6}) (M s^{-1})$	
	Run 1	Run 2
-CN	29.3	29.6
-Br	22.2	21.3
-H	10.0	9.67
-Me	5.55	6.55
-OMe	7.21	7.80

The best fits to the data were obtained using pK_a and σ_m values (Figure S10 and Figure S11).⁶ Fits using σ_p , σ^+ , and σ^- are also shown here (Figure S12–Figure S14).

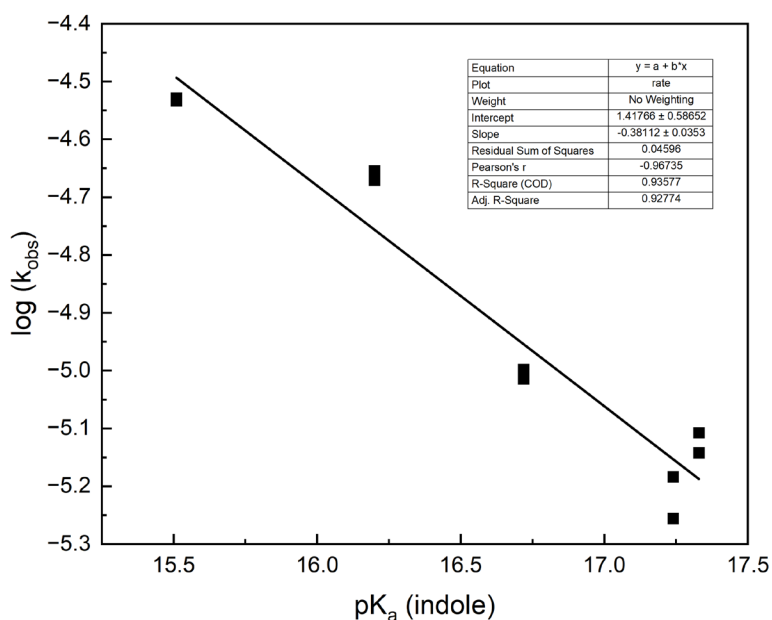


Figure S10. Brønsted plot varying indole substituent, plotted against pK_a values (data in Table S8).

⁶ Muñoz, M. A.; Guardado, P.; Hidalgo, J.; Carmona, C.; Balón, M. An Experimental and Theoretical Study of the Acid-base Properties of Substituted Indoles. *Tetrahedron*, **1992**, 48, 5901–5914.

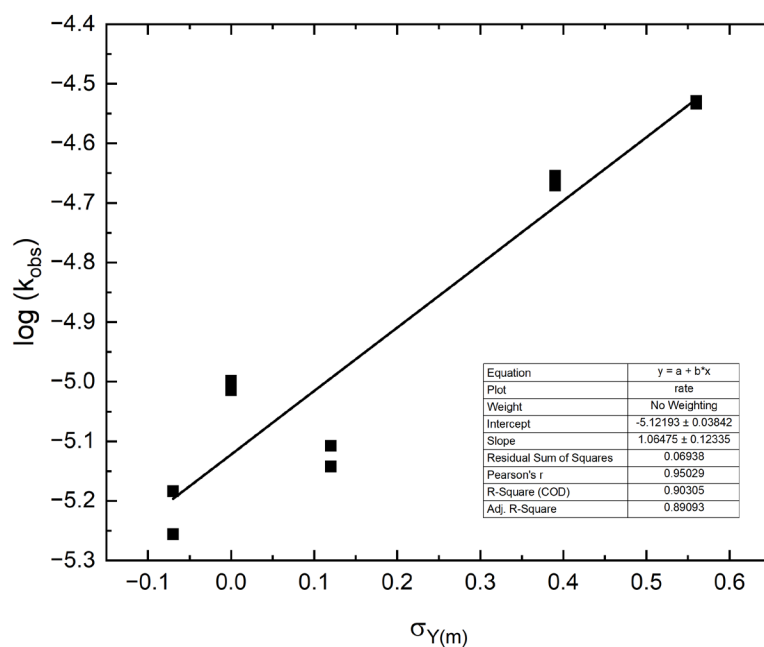


Figure S11. Hammett plot varying indole substituent, plotted against σ_m (data in Table S8).

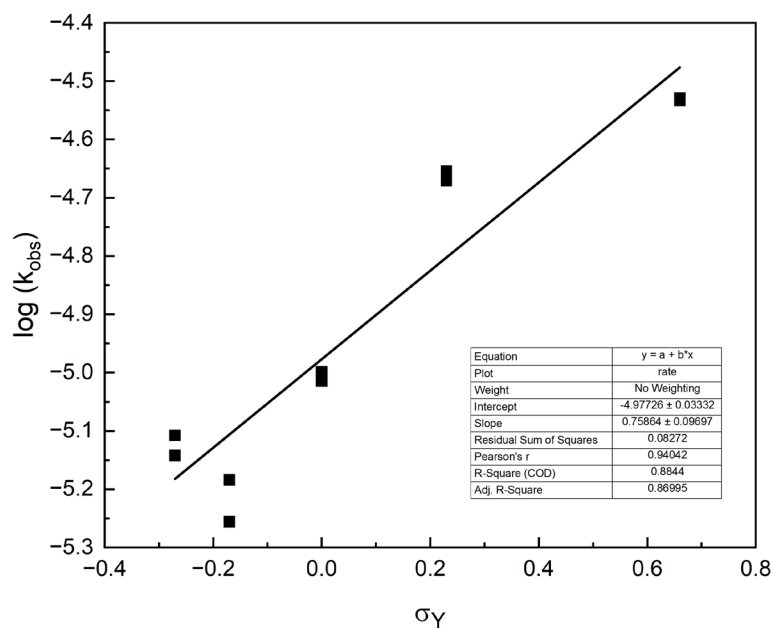


Figure S12. Hammett plot varying indole substituent, plotted against σ_p (data in Table S8)

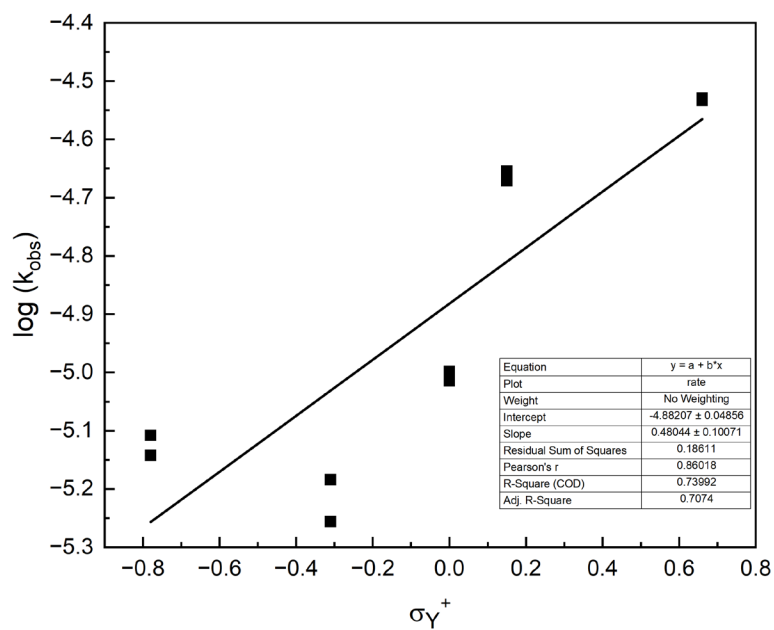


Figure S13. Hammett plot varying indole substituent, plotted against σ^+ (data in Table S8).

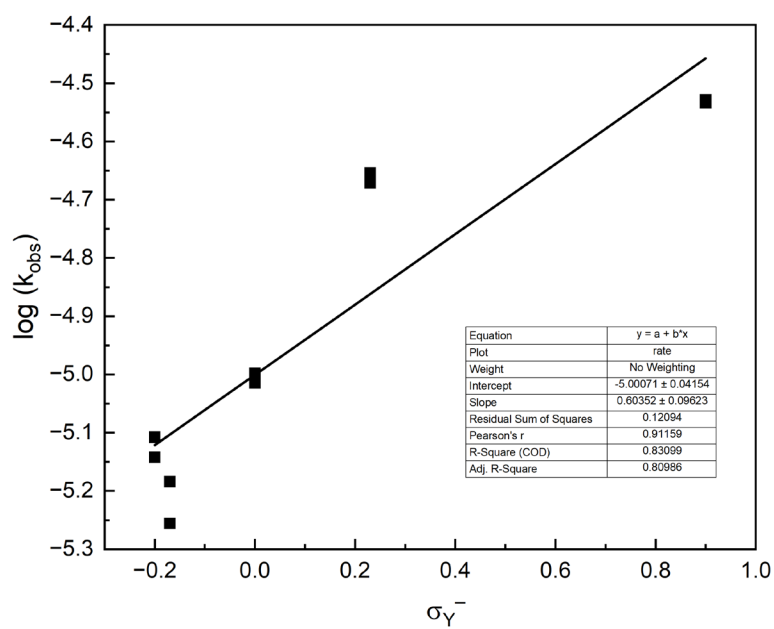
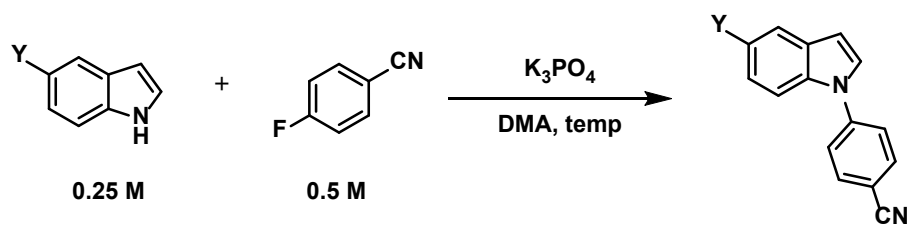


Figure S14. Hammett plot varying indole substituent, plotted against σ^- (data in Table S8)

F. Eyring Analysis

The data for the Eyring analysis were collected using the general procedure for kinetics experiments, adjusting the temperature accordingly (Table S9). We note that these initial rate constants were determined from a concentration vs. time plot using seconds as the x-axis unit (consistent with the units required for the Eyring analysis), whereas all previous data were collected from a concentration vs. time plot using minutes as the x-axis unit.

Table S9. Initial rate constants for Eyring analysis



T (°C)	k_{obs} ($\times 10^{-5}$) ($M s^{-1}$)	
	Run 1	Run 2
100	3.77	3.84
90	2.09	1.91
80	1.00	0.97
70	0.66	0.67
60	0.35	0.28

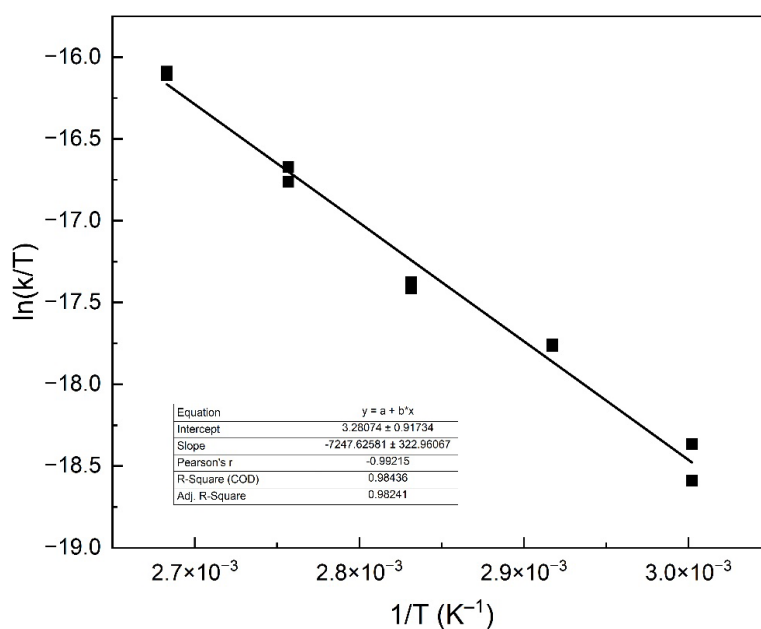


Figure S15. Eyring analysis for reaction of indole (0.25 M) with 4-fluorobenzonitrile (0.5 M).

III. Kinetic Isotope Measurements

A. Overview

This section discusses the measurement of $^{12}\text{C}/^{13}\text{C}$ kinetic isotope effects (KIEs). Typically, these KIEs are measured by conducting an intermolecular competition experiment between isotopologous substrates. For example, a reaction can be run to high conversion, which enriches the remaining starting material in the slower-reacting isotope. By comparing the isotope ratio, $R=[^{13}\text{C}]/[^{12}\text{C}]$, in the recovered starting material, to the analogous ratio R_0 in the unreacted starting material, the KIE can be calculated. The required isotope ratios can be measured by NMR spectroscopy.

B. Strategy and Pulse Sequence Development

Traditionally, $^{12}\text{C}/^{13}\text{C}$ ratio measurements have been obtained via quantitative ^{13}C NMR spectroscopy, which suffers from low natural abundance and low sensitivity. As a result, indirect methods that detect ^{13}C magnetization through a more sensitive reporter nucleus have been developed. For carbons that are directly attached to fluorine, we previously showed that multiple quantum filtration (MQF) is an effective method. The idea is to acquire a ^{19}F spectrum in which the very large ^{19}F - ^{12}C signal has been suppressed and the ^{19}F - ^{13}C satellites remain as an antiphase doublet. Integration of this doublet reports on the ^{13}C content, while the integration of the ^{19}F - ^{12}C signal in a separate standard ^{19}F spectrum reports on ^{12}C content.

While the MQF method is substantially more sensitive than direct detection, it has some drawbacks. For example, splitting the satellite signals into doublets reduces the sensitivity by a factor of $\sqrt{2}$. Additionally, because the ^{13}C and ^{12}C content are being assessed in different experiments, and instrument drift or temperature fluctuations can occur during acquisition, small systematic errors can develop. Here, we report the use of a new pulse sequence, pMODO (permuted MODulated echo), which provides the satellites as singlets and simultaneously measures ^{13}C and ^{12}C content.

In the MQF method, magnetization is transferred from ^{19}F to ^{13}C and back to ^{19}F via the $^1J_{\text{CF}}$ coupling and multiple quantum coherence. Because the undesired ^{19}F - ^{12}C signal retains a coherence order of zero during this process, it can be eliminated by gradient dephasing or phase cycling. In pMODO,^{7,8} magnetization is not transferred between nuclei. Instead, a heteronuclear J -modulated spin echo is employed in which chemical shift evolution is refocused, but fluorine-carbon coupling is allowed to evolve. By judicious choice of the evolution delays, the satellite peaks can be made to appear with positive or negative phase, while the parent peak is left unaffected (as $J=0$). Overall, pMODO acquires the ^{19}F - ^{12}C signal as a large main peak and smaller

⁷ Dal Poggetto, G.; Soares, J.V.; Tormena, C. F. Selective Nuclear Magnetic Resonance Experiments for Sign Sensitive Determination of Heteronuclear Couplings: Expanding the Analysis of Crude Reaction Mixtures. *Anal. Chem.* **2020**, 92, 14047–14053.

⁸ Mycroft, C.; Dal Poggetto, G.; Barbosa, T. M.; Tormena, C. F.; Nilsson, M.; Morris, G. A. Castañar, L. Rapid Measurement of Heteronuclear Coupling Constants in Complex NMR Spectra. *J. Am. Chem. Soc.* **2023**, 145, 19824–19831.

^{19}F - ^{13}C satellites as a small singlet (rather than a doublet). The pulse sequence is shown below (Figure S17).

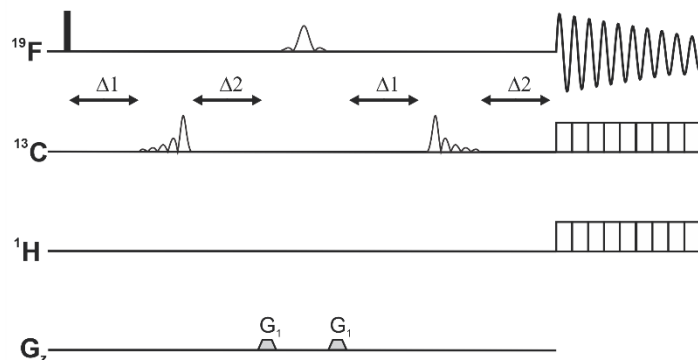
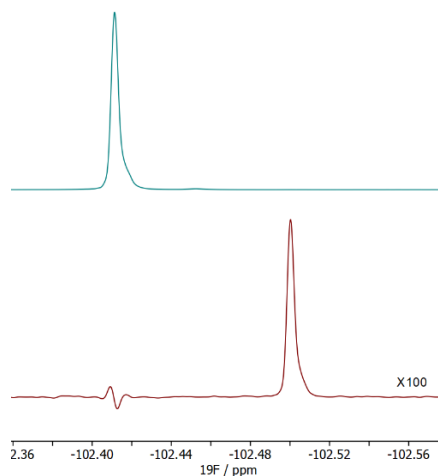
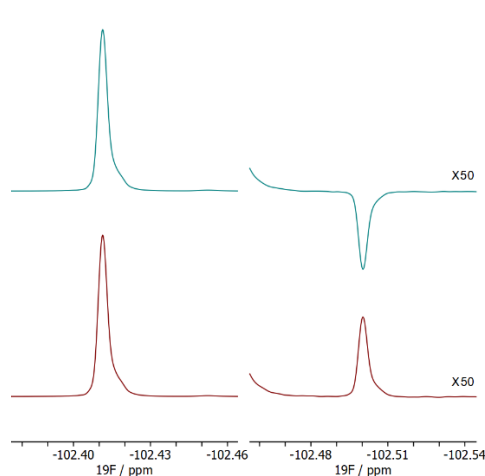


Figure S16. pMODO pulse sequence

The black rectangle represents a 90° hard pulse, while white-shaped pulses represent selective pulses. White rectangles during acquisition represent decoupling sequences. A selective refocusing pulse is applied at the center of the pulse sequence for refocusing the ^{19}F chemical shift. Gradients (G_1) flanking the refocusing pulse are used for coherence transfer pathway (CTP) selection. Selective inversion pulses are applied in the ^{13}C signal relative to the one-bond carbon to the fluorine atom. The experiment is recorded in a pseudo-2D fashion where the total delay is $2\Delta_1 + 2\Delta_2 = 1/{}^1J_{\text{CF}}$. In even-numbered increments, Δ_1 is set to zero and Δ_2 is set to $0.5/{}^1J_{\text{CF}}$, which inverts the ^{19}F signal one-bond to the ^{13}C (i.e., satellite signals) in relationship with the ^{19}F signal bonded to ^{12}C (i.e., the reference signal). In odd-numbered increments, Δ_1 must be set equal to Δ_2 , which keeps all signals positive. To avoid differential relaxation losses, we set $\Delta_1 = \Delta_2 = 0.25/{}^1J_{\text{CF}}$ in odd-numbered increments. Summing even and odd increments gives the reference ^{12}C signal, while subtracting them gives only the ^{13}C satellite signals:

Even (top) and odd (bottom) increments.

Sum (top) and subtraction (bottom)



We can consider the mechanics of pMOD0 for the even and odd increments via the product operator formalism. Let the product operator for the ^{19}F - ^{12}C signals be represented by the ^{19}F operator I and the product operators for the ^{19}F - ^{13}C signals be described by M and S , where M indicates ^{19}F and S indicates ^{13}C . Let J represent $^1J_{\text{CF}}$. In general, after initial excitation, we have:

$$I_y + M_y \rightarrow I_y + \cos[2\pi J(\Delta 1 - \Delta 2)] M_y + \sin[2\pi J(\Delta 1 - \Delta 2)] 2M_x S_z$$

Of course, both I_y and M_y will be unaffected by chemical shift evolution because of the central refocusing pulse. In contrast, I_y is unaffected by J evolution, whereas M_y will evolve for a period of $\Delta 1 - \Delta 2$, which is the amount of J evolution that the spin echo does not compensate for. In even increments, where $\Delta 1=0$ and $\Delta 2=0.5/{}^1J_{\text{CF}}$, we have inversion of the satellite signal:

$$I_y + M_y \rightarrow I_y - M_y$$

Conversely, for odd increments, where $\Delta 1=\Delta 2=0.25/{}^1J_{\text{CF}}$, we have a positive satellite signal:

$$I_y + M_y \rightarrow I_y + M_y$$

Summing or subtracting these two results will produce the ^{12}C and ^{13}C signals, respectively. Note that because gradient selection is only being used to select for the inversion of coherence order ($\pm p$ to $\mp p$), there is no loss of sensitivity. Because ^1H and ^{13}C decoupling are both applied during acquisition, the satellite signals are not split by the heteronuclear coupling. However, any ^{19}F - ^{19}F couplings will remain.

C. Pulse Sequence Parameters

All data were acquired in a Bruker Avance NEO NMR spectrometer, equipped with a 5-mm TBO probe with a maximum nominal gradient strength of 53.5 G/cm, operating at 599.301 MHz for ^1H frequency. All data were acquired at 298 K, stabilized by a BCU-I unit. Hard ^{19}F 90° pulse was set to 25.75 μs with a power of 43.302 W. cnst2 ($^1J_{\text{CF}}$) was set to 257 Hz. Selective refocusing pulse (RSNOB with 1 kHz bandwidth) was set with a duration of 1.85 ms and power of 0.73524 W at -102.40 ppm for the fluorine channel. Selective inversion pulses (IBURP with 1 kHz bandwidth) were set with a duration of 4.653 ms and power of 0.26963 W at 165 ppm for the carbon channel. Shaped pulses were created using the wavemaker. 8 increments were acquired in each pseudo-2D experiment, using 32 scans. Relaxation delay ($d1$) was set to 30s, and FID was recorded for 0.6 s (AQ). Constant-adiabaticity WURST-2 and WURST-40 were used for ^1H and ^{13}C decoupling, respectively. Total experiment duration of 2 h and 43 min.

D. Pulse Sequence Code

```
;pMOD019F{1H,13C}
; updated 23/02/2023 RAHWAY
;
;   Guilherme Dal Poggetto, PhD
;   email: guilherme.dal.poggetto@merck.com
```

```

; Analytical Enabling Capabilities - Rahway, NJ
;
; pseudo-2D F-19/X correlation
; via selective permuted modulated echo (pMOD0)
; using shaped pulses for inversion and refocusing
; decoupling 1H during acquisition in f3
; decoupling 13C during acquisition
;
;
; $CLASS=HighRes
; $DIM=2D
; $TYPE=
; $SUBTYPE=
; $COMMENT=

#include <Avance.incl>
#include <Grad.incl>
#include <Delay.incl>
#include <De.incl>

"l0=0"
"d11=30m"
"p2=p1*2"
"p4=p3*2"
"d12=20u"

;%%%%%%%%%% WaveMaker Parameters %%%%%%%%%%%
"d11=30m+1s/(cnst12)-1s/(cnst12)"
"d11=30m+1s/(cnst13)-1s/(cnst13)"
"d11=30m+1s/(cnst14)-1s/(cnst14)"
"d11=30m+1s/(cnst15)-1s/(cnst15)"
;sp11:wvm:gdp_Frsnob:f1 rsnob(cnst12 Hz, cnst13 ppm; PA=0.5, NPOINTS=5000);
;sp14:wvm:gdp_Ciburp1:f2 iburp2(cnst14 Hz, cnst15 ppm; PA=1, NPOINTS=5000);
;sp13:wvm:gdp_Ciburp2:f2 iburp2(cnst14 Hz, cnst15 ppm; TR=1, NPOINTS=5000);

;sp15(pcpd3,pl12):wvm:gdp_W2:f3 cawurst-2(cnst50 kHz, cnst51 us; Q=cnst53
SUCYC=[p5]m4) ss=cnst54 us p90=p5;
;sp31(p63,pl15):wvm:gdp_W40:f2 cawurst-40(cnst40 kHz, cnst41 us; Q=cnst43
SUCYC=[p5]m4) ss=cnst44 us p90=p3;
"d11=30m+1s/(cnst40)-1s/(cnst40)"
"d11=30m+1s/(cnst41)-1s/(cnst41)"
"d11=30m+1s/(cnst43)-1s/(cnst43)"
"d11=30m+1s/(cnst44)-1s/(cnst44)"
"d11=30m+1s/(cnst50)-1s/(cnst50)"
"d11=30m+1s/(cnst51)-1s/(cnst51)"
"d11=30m+1s/(cnst53)-1s/(cnst53)"
"d11=30m+1s/(cnst54)-1s/(cnst54)"

```

```

;%%%%%%%% Other Parameters %%%%%%%%%
"d4=((1s*0.5)/(cnst2*cnst3))"
"DELTA=d4*0.5"

"acqt0 = 0"
baseopt_echo

1 ze
2 d11 do:f3 do:f2
  d12 pl1:f1
  d12 pl0:f2
  d12 pl12:f3
  10u BLKGRAD
  50u LOCKH_OFF
  d1
  50u LOCKH_ON
  10u UNBLKGRAMP

"if ( l0>1 ) {l0=0;}"

3 d12 pl1:f1

if "l0%2 == 1"
{
  (p1 ph1):f1

  5u
  (p14:sp14 ph3):f2
  5u

  d4

  p16:gp1
  d16 pl0:f1
  (p11:sp11 ph2):f1
  p16:gp1
  d16

  5u
  (p13:sp13 ph3):f2
  5u

  d4 BLKGRAMP
}
else
{
  (p1 ph1):f1

```

```

DELTA

5u
(p14:sp14 ph3):f2
5u

DELTA

p16:gp1
d16 pl0:f1
(p11:sp11 ph2):f1
p16:gp1
d16

DELTA

5u
(p13:sp13 ph3):f2
5u

DELTA BLKGRAMP

}
1u pl15:f2

go=2 ph31 cpd3:f3 cpd2:f2
d11 do:f3 do:f2 mc #0 to 2 F1QF(calclc(l0, 1) )

50u LOCKH_OFF

exit

ph1=0 0 0 0 2 2 2 2 1 1 1 1 3 3 3 3
ph2=0 1 2 3
ph3=0

ph11=2
ph31=0 2 0 2 2 0 2 0 3 1 3 1 1 3 1 3

;POWER LEVEL
;p10 : f2 channel - zero power [0 W]
;p11 : f1 channel - power level for pulse (default)
;p12 : f2 channel - power level for pulse (default)
;p13 : f3 channel - power level for pulse (default)
;p14 : f1 channel - zero power [0 W]
;p112 : f3 channel - power level for decoupling

```

```

;PULSES
;p1 : f1 channel - 90 degree high power pulse
;p2 : f1 channel - 180 degree high power pulse
;p3 : f2 channel - 90 degree high power pulse
;p4 : f2 channel - 180 degree high power pulse
;p11
;p14: f2 channel - 180 degree shaped pulse for inversion
;p15: f2 channel - 180 degree shaped pulse for inversion
;p16 : duration of CTP gradients [1m]

;DELAYS
;d1 : relaxation delay; 1-5 * T1
;d4 : 1/(4 nJ)XH (long range coupling constant)
;d11 : delay for disk I/O [30 msec]
;d16 : recovery delay for CTP gradients [200u]

;SHAPE PULSE
;spnam12: rsnob (wavemaker)

;GRADIENTS
;gpz1: CTP gradient (17%)
;gpnam1: SMSQ10.100

;CONSTANTS
;cnst2: f1 channel - nJ(X,H) Hz
;cnst3: number of X elements (use 1 for AX and AX3, use 2 for AX2)
;cnst12: f1 channel - bandwidth for selective refocusing pulse (in Hz)
;cnst13: f1 channel - chemical shift for selective refocusing pulse (in ppm)
;cnst14: f2 channel - bandwidth for selective refocusing pulse (in Hz)
;cnst15: f2 channel - chemical shift for selective refocusing pulse (in ppm)
;cnst40: f2 channel - sweep-width [kHz]
;cnst41: f2 channel - duration of the low-level W40 pulse [us]
;cnst43: f2 channel - adiabaticity factor of the low-level W40 pulse [Q=2.0]
;cnst44: f2 channel - step size of the low-level W40 pulse [ss > 2 us]
;cnst50: f3 channel - sweep-width [kHz]
;cnst51: f3 channel - duration of the low-level W2 pulse [us]
;cnst53: f3 channel - adiabaticity factor of the low-level W40 pulse [Q=2.0]
;cnst54: f3 channel - step size of the low-level W40 pulse [ss > 2 us]

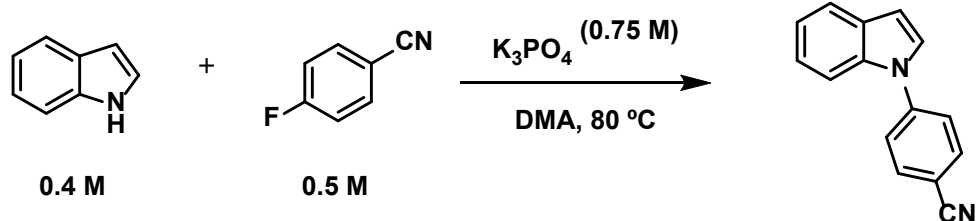
;OTHERS
;NS: 4 * n
;DS: >= 2

```


E. Data Processing

Data were phased in TopSpin in pseudo-2D mode. Further processing was performed in Python using the nmrglue library for data ingestion.

F. Sample Preparation



A sample of partially converted starting material was obtained as follows: An oven-dried large microwave vial was charged with 1.59 g of the base and a magnetic stir bar and was sealed. Stock solutions of indole (2.135 g) in 10 mL DMA and 4-fluorobenzonitrile (2.752 g) in 10 mL DMA were prepared. Under an atmosphere of argon, 2.2 mL of each stock solution and 5.6 mL of DMA were added. The vial was heated in an oil bath that had been pre-heated to 80 °C. The vial was sealed and DMA (9.3 mL) was added under an atmosphere of argon. The vial was then heated in an oil bath that had been pre-heated to the desired temperature. A 50 μ L aliquot was collected to determine conversion prior to workup. Conversion was determined using the HPLC method described previously, using the response factor determined for 4-fluorobenzonitrile (148335 M^{-1} at $240 \pm 2 \text{ nm}$). After measuring the conversion, the samples were subjected to an aqueous workup: the reaction mixture was washed with H_2O (5x) and brine. The organic phase was dried over Na_2SO_4 , filtered, and concentrated *in vacuo*, and the crude mixture was purified by column chromatography using the Biotage Isolera One.

The samples of recovered starting material and unreacted starting material were prepared in standard 5 mm glass tubes with 0.5 mM $Cr(acac)_3$ in $CDCl_3$ which were subsequently flame-sealed. Duplicate samples were prepared for each experiment and for the unreacted starting material.

Table S10. Samples used for $^{12}C/^{13}C$ kinetic isotope effect measurements

Description	% Remaining SM	
	Sample 1	Sample 2
Recovered SM from reaction with K_3PO_4	14.1%	15.7%
Unreacted SM	100%	100%

G. Results

The error bars due to random errors in conversion were estimated to be 0.003-0.004. Systematic errors can be judged by the spread between replicates. The spreads are smaller than the random errors, which indicates that the measurements are of high quality.

Table S11. Results of $^{12}\text{C}/^{13}\text{C}$ kinetic isotope effect measurements

Description	KIE	
	Sample 1	Sample 2
Recovered SM from reaction with K_3PO_4	1.032	1.035

IV. Computational Methods and Results

A. General Information

All DFT computations were carried out using Gaussian 16 version C.01.⁹ Stationary points were verified to be true local minima or saddle points by frequency analysis. Computational

⁹ Frisch, M. J.; Trucks, G. W.; Schlegel, H. B.; Scuseria, G. E.; Robb, M. A.; Cheeseman, J. R.; Scalmani, G.; Barone, V.; Petersson, G. A.; Nakatsuji, H.; Li, X.; Caricato, M.; Marenich, A. V.; Bloino, J.; Janesko, B. G.; Gomperts, R.; Mennucci, B.; Hratchian, H. P.; Ortiz, J. V.; Izmaylov, A. F.; Sonnenberg, J. L.; Williams, D.; Ding, F.; Lipparini, F.; Egidi, F.; Goings, J.; Peng, B.; Petrone, A.; Henderson, T.; Ranasinghe, D.; Zakrzewski, V. G.; Gao, J.; Rega, N.; Zheng, G.; Liang, W.; Hada, M.; Ehara, M.; Toyota, K.; Fukuda, R.; Hasegawa, J.; Ishida, M.; Nakajima, T.; Honda, Y.; Kitao, O.; Nakai, H.; Vreven, T.; Throssell, K.; Montgomery Jr., J. A.; Peralta, J. E.; Ogliaro, F.; Bearpark, M. J.; Heyd, J. J.; Brothers, E. N.; Kudin, K. N.; Staroverov, V. N.; Keith, T. A.; Kobayashi, R.; Normand, J.; Raghavachari, K.; Rendell, A. P.; Burant, J. C.; Iyengar, S. S.; Tomasi, J.; Cossi, M.; Millam, J. M.; Klene, M.; Adamo, C.; Cammi, R.; Ochterski, J. W.; Martin, R. L.; Morokuma, K.; Farkas, O.; Foresman, J. B.; Fox, D. J. *Gaussian 16 Rev. C.01*, Wallingford, CT, 2016

structures were visualized using Chemcraft 1.8.¹⁰ KIEs were calculated using *PyQuiver*.¹¹ Geometry optimizations were carried out at B3LYP-D3(BJ)/6-31+g*/CPCM(DMA).^{12–19}

B. Grid Calculations

To probe the influence of starting material structure on the mechanism of S_NAr , we computed a grid of potential energy surfaces for 72 S_NAr reactions constructed from the union of 9 aryl fluoride electrophiles and 8 nitrogen nucleophiles (Figure S17).

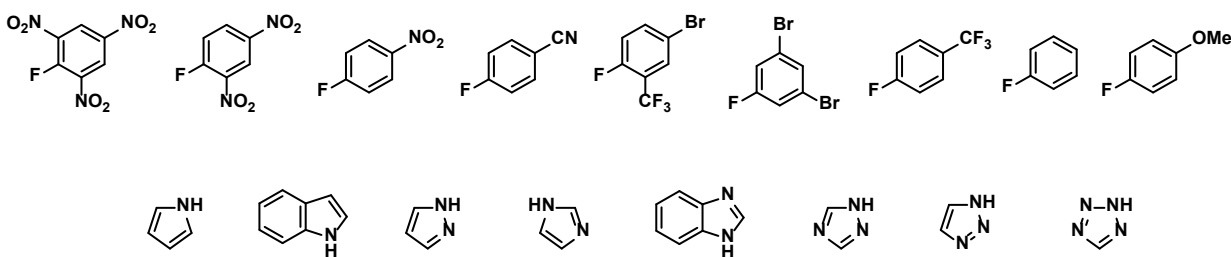


Figure S17. Selection of electrophiles and nucleophiles for potential energy surface calculations.

The electrophiles span a large range of Hammett σ values. Because not all of the σ values are readily available, and to isolate the computational factors responsible for the trends in mechanistic variation, computational σ values were determined using a series of isodesmic reactions in which the fluoride was replaced either by a carboxylic acid or carboxylate anion. Isodesmic energies were then computed as:

¹⁰ Zhurko G. A. Chemcraft - graphical program for visualization of quantum chemistry computations. Ivanovo, Russia, **2005**. <https://chemcraftprog.com>

¹¹ Anderson, T. L.; Kwan, E. E. *PyQuiver* **2020**, [www.github.com/ekwan/PyQuiver](https://github.com/ekwan/PyQuiver)

¹² Becke, A. D., Density-functional thermochemistry. III. The role of exact exchange. *J. Chem. Phys.* **1993**, *98*, 5648–5652;

¹³ Becke, A. D. A new mixing of Hartree–Fock and local density-functional theories. *J. Chem. Phys.* **1993**, *98*, 1372–1377.

¹⁴ Grimme, S.; Ehrlich, S.; Goerigk, L., Effect of the damping function in dispersion corrected density functional theory. *J. Comput. Chem.* **2011**, *32* (7), 1456–1465.

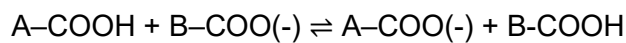
¹⁵ Lee, C.; Yang, W.; Parr, R. G. Development of the Colle-Salvetti correlation-energy formula into a functional of the electron density. *Phys. Rev. B* **1988**, *37*, 785–789.

¹⁶ Grimme, S.; Antony, J.; Ehrlich, S.; Krieg, H. A consistent and accurate *ab initio* parametrization of density functional dispersion correction (DFT-D) for the 94 elements H–Pu. *J. Chem. Phys.* **2010**, 154104–154119.

¹⁷ Grimme, S.; Ehrlich, S.; Goerigk, L. Effect of the Damping Function in Dispersion Corrected Density Functional Theory. *J. Comput. Chem.* **2011**, *32*, 1456–1465.

¹⁸ Hehre, W. J.; Ditchfield, R.; Pople, J. A. Self-Consistent Molecular Orbital Methods. XII. Further Extensions of Gaussian-Type Basis Sets for Use in Molecular Orbital Studies of Organic Molecules. *J. Chem. Phys.* **1972**, *56*, 2257–2261.

¹⁹ Barone, V.; Cossi, M. Quantum Calculation of Molecular Energies and Energy Gradients in Solution by a Conductor Solvent Model. *J. Phys. Chem. A* **1008**, 102, 1995–2001.



A similar procedure was carried out for the pK_a values of the nucleophiles by comparing the nitrogen anions with their neutral protonated counterparts. While these isodesmic energies could be used directly in the regressions presented below, they were rescaled to standard σ and pK_a scales for easier interpretation. The isodesmic σ and pK_a values are shared below (Table S12 and Table S13).

Table S12. Isodesmic σ values for the electrophiles computed from electronic energies.

				isodesmic_sigma				
2_4_6_trinitro	-1034.3973	-1033.9592	0	2.76				
3_4_dinitro	-829.8911	-829.44306	-6.23	1.49	1.49		slope	0.20307214
para_nitro	-625.39382	-624.9406	-9.48	0.83	0.78		intercept	2.75570174
meta_dibromo	-5563.1388	-5562.685	-9.85	0.76	0.78			
para_bromo_ortho_CF3	-3329.0618	-3328.6121	-7.26	1.28				
para_cyano	-513.12887	-512.67425	-10.36	0.65	0.66			
para_CF3	-757.9417	-757.48595	-11.07	0.51	0.54			
parent	-420.87622	-420.41656	-13.53	0.01	0			
para_methoxy	-535.41409	-534.95228	-14.87	-0.26	-0.27			

Table S13. Isodesmic pK_a values for the nucleophiles computed from electronic energies.

	with H	without H	isodesmic	isodesmic_pKa	pKa			627.509469
pyrrole	-210.1975	-209.70051	0.00	22.7	23			
indole	-363.86937	-363.37695	2.87	21.2	21		slope	-0.5396377
pyrazole	-226.23084	-225.74308	5.79	19.6	19.8		intercept	22.7315131
imidazole	-226.24984	-225.7655	7.94	18.4	18.6			
benzimidazole	-379.92143	-379.44132	10.59	17.0	16.4			
1_2_4_triazole	-242.28324	-241.80952	14.60	14.9	14.8			
1_2_3_triazole	-242.25816	-241.78748	16.51	13.8	13.9			
tetrazole	-258.28681	-257.83319	27.21	8.0	8.2			

The electrophiles range from very electron-deficient ($\sigma = +2.76$) to moderately electron rich ($\sigma = -0.26$). The nucleophiles also span 15 pK_a units.

The potential energy surfaces for all 72 reactions are shared below (Figure S18). To calculate each individual PES, the C–N and C–F bond lengths were systematically varied in constrained optimizations. The color scale in each square has been chosen to show the variation in relative energy from 10% to 80% of the energy span. That is, the energy scale in each square is different so that we can see the change in qualitative mechanism.

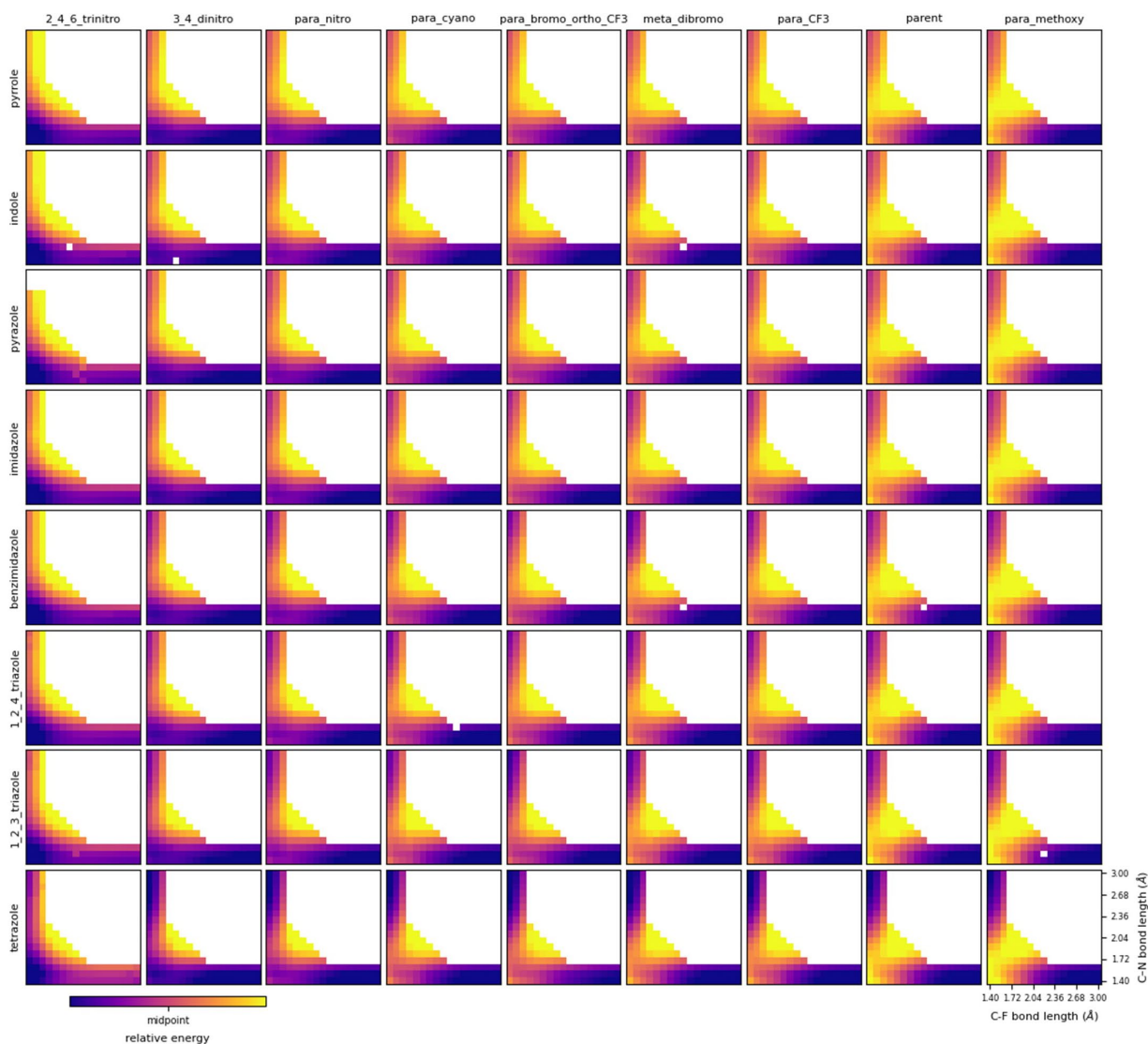


Figure S18. Complete grid of potential energy surfaces for all 72 nucleophiles and electrophiles B3LYP-D3(BJ)/6-31+g*/CPCM(DMA).²⁰

Within each PES, the starting materials (nitrogen anion and aryl fluoride) are in the upper left. The Meisenheimer region is in the lower left and will be dark if it is stable. The products (N-arylated product + fluoride) are in the bottom right. The upper left PES (pyrrole + 2,4,6-trinitrofluorobenzene) represents a “traditional” stepwise mechanism with a very electron-deficient substrate. There is a very stable Meisenheimer intermediate with a very early addition transition state. As the nucleophilicity decreases down the grid, the barrier increases and the transition state shifts later due to the Hammond postulate. The upper right PES (pyrrole + 4-methoxyfluorobenzene) represents a fully concerted mechanism with an electron-rich substrate. Because the electrophile is less reactive, all transition states in this vertical series are later.

²⁰ Data were visualized using cctk: Wagen, C.C.; Kwan, E.E. *cctk* 2020, www.github.com/ekwan/cctk.

Moving across the grid, from highly reactive electrophiles to less reactive electrophiles, the Meisenheimer region gradually increases in energy. The middle potential energy surfaces fall in the borderline region, in which a single transition state leads to a “shoulder” in the energy along the minimum energy path. These reactions are formally concerted but have some of the characteristics of a stepwise reaction. In all cases, the reaction is driven by the conversion of a nitrogen anion into a fluoride anion, and in most cases, the addition coordinate is higher in energy than the elimination coordinate.

We located all 72 transition states. Plotting their positions on the same axes reveals that, consistent with the Hammond postulate, as the electrophile gets more reactive, the transition states become earlier. Remarkably, the transition structures vary smoothly between the substrates and mechanisms. Thus, regardless of whether the reaction is stepwise, borderline, or concerted, the transition structure is similar, with advanced C–N bond formation and relatively little C–F bond cleavage.

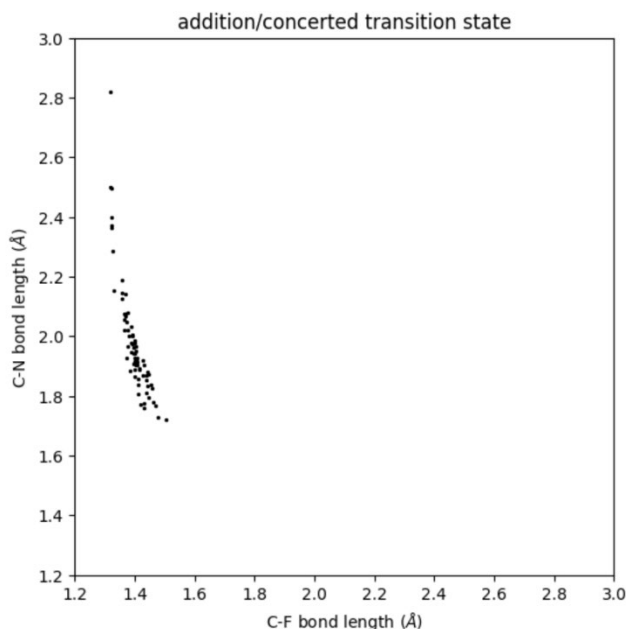


Figure S19. Plot of transition state locations for all 72 nucleophile-electrophile combinations.

Zooming in and coloring by electrophile further reveals trends with respect to both the electrophile and the nucleophile (Figure S20).

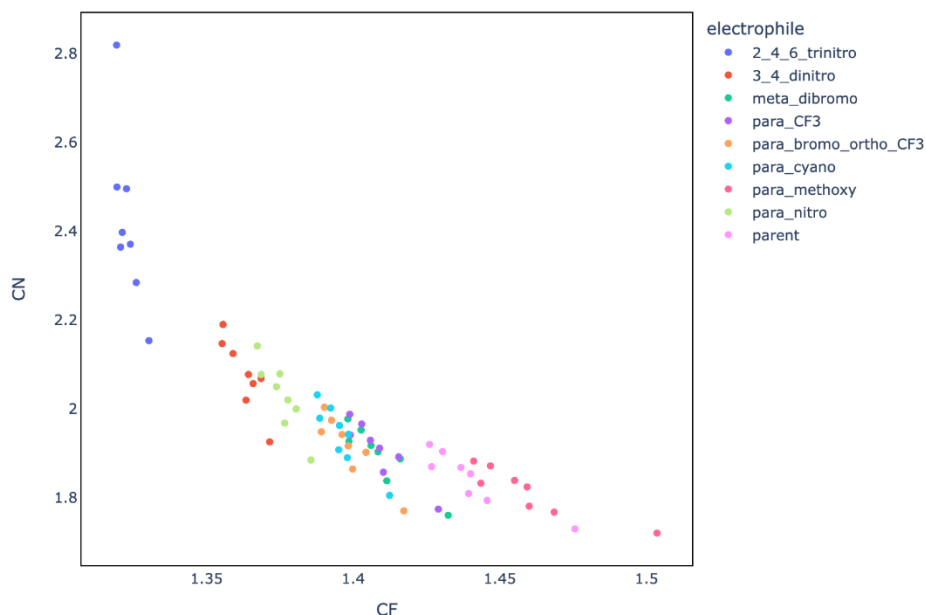


Figure S20. Plot of transition state locations for all 72 nucleophile-electrophile combinations, zoomed in and color-coded by electrophile.

Remarkably, we can predict how early or late the transition state will be with a simple linear model:

$$CN \text{ distance} = 0.015(pK_{a_{nuc}}) + 0.1918(\sigma_{e-phile}) + 1.5581 (R^2 = 0.802)$$

$$CF \text{ distance} = -0.0019(pK_{a_{nuc}}) - 0.0431(\sigma_{e-phile}) + 1.5581 (R^2 = 0.877)$$

These models simply show that as the nucleophile gets better (pK_a increases), the C–N distance increases and the C–F distance decreases (in other words, the transition state gets earlier). However, the influence of the electrophile is much larger (bigger coefficients), with more reactive electrophiles (more positive σ) resulting in earlier transition states. The C–N distance increases is also affected to a larger degree than the C–F distance.

Taking zero energy to mean isolated starting materials, we find that the energies of the transition state, Meisenheimer intermediate, and product structures are all predictable. The Meisenheimer intermediate was defined as the constrained structure where both the C–N and C–F bonds were set to 1.45 Å.

From calculating the TS energies for these reactions, we can see that the range of reactions chosen for our experimental study (the indole row, extending from para_nitro to para_CF3) are quite feasible at room temperature (Table S14). Note that these are electronic energies and neglect the free energy cost of association. In contrast, electron-rich substrates are not predicted to undergo the reaction in a reasonable timeframe. The plots are color coded such that dark purple = low energy and yellow = high energy (the same scale as the grid).

Table S14. Calculated transition state energies for 72 nucleophile-electrophile combinations.

$$TS \text{ energy} = -0.8223(pK a_{nuc}) - 11.2980(\sigma_{e-phile}) + 36.2412 (R^2 = 0.940)$$

electrophile nucleophile	2_4_6_trinitro	3_4_dinitro	para_bromo_ortho_CF3	para_nitro	meta_dibromo	para_cyano	para_CF3	parent	para_methoxy
pyrrole	-11.7	-0.7	8.8	4.7	9.6	9.3	12.1	19.0	22.3
indole	-11.7	-1.4	7.5	5.1	8.5	9.8	12.6	19.6	22.8
pyrazole	-7.8	1.1	10.5	6.4	11.8	11.2	14.1	21.0	24.6
imidazole	-7.3	2.5	11.9	7.7	13.2	12.5	15.4	22.4	25.8
benzimidazole	-8.5	2.7	10.7	8.0	11.7	12.7	15.5	22.5	25.9
1_2_4_triazole	-6.6	4.7	14.2	10.0	15.7	15.2	17.8	25.2	28.8
1_2_3_triazole	-6.3	5.5	15.2	10.7	16.8	15.8	18.8	26.0	29.7
tetrazole	-3.1	10.4	20.9	15.8	22.7	21.2	24.3	31.7	35.4

Evidently, the reaction barrier is largely determined by the choice of electrophile. The nearly smooth gradation of this colored plot indicates that it is largely described by the equation of a two-dimensional plane.

Unsurprisingly, the Meisenheimer energy is largely determined by the nature of the electrophile (Table S15).

Table S15. Calculated Meisenheimer energies for 72 nucleophile-electrophile combinations.

$$\begin{aligned} \text{Meisenheimer relative energy} \\ = -1.7330(pK a_{nuc}) - 19.8798(\sigma_{e-phile}) + 47.5990 (R^2 = 0.929) \end{aligned}$$

electrophile nucleophile	2_4_6_trinitro	3_4_dinitro	para_bromo_ortho_CF3	para_nitro	meta_dibromo	para_cyano	para_CF3	parent	para_methoxy
pyrrole	-48.1	-25.5	-5.6	-16.9	-3.2	-6.2	-1.2	10.4	14.3
indole	-46.9	-23.0	-4.5	-14.4	-2.6	-4.0	1.0	12.5	16.3
pyrazole	-43.2	-20.0	0.9	-11.5	2.6	-0.9	4.0	15.3	20.6
imidazole	-39.8	-17.3	1.4	-8.9	4.0	1.1	5.8	16.9	20.8
benzimidazole	-39.1	-15.6	2.1	-7.4	4.0	2.4	7.1	18.1	22.0
1_2_4_triazole	-34.1	-11.0	7.0	-2.9	9.7	6.8	11.4	22.2	27.2
1_2_3_triazole	-31.5	-8.6	10.3	-0.7	12.4	9.0	13.6	24.2	29.2
tetrazole	-18.8	1.4	20.0	9.0	21.6	18.3	22.7	32.9	37.6

In contrast, the energetics of the reaction are largely determined by the nucleophile (Table S16). Evidently, remote substitution has little effect on the strength of the C–F bond, and we can see that this chart is not tilted.

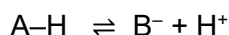
Table S16. Calculated product energies for 72 nucleophile-electrophile combinations.

$$\text{Product energy} = -1.9592(pK_{a_{nuc}}) + 12.6973 (R^2 = 0.977)$$

electrophile	2_4_6_trinitro	3_4_dinitro	para_bromo_ortho_CF3	para_nitro	meta_dibromo	para_cyano	para_CF3	parent	para_methoxy
nucleophile									
pyrrole	-32.6	-33.5	-30.3	-32.1	-33.7	-31.6	-31.3	-30.9	-31.4
indole	-31.4	-30.5	-29.0	-29.1	-31.5	-28.6	-28.4	-28.1	-28.9
pyrazole	-26.1	-28.1	-24.2	-26.5	-28.3	-26.1	-25.9	-25.6	-26.3
imidazole	-21.8	-22.7	-21.4	-22.1	-24.3	-21.9	-21.9	-22.1	-23.0
benzimidazole	-20.7	-20.5	-20.4	-19.9	-22.6	-19.7	-19.8	-20.0	-21.1
1_2_4_triazole	-14.3	-16.2	-14.7	-15.8	-16.1	-15.8	-15.9	-16.3	-17.3
1_2_3_triazole	-12.1	-14.0	-12.5	-13.5	-15.7	-13.6	-13.7	-14.3	-15.5
tetrazole	0.1	-3.6	-1.5	-3.5	-6.1	-3.8	-4.0	-4.9	-6.4

C. Specific Base and General Base Calculations

In an attempt to find a general base transition state, several different bases were explored computationally. The pK_a values for the conjugate acids were predicted as follows. The DFT acidities were predicted as follows:



$$\text{Acidity(energy)} = B^-(\text{energy}) - A-H(\text{energy})$$

The resulting DFT acidities are calculated in kcal/mol. To scale the acidities according to experimental pK_a values, the following linear regression was performed:

$$pK_a(\text{DMSO}) = \text{slope} * \text{acidity(energy)} + \text{intercept}$$

Computations were carried out with each of the bases to locate a specific base or general base transition state. The geometries and predicted KIEs are shown in Table S17. General base mechanism are only located when the pK_a of the base is less than 13; stronger bases result in predictions of specific base mechanisms only. The geometries are also clustered according to mechanism: specific base transition states fall fairly early along the addition coordinate (C–N ~ 1.9 Å, C–F ~ 1.4 Å), whereas the general base transition states lie in the Meisenheimer region (C–N ~ 1.6 Å, C–F ~ 1.5 Å). The geometries and KIEs are independent of base, and depend solely on whether the specific or general base mechanism is operative.

Table S17. Predicted KIEs for general base and specific base transition states

conjugate_acid	mechanism	pKa	CF	CN	NH	BH	KIE
hydrogen_chloride	GENERAL	-3.6	1.565	1.585	1.074	1.971	1.030
tri_hydrogen_phosphate	GENERAL	3.4	1.527	1.612	1.084	1.549	1.030
tri_hydrogen_phosphate	specific	3.4	1.415	1.865	1.682	1.021	1.052
hydrogen_isocyanide	GENERAL	4.6	1.52	1.613	1.086	1.624	1.028
hydrogen_isocyanide	specific	4.6	1.418	1.865	1.612	1.079	1.051
di_hydrogen_carbonate	GENERAL	6.5	1.511	1.62	1.1	1.525	1.030
di_hydrogen_carbonate	specific	6.5	1.42	1.857	1.598	1.043	1.050
tetrazole	specific	8.0	1.414	1.886	1.71	1.062	1.052
tetrazole	GENERAL	8.0	1.512	1.624	1.098	1.617	1.031
hydrogen_fluoride	specific	9.2	1.426	1.825	1.463	1.04	1.050
hydrogen_cyanide	specific	12.8	1.397	1.958	2.019	1.091	1.050
hydrogen_cyanide	GENERAL	12.8	1.479	1.666	1.128	1.634	1.040
1_2_3_triazole	specific	13.8	1.407	1.919	1.819	1.041	1.051
1_2_4_triazole	specific	14.9	1.415	1.904	1.802	1.043	1.052
1_2_4_triazole	specific	14.9	1.415	1.904	1.802	1.043	1.052
benzimidazole	specific	17.0	1.397	1.957	2.042	1.022	1.051
di_hydrogen_phosphate	specific	17.3	1.404	1.921	1.888	0.991	1.052
imidazole	specific	18.4	1.403	1.921	1.875	1.033	1.051
pyrazole	specific	19.6	1.411	1.917	1.859	1.034	1.052
indole	specific	21.0	1.396	1.963	2.082	1.018	1.050
pyrrole	specific	23.0	1.396	1.965	2.093	1.019	1.050
hydrogen_carbonate	specific	24.1	1.401	1.951	2.015	0.985	1.051
hydrogen_phosphate	specific	28.7	1.401	1.953	2.002	0.983	1.050

The charge distribution on the arene was calculated using a Hirshfeld population analysis for the specific base and general base transition states using tetrazole anion as the base (Table S18). In addition, we calculated the charge distribution in the starting material (4-fluorobenzonitrile), the transition state with no base, and the Meisenheimer intermediate (defined here as the structure in which both the C–N and C–F bonds are constrained at 1.4 Å). This analysis provides further evidence for the general base mechanism, as the charges in the general base transition state are more consistent with the LFER data obtained experimentally.

Table S18. Hirshfeld population analysis of arene carbons.

structure	ortho1 charge	ortho2 charge	para charge	sum charges	C–F (Å)	C–N (Å)	B–H (Å)
4-fluorobenzonitrile	-0.086	-0.086	0.001	-0.171	N/A	N/A	N/A
no base TS	-0.134	-0.134	-0.049	-0.317	1.39	2.00	N/A
Specific base TS	-0.156	-0.151	-0.071	-0.379	1.41	1.89	1.06
General base TS	-0.140	-0.140	-0.060	-0.340	1.51	1.62	1.62
Meisenheimer intermediate	-0.166	-0.169	-0.094	-0.429	1.40	1.40	1.00

D. Calculations using Indole Anion

The singly anionic system containing indole anion and 4-fluorobenzonitrile was explored with B3LYP-D3(BJ)/CPCM(DMF) with several basis sets.

The PES was calculated by systematically varying the C–N and C–F bond lengths in constrained optimizations (Figure S22). At the 6-31+G* level, the reaction appears to be “borderline,” with a single transition state for addition and no stationary point for elimination.

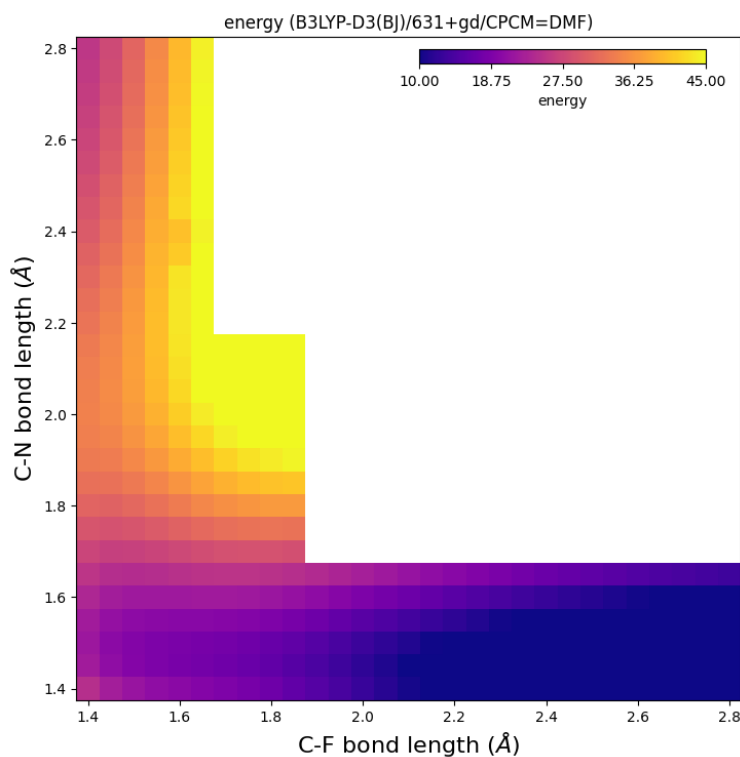


Figure S21. PES for the reaction between indole anion and 4-fluorobenzonitrile (B3LYP-D3(BJ)/6-31+g*/CPCM(DMF))

There is a blended intermediate/transition state in the Meisenheimer region that is best thought of as a shoulder along the minimum energy path (Figure S22).

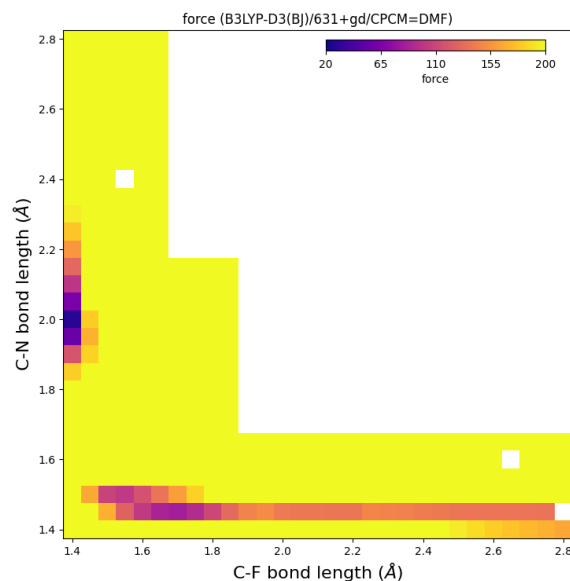


Figure S22. Force analysis of the PES for the reaction between indole anion and 4-fluorobenzonitrile (B3LYP-D3(BJ)/jun-cc-pVTZ/CPCM(DMF))

The surface is qualitatively unchanged at the much larger jun-cc-pVTZ level (some points are missing due to convergence issues):

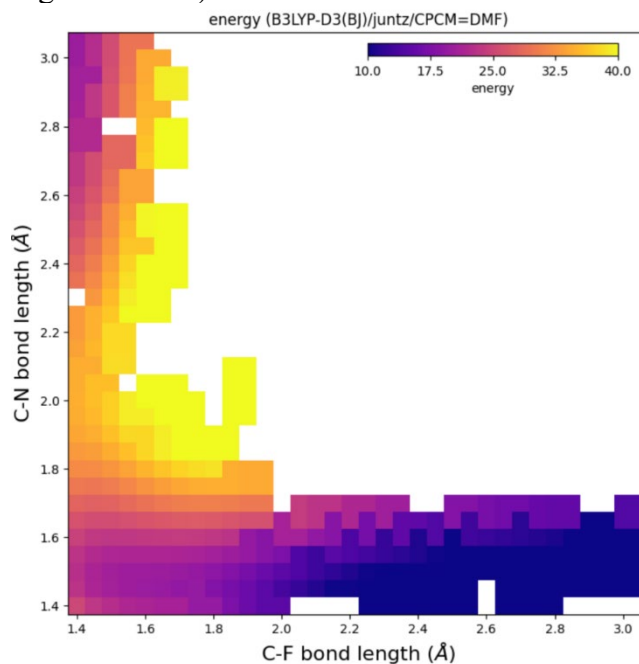


Figure S23. PES for the reaction between indole anion and 4-fluorobenzonitrile (B3LYP-D3(BJ)/jun-cc-pVTZ/CPCM(DMF))

The Hirshfeld charge on the indole nitrogen abruptly decreases significantly at a C–N distance of 2.2 Å as the system gets close to its transition state distance of ~2.0 Å (Figure S24). Concurrently, the charge on the arene carbons increases as we approach the Meisenheimer region (Figure S25).

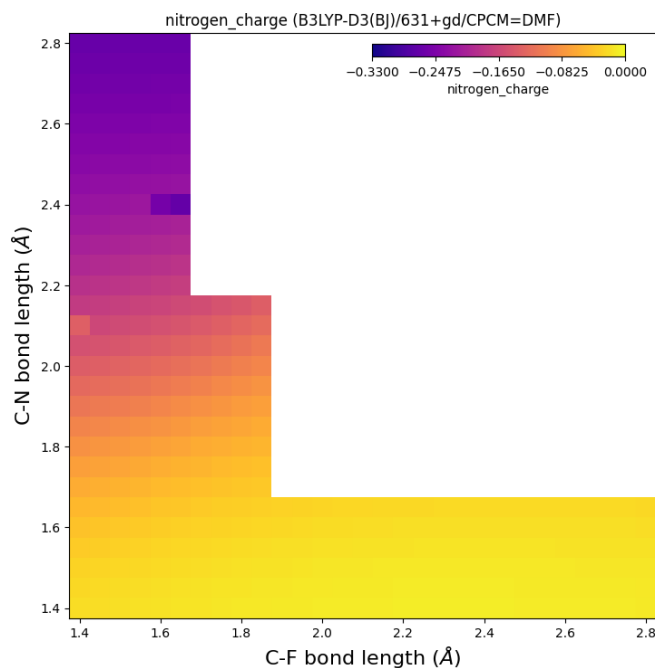


Figure S24. Hirshfeld population analysis of indole nitrogen

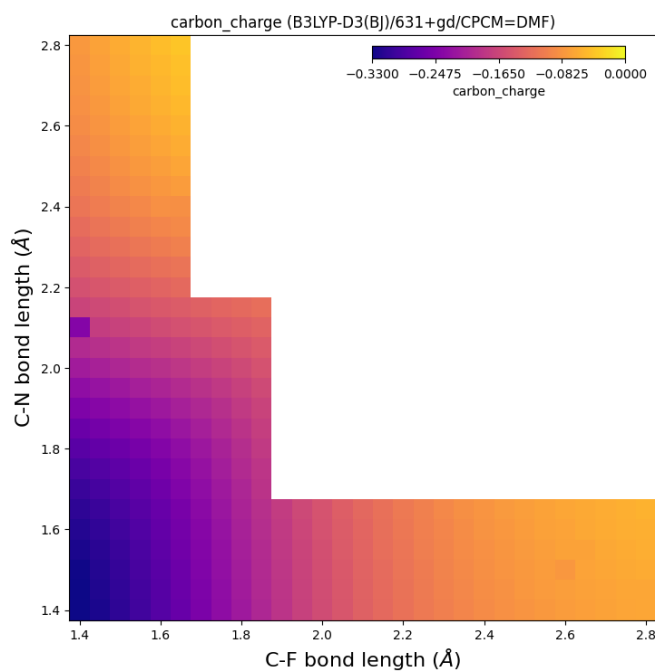


Figure S25. Hirshfeld population analysis of arene carbons

A plot of the predicted KIEs shows that they are largest in the concerted regime of the addition-elimination coordinate (Figure S26).

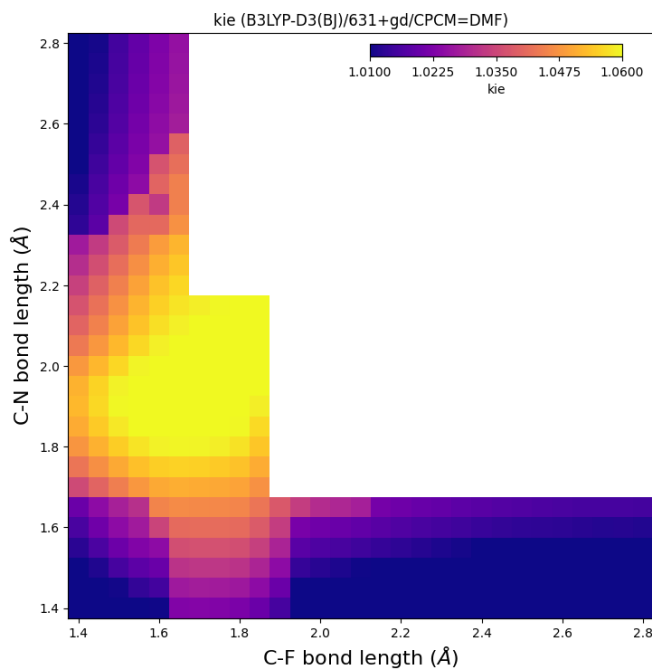
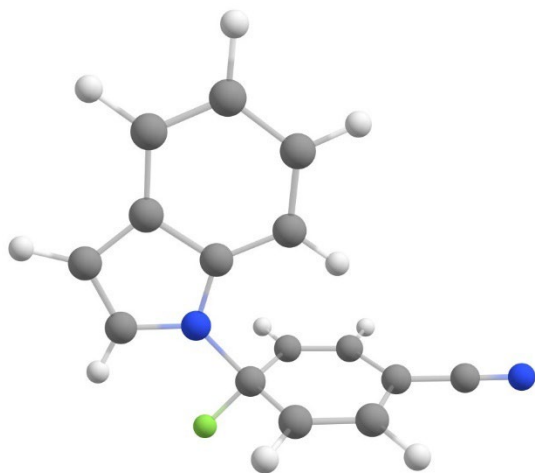


Figure S26. Predicted KIEs as a function of geometry.

E. Coordinates for Key Structures

“Anionic/No Base” Transition State: Indole Anion + 4-Fluorobenzonitrile



Charge: -1

Multiplicity: 1

Electronic Energy: -787.1398684

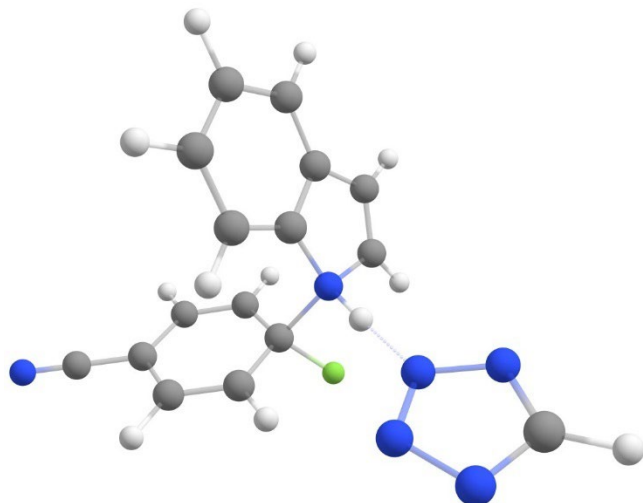
Imaginary Frequencies: 1 (-301.8608)

Reduced Mass: 8.7115

C	3.234382000	-1.248453000	0.000865000
C	2.051711000	-1.958535000	0.000506000
C	2.883066000	0.143788000	0.000296000
H	1.885871000	-3.025218000	0.000696000
C	1.452849000	0.205571000	-0.000269000
C	3.622373000	1.342969000	0.000265000
C	0.768043000	1.431935000	-0.000829000
C	2.943182000	2.557503000	-0.000275000
H	4.709781000	1.316941000	0.000705000
H	-0.315140000	1.474063000	-0.001274000
C	1.529555000	2.598384000	-0.000833000
H	3.503362000	3.489183000	-0.000273000
H	1.024520000	3.561096000	-0.001277000
H	4.231294000	-1.670690000	0.001380000
N	0.977871000	-1.091599000	-0.000227000
C	-2.303229000	-0.147585000	1.218933000
C	-2.883694000	0.313023000	0.000294000
C	-2.303305000	-0.146893000	-1.218645000
C	-1.216108000	-0.977380000	-1.236144000
C	-0.578915000	-1.460945000	-0.000284000
C	-1.216031000	-0.978082000	1.235889000
H	-2.728359000	0.186308000	2.162932000
H	-2.728508000	0.187520000	-2.162426000
H	-0.762008000	-1.284255000	-2.174520000
H	-0.761865000	-1.285482000	2.174062000
F	-0.489923000	-2.858113000	-0.000684000
C	-3.992608000	1.177538000	0.000575000

N -4.920338000 1.899676000 0.000810000

General Base Transition State: Indole + 4-Fluorobenzonitrile + Tetrazole anion



Charge: -1

Multiplicity: 1

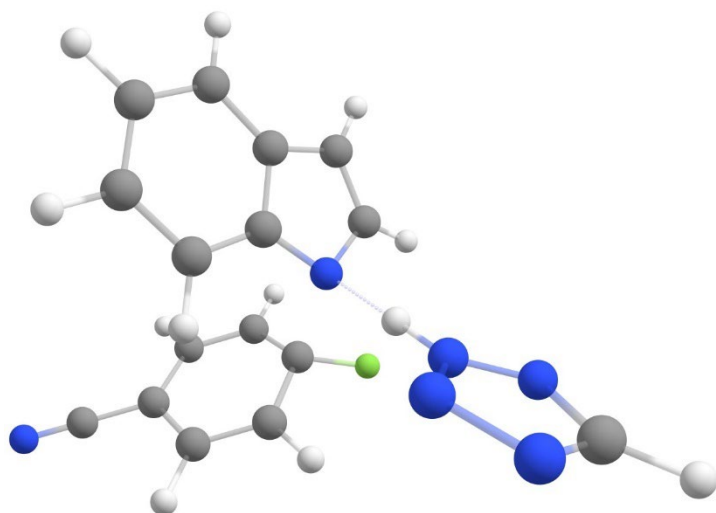
Electronic Energy: -1045.4413125

Imaginary Frequencies: 1 (-47.9927)

Reduced Mass: 6.5813

C	1.986282000	-1.908168000	-0.654012000
C	3.169252000	-1.346611000	-0.107895000
C	3.036447000	-0.484402000	1.011623000
C	1.810014000	-0.195106000	1.559241000
C	0.596482000	-0.773816000	1.024783000
C	0.746109000	-1.629630000	-0.132563000
H	2.059676000	-2.568639000	-1.514169000
H	3.926566000	-0.035879000	1.445097000
H	1.727046000	0.478488000	2.406187000
H	-0.150820000	-2.050537000	-0.576017000
F	-0.173973000	-1.506232000	2.099930000
C	4.435933000	-1.626810000	-0.666298000

N	5.487568000	-1.858690000	-1.129625000
H	-1.424792000	-0.211695000	0.411466000
C	-0.751648000	2.396774000	1.834821000
C	-0.926152000	1.074807000	2.004643000
C	-0.274245000	2.632992000	0.475202000
H	-1.266078000	0.504057000	2.853421000
C	-0.173194000	1.382220000	-0.155996000
C	0.042891000	3.793777000	-0.233230000
C	0.220145000	1.236433000	-1.475690000
C	0.453869000	3.666033000	-1.564666000
H	-0.032529000	4.769871000	0.236334000
H	0.286060000	0.263446000	-1.945843000
C	0.538777000	2.408147000	-2.177757000
H	0.705859000	4.555518000	-2.134697000
H	0.854749000	2.335126000	-3.213921000
H	-0.949555000	3.159112000	2.577472000
N	-0.558466000	0.344286000	0.792166000
C	-4.728986000	-1.523084000	-0.532164000
H	-5.804487000	-1.599451000	-0.452551000
N	-3.978368000	-0.726922000	0.239670000
N	-2.728286000	-0.949387000	-0.198453000
N	-2.726030000	-1.831281000	-1.180991000
N	-3.990388000	-2.215812000	-1.415966000

Specific Base Transition State: Indole + 4-Fluorobenzonitrile + Tetrazole anion

Charge: -1

Multiplicity: 1

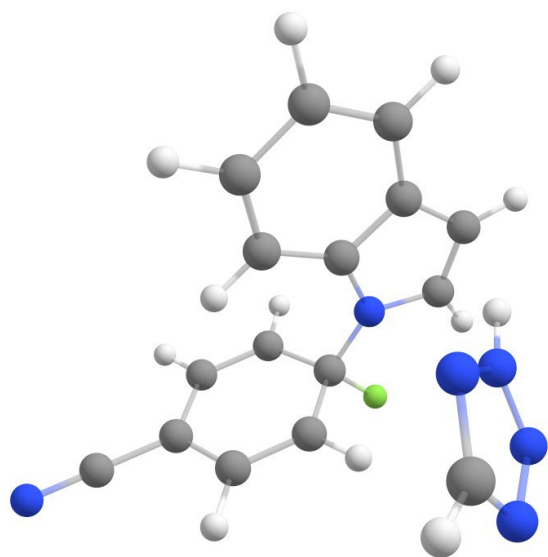
Electronic Energy: -1045.4451597

Imaginary Frequencies: 1 (-403.8768)

Reduced Mass: 9.0549

C	1.658352000	-2.115421000	-0.643363000
C	2.879607000	-1.605209000	-0.138622000
C	2.854322000	-0.900565000	1.093050000
C	1.674574000	-0.688561000	1.769930000
C	0.424412000	-1.091041000	1.196885000
C	0.467251000	-1.896064000	0.012806000
H	1.662298000	-2.700012000	-1.559301000
H	3.786471000	-0.541446000	1.520763000
H	1.660244000	-0.154633000	2.714720000
H	-0.462627000	-2.296742000	-0.377154000
F	-0.532261000	-1.533503000	2.139700000
C	4.096259000	-1.819754000	-0.827565000
N	5.103630000	-1.993845000	-1.399485000
H	-1.946168000	-0.198345000	0.144553000

C	-0.563003000	2.554996000	1.859455000
C	-0.881968000	1.226286000	1.992564000
C	0.035199000	2.704602000	0.554463000
H	-1.335635000	0.722292000	2.835638000
C	0.037000000	1.402074000	-0.029803000
C	0.547842000	3.795627000	-0.167798000
C	0.551146000	1.187553000	-1.313954000
C	1.066209000	3.574384000	-1.443641000
H	0.540560000	4.795588000	0.260120000
H	0.548514000	0.198753000	-1.757747000
C	1.069980000	2.282050000	-2.008688000
H	1.468878000	4.407799000	-2.013917000
H	1.477968000	2.135633000	-3.005601000
H	-0.746412000	3.339209000	2.584159000
N	-0.549192000	0.487396000	0.853746000
C	-4.633991000	-1.523138000	-0.622765000
H	-5.590431000	-1.996158000	-0.458235000
N	-3.828174000	-1.123036000	0.361263000
N	-2.805252000	-0.617381000	-0.318678000
N	-2.945144000	-0.689609000	-1.628650000
N	-4.114792000	-1.268854000	-1.845770000

Meisenheimer Intermediate

Charge: -1

Multiplicity: 1

Electronic Energy: -1045.4543674

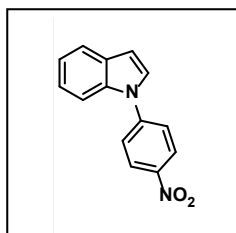
Imaginary Frequencies: 3

C	-2.329871000	-1.204545000	0.365634000
C	-3.385062000	-0.246157000	0.274990000
C	-3.204984000	0.840448000	-0.634507000
C	-2.079204000	0.972537000	-1.395605000
C	-0.968927000	-0.026257000	-1.389627000
C	-1.190469000	-1.104194000	-0.379436000
H	-2.426313000	-2.025230000	1.073801000
H	-3.978455000	1.603329000	-0.698540000
H	-1.935708000	1.840123000	-2.035940000
H	-0.380473000	-1.817615000	-0.255731000
F	-0.896920000	-0.616528000	-2.657063000
C	-4.541803000	-0.355051000	1.063112000
N	-5.512408000	-0.446027000	1.722346000
H	2.659767000	-0.634005000	-0.374800000

C	2.412300000	1.269625000	-1.606762000
C	1.342658000	0.580071000	-2.135065000
C	2.005013000	1.750352000	-0.313506000
H	1.249113000	0.071709000	-3.080953000
C	0.665980000	1.303450000	-0.112092000
C	2.644427000	2.492624000	0.698397000
C	-0.037185000	1.583327000	1.069277000
C	1.948051000	2.773140000	1.868305000
H	3.666487000	2.836858000	0.562328000
H	-1.052532000	1.236559000	1.217589000
C	0.620620000	2.321768000	2.048879000
H	2.428063000	3.345408000	2.657673000
H	0.100874000	2.553704000	2.974642000
H	3.364316000	1.431547000	-2.094774000
N	0.281897000	0.585023000	-1.242057000
C	2.042384000	-2.785631000	1.659764000
H	1.860782000	-3.211812000	2.634623000
N	2.339153000	-1.503107000	1.459166000
N	2.467452000	-1.470024000	0.139095000
N	2.266513000	-2.630197000	-0.460114000
N	1.993506000	-3.489219000	0.502009000

V. Characterization of S_NAr Products

The compounds described in this section were isolated from various kinetics experiments for the purposes of characterization and acquiring the calibration plots. As such, the yields reported here are not optimized.

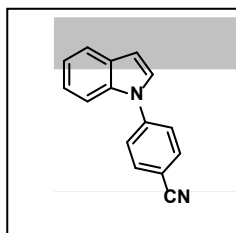


1-(4-nitrophenyl)-1H-indole²¹

Previously reported compound; isolated from a kinetics experiment following Procedure A as a yellow powdery solid (127 mg, 21% yield).

¹H NMR (500 MHz, CDCl₃) δ 8.44–8.32 (m, 2H), 7.76–7.59 (m, 4H), 7.37 (d, *J* = 3.4 Hz, 1H), 7.29 (ddd, *J* = 8.4, 7.1, 1.3 Hz, 1H), 7.26–7.20 (m, 1H), 6.77 (dd, *J* = 3.4, 0.9 Hz, 1H).

HPLC (C18, water/acetonitrile = 10/90, flow rate = 0.6–0.7 mL/min, λ = 363 nm) t_R = 5.4 min.

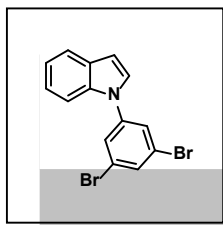


4-(1H-indol-1-yl)benzonitrile²²

Previously reported compound; isolated from a kinetics experiment following Procedure A as an off-white powdery solid (233 mg, 43% yield).

¹H NMR (500 MHz, CDCl₃) δ 7.77–7.72 (m, 2H), 7.63 (d, *J* = 7.8 Hz, 1H), 7.58 (d, *J* = 8.5 Hz, 2H), 7.54 (d, *J* = 8.3 Hz, 1H), 7.28 (d, *J* = 3.4 Hz, 1H), 7.25–7.18 (m, 1H), 7.15 (t, *J* = 7.4 Hz, 1H), 6.68 (d, *J* = 3.4 Hz, 1H).

HPLC (C18, water/acetonitrile = 10/90, flow rate = 0.6–0.7 mL/min, λ = 315 nm) t_R = 5.2 min.



1-(3,5-dibromophenyl)-1H-indole

Isolated from a kinetics experiment following Procedure B as a yellow-orange oil (69 mg, 8% yield).

¹H NMR (500 MHz, DMSO-*d*₆) δ 7.83 (s, 3H), 7.71 (d, *J* = 3.4 Hz, 1H), 7.65 (d, *J* = 7.8 Hz, 1H), 7.57 (d, *J* = 8.3 Hz, 1H), 7.26–7.19 (m, 1H), 7.15 (t, *J* = 7.4 Hz, 1H), 6.72 (d, *J* = 3.4 Hz, 1H).

¹³C NMR: (126 MHz, DMSO-*d*₆) δ 141.93, 135.24, 131.58, 129.85, 128.93, 125.92, 123.69, 123.34, 121.60, 121.39, 110.77, 105.19.

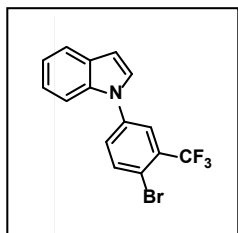
IR (FT-ATR, cm⁻¹) ν_{max} 3081, 1576, 1556, 1514, 1475, 1461, 1425, 1341, 1328, 1300, 1234, 1209, 1133, 1113, 1096, 1015, 983, 929, 882, 862, 841, 762, 738, 717, 678, 614, 601, 573, 483, 427, 415

²¹ Klapars, A.; Antilla, J. C.; Huang, X.; Buchwald, S. L. A General and Efficient Copper Catalyst for the Amidation of Aryl Halides and the *N*-Arylation of Nitrogen Heterocycles. *J. Am. Chem. Soc.* **2001**, *123*, 7727–7729.

²² Smith III, W. J.; Sawyer, J. S. A novel and selective method for the *N*-arylation of indoles mediated by KFAI₂O₃. *Tetrahedron Lett.* **1996**, *37*, 299–302.

HRMS (ESI) (m/z) for $[M+H]^+$ for $C_{14}H_{10}Br_2N$ requires 349.9175, observed 349.9169.

HPLC (C18, water/acetonitrile = 10/90, flow rate = 0.6-0.7 mL/min, λ = 363 nm) t_R = 5.9 min.



1-(4-bromo-3-(trifluoromethyl)phenyl)-1H-indole

Isolated from a kinetics experiment following Procedure B as a colorless oil (52.4 mg, 6% yield).

1H NMR (500 MHz, $CDCl_3$) δ 7.85 (d, J = 6.9 Hz, 1H), 7.84 (s, 1H), 7.70 (d, J = 7.8 Hz, 1H), 7.55 (dd, J = 8.5, 2.6 Hz, 1H), 7.51 (d, J = 8.2 Hz, 1H), 7.30 (d, J = 3.3 Hz, 1H), 7.29 – 7.24 (m, 2H), 7.21 (td, J = 7.4, 7.0, 1.0 Hz, 1H),

6.73 (d, J = 3.3 Hz, 1H)

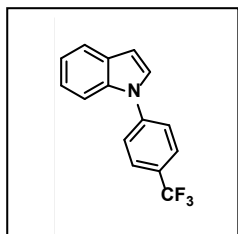
^{13}C NMR (126 MHz, $CDCl_3$) δ 139.21, 136.30, 135.49, 131.63 (q, J = 31.8 Hz), 129.62, 128.10, 127.24, 123.41 (q, J = 5.5 Hz), 123.15, 122.50 (q, J = 274.0 Hz), 121.55, 121.14, 116.90, 109.97, 105.18

^{19}F NMR (471 MHz, $CDCl_3$) δ –63.45

IR (FT-ATR, cm^{-1}) ν_{max} 3053, 1736, 1603, 1570, 1519, 1482, 1455, 1423, 1351, 1337, 1299, 1271, 1257, 1232, 1211, 1173, 1125, 1095, 1022, 974, 896, 883, 848, 830, 810, 761, 738, 718, 663, 630, 587, 565, 533, 488, 468, 453, 424

HRMS (ESI) (m/z) for $[M+H]^+$ for $C_{15}H_{10}BrF_3N$ requires 339.9943, observed 339.9938.

HPLC (C18, water/acetonitrile = 10/90, flow rate = 0.6-0.7 mL/min, λ = 363 nm) t_R = 5.9 min.



1-(4-(trifluoromethyl)phenyl)-1H-indole²³

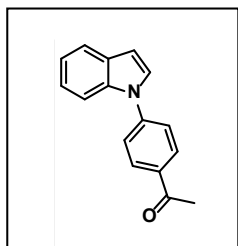
Previously reported compound; isolated from a kinetics experiment following Procedure B as white needles (44.2 mg, 14% yield).

1H NMR (500 MHz, $CDCl_3$) δ 7.83–7.74 (m, 2H), 7.70 (dt, J = 7.8, 1.1 Hz, 1H), 7.67–7.62 (m, 2H), 7.60 (dq, J = 8.3, 0.9 Hz, 1H), 7.36 (d, J = 3.3 Hz, 1H), 7.29–7.23 (m, 1H), 7.21 (ddd, J = 7.9, 7.1, 1.1 Hz, 1H), 6.73 (dd, J =

3.3, 0.9 Hz, 1H).

HPLC (C18, water/acetonitrile = 10/90, flow rate = 0.6-0.7 mL/min, λ = 265 nm) t_R = 5.9 min.

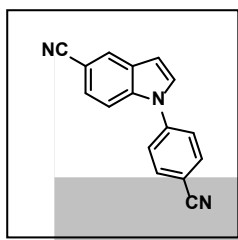
²³ Mann, G.; Hartwig, J. F.; Driver, M. S.; Fernández-Rivas, C. Palladium-Catalyzed C–N(sp²) Bond Formation: *N*-Arylation of Aromatic and Unsaturated Nitrogen and the Reductive Elimination Chemistry of Palladium Azolyl and Methyleneamido Complexes. *J. Am. Chem. Soc.* **1998**, *120*, 827–828.

**1-(4-(1H-indol-1-yl)phenyl)ethan-1-one²⁴**

Previously reported compound; isolated from a kinetics experiment following Procedure B as a tan solid (97.7 mg, 33% yield).

¹H NMR (500 MHz, CDCl₃) δ 8.09 (d, *J* = 8.3 Hz, 2H), 7.68 (d, *J* = 7.8 Hz, 1H), 7.58 (d, *J* = 8.2 Hz, 2H), 7.35 (d, *J* = 3.4 Hz, 1H), 7.29–7.22 (m, 1H), 7.19 (t, *J* = 7.4 Hz, 1H), 6.72 (d, *J* = 3.4 Hz, 1H), 2.63 (s, 3H).

HPLC (C18, water/acetonitrile = 10/90, flow rate = 0.6–0.7 mL/min, λ = 363 nm) t_R = 5.2 min.

**1-(4-cyanophenyl)-1H-indole-5-carbonitrile**

Isolated from a kinetics experiment following Procedure A as an off-white powdery solid (219 mg, 36% yield).

¹H NMR (500 MHz, CDCl₃) δ 8.07 (d, *J* = 1.6 Hz, 1H), 7.89 (d, 2H, *J* = 8.9 Hz), 7.66 (d, 2H, *J* = 8.6 Hz), 7.64 (d, *J* = 8.9 Hz, 1H), 7.52 (dd, *J* = 8.6, 1.6 Hz, 1H), 7.49 (d, *J* = 3.4 Hz, 1H), 6.86 (d, *J* = 3.4 Hz, 1H)

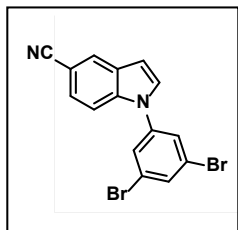
¹³C NMR (126 MHz, CDCl₃) δ 142.43, 136.90, 134.07, 129.57, 126.96, 126.10, 124.61, 120.04, 118.00, 111.23, 110.93, 106.00, 104.64

IR (FT-ATR, cm⁻¹) ν_{max} 3142, 3060, 2222, 1601, 1524, 1469, 1447, 1377, 1309, 1294, 1282, 1250, 1218, 1187, 1142, 1106, 955, 907, 842, 806, 793, 761, 653, 622, 588, 559, 547, 534, 492, 449, 421, 404

HRMS (ESI) (*m/z*) for [M+H]⁺ for C₁₆H₁₀N₃ requires 244.0869, observed 244.0869

HPLC (C18, water/acetonitrile = 10/90, flow rate = 0.6–0.7 mL/min, λ = 363 nm) t_R = 4.9 min.

²⁴ Monguchi, Y.; Marumoto, T.; Takamatsu, H.; Sawama, Y.; Sajiki, H. Palladium on Carbon-Catalyzed One-Pot *N*-Arylindole Synthesis: Intramolecular Aromatic Amination, Aromatization, and Intermolecular Aromatic Amination. *Adv. Synth. Catal.*, **2014**, 356, 1649–1882.

**1-(3,5-dibromophenyl)-1H-indole-5-carbonitrile**

Isolated from a kinetics experiment following Procedure B as a white powdery solid (125 mg, 13% yield).

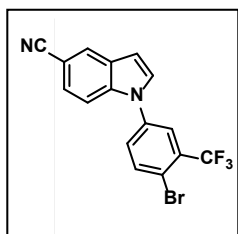
^1H NMR (500 MHz, CDCl_3) δ 8.03 (d, $J = 1.6$ Hz, 1H), 7.73 (t, $J = 1.7$ Hz, 1H), 7.60 (d, $J = 1.7$ Hz, 2H), 7.56 (dt, $J = 8.8, 0.8$ Hz, 1H), 7.50 (dd, $J = 8.6, 1.6$ Hz, 1H), 7.39 (d, $J = 3.4$ Hz, 1H), 6.78 (dd, $J = 3.4, 0.8$ Hz, 1H).

^{13}C NMR (126 MHz, CDCl_3) δ 140.69, 137.12, 133.13, 129.75, 129.20, 126.88, 126.37, 126.00, 123.90, 120.14, 111.13, 105.45, 104.42.

IR (FT-ATR, cm^{-1}) ν_{max} 3128, 3100, 3066, 2923, 2852, 2217, 1888, 1725, 1606, 1575, 1556, 1519, 1472, 1436, 1423, 1325, 1283, 1247, 1214, 1141, 1100, 1072, 983, 936, 891, 868, 844, 804, 794, 777, 762, 721, 675, 630, 623, 567, 544, 511, 499, 484, 435, 419, 404

HRMS (ESI) (m/z) for $[\text{M}+\text{H}]^+$ for $\text{C}_{15}\text{H}_9\text{Br}_2\text{N}_2$ requires 376.9127, observed 376.9122

HPLC (C18, water/acetonitrile = 10/90, flow rate = 0.6-0.7 mL/min, $\lambda = 363$ nm) $t_R = 5.7$ min.

**1-(4-bromo-3-(trifluoromethyl)phenyl)-1H-indole**

Isolated from a kinetics experiment following Procedure B as a white powdery solid (333 mg, 37% yield).

^1H NMR (500 MHz, CDCl_3) δ 8.04 (t, $J = 1.1$ Hz, 1H), 7.91 (d, $J = 8.5$ Hz, 1H), 7.81 (d, $J = 2.6$ Hz, 1H), 7.54 (dd, $J = 8.5, 2.7$ Hz, 1H), 7.52 – 7.47 (m, 2H), 7.43 (d, $J = 3.4$ Hz, 1H), 6.82 (d, $J = 3.4$ Hz, 1H)

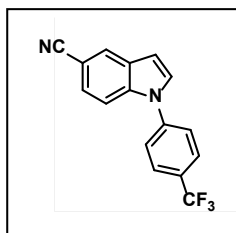
^{13}C NMR (126 MHz, CDCl_3) δ 138.03, 137.17, 136.66, 132.02 (q, $J = 32.1$ Hz), 129.76, 129.25, 128.63, 126.95, 126.02, 123.93 (q, $J = 5.4$ Hz), 122.31 (q, $J = 273.9$ Hz), 120.11, 118.53, 110.92, 105.56, 104.42

^{19}F NMR (471 MHz, CDCl_3) δ -63.50

IR (FT-ATR, cm^{-1}) ν_{max} 3078, 2218, 1718, 1602, 1579, 1563, 1519, 1495, 1467, 1526, 1376, 1331, 1311, 1291, 1270, 1261, 1242, 1220, 1176, 1133, 1100, 1075, 1022, 980, 945, 899, 886, 839, 817, 805, 789, 747, 7211, 708, 661, 626, 619, 538, 505, 493, 470, 452, 425, 416

HRMS (ESI) (m/z) for $[\text{M}+\text{H}]^+$ for $\text{C}_{16}\text{H}_9\text{BrF}_3\text{N}_2$ requires 364.9896, observed 364.9890

HPLC (C18, water/acetonitrile = 10/90, flow rate = 0.6-0.7 mL/min, $\lambda = 363$ nm) $t_R = 5.5$ min.

**1-(4-(trifluoromethyl)phenyl)-1H-indole-5-carbonitrile**

Isolated from a kinetics experiment following Procedure B as a white powdery solid (188 mg, 26% yield).

^1H NMR (500 MHz, CDCl_3) δ 8.07 (d, J = 1.4 Hz, 1H), 7.86 (d, J = 8.5 Hz, 2H), 7.65 (d, J = 8.3 Hz, 2H), 7.62 (dd, J = 8.7, 0.9 Hz, 1H), 7.54 – 7.47 (m, 2H), 6.84 (dd, J = 3.4, 0.9 Hz, 1H)

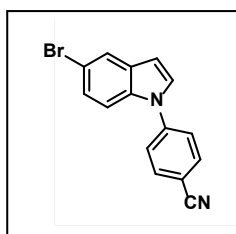
^{13}C NMR (126 MHz, CDCl_3) δ 141.68, 137.16, 129.89, 129.49 (q, J = 33.2 Hz), 129.34, 127.24 (q, J = 3.7 Hz), 126.87, 125.82, 124.57, 123.75 (q, J = 272.2 Hz), 120.22, 111.23, 105.33, 104.23

^{19}F NMR (471 MHz, CDCl_3) δ -62.95

IR (FT-ATR, cm^{-1}) ν_{max} 2219, 1738, 1604, 1527, 1471, 1449, 1377, 1328, 1252, 1216, 1192, 1165, 1098, 1073, 1064, 1017, 887, 843, 795, 764, 725, 687, 622, 595, 526, 494, 483, 416

HRMS (ESI) (m/z) for $[\text{M}+\text{H}]^+$ for $\text{C}_{16}\text{H}_{10}\text{F}_3\text{N}_2$ requires 287.0791, observed 287.0784

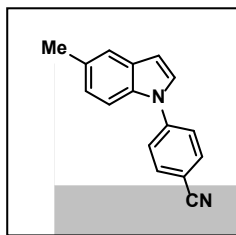
HPLC (C18, water/acetonitrile = 10/90, flow rate = 0.6-0.7 mL/min, λ = 363 nm) t_R = 5.2 min.

**4-(5-bromo-1H-indol-1-yl)benzonitrile²⁵**

Previously reported compound; isolated from a kinetics experiment following Procedure A as a tan powdery solid (233 mg, 31% yield).

^1H NMR (500 MHz, CDCl_3) δ 7.87–7.78 (m, 3H), 7.67–7.56 (m, 2H), 7.46 (d, J = 8.8 Hz, 1H), 7.35 (dd, J = 8.8, 2.5 Hz, 2H), 6.69 (d, J = 3.3 Hz, 1H).

HPLC (C18, water/acetonitrile = 10/90, flow rate = 0.6-0.7 mL/min, λ = 315 nm) t_R = 5.3 min.

**4-(5-methyl-1H-indol-1-yl)benzonitrile**

Isolated from a kinetics experiment following Procedure A as a white powdery solid (76 mg, 13% yield).

^1H NMR (500 MHz, CDCl_3) δ 7.78 (d, J = 8.6 Hz, 2H), 7.60 (d, J = 8.6 Hz, 2H), 7.50 (d, J = 8.5 Hz, 1H), 7.47 (dt, J = 1.7, 0.8 Hz, 1H), 7.29 (d, J = 3.3 Hz, 1H), 7.09 (dd, J = 8.5, 1.7 Hz, 1H), 6.66 (dd, J = 3.3, 0.9 Hz, 1H), 2.47 (s, 3H)

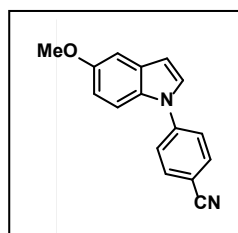
²⁵ Frayne, G. L.; Green, G. M. Investigation of the N-arylation of various substituted indoles using microwave-assisted technology. *Tetrahedron Lett.* **2008**, 49, 7328–7329

^{13}C NMR (126 MHz, CDCl_3) δ 143.75, 133.80, 133.54, 130.86, 130.33, 127.05, 124.78, 123.54, 121.32, 118.54, 110.12, 109.03, 105.42, 21.35

IR (FT-ATR, cm^{-1}) ν_{max} 3135, 3113, 3021, 2916, 2222, 1707, 1602, 1507, 1469, 1376, 1333, 1307, 1296, 1283, 1215, 1179, 1108, 1033, 951, 909, 886, 872, 855, 842, 828, 802, 761, 748, 715, 704, 623, 603, 581, 569, 554, 546, 512, 473, 461, 430

HRMS (ESI) (m/z) for $[\text{M}+\text{H}]^+$ for $\text{C}_{16}\text{H}_{13}\text{N}_2$ requires 233.1074, observed 233.1077

HPLC (C18, water/acetonitrile = 10/90, flow rate = 0.6-0.7 mL/min, λ = 363 nm) t_R = 5.2 min.



4-(5-methoxy-1H-indol-1-yl)benzonitrile²⁵

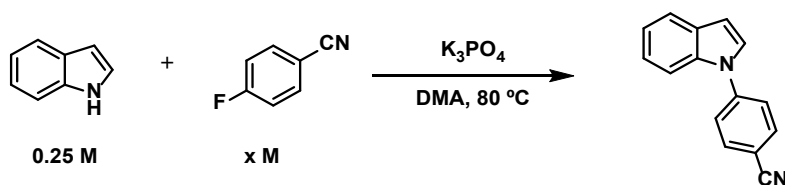
Previously reported compound; isolated from a kinetics experiment following Procedure A as a white solid (25 mg, 4% yield).

^1H NMR (500 MHz, CDCl_3) δ 7.84–7.76 (m, 2H), 7.66–7.59 (m, 2H), 7.55–7.49 (m, 1H), 7.32 (d, J = 3.3 Hz, 1H), 7.14 (d, J = 2.5 Hz, 1H), 6.92 (dd, J = 9.0, 2.5 Hz, 1H), 6.67 (dd, J = 3.4, 0.8 Hz, 1H), 3.88 (s, 3H).

HPLC (C18, water/acetonitrile = 10/90, flow rate = 0.6-0.7 mL/min, λ = 325 nm) t_R = 4.8 min.

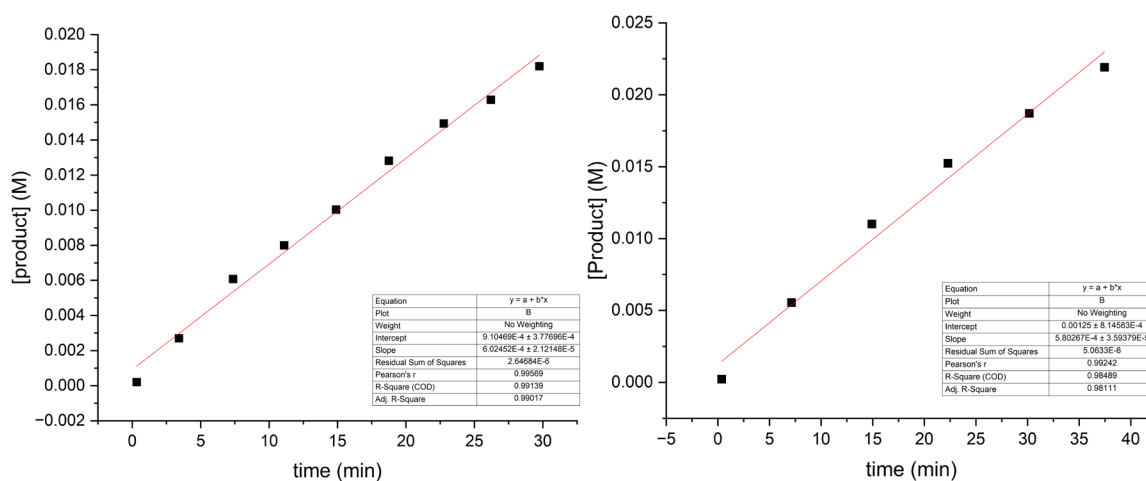
VI. Kinetic Data

A. Experiments varying aryl fluoride concentration (Table S2 Data)



A1. 0.5 M 4-fluorobenzonitrile

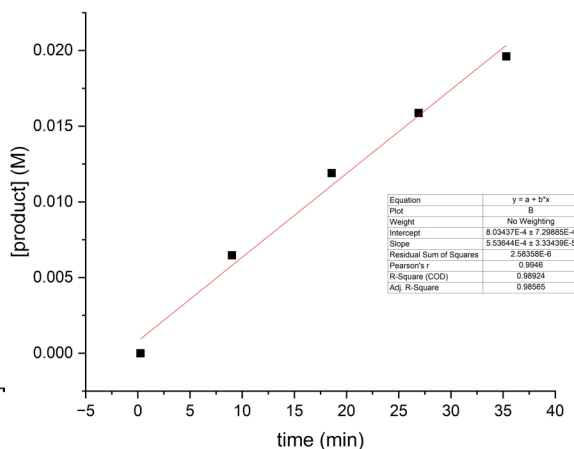
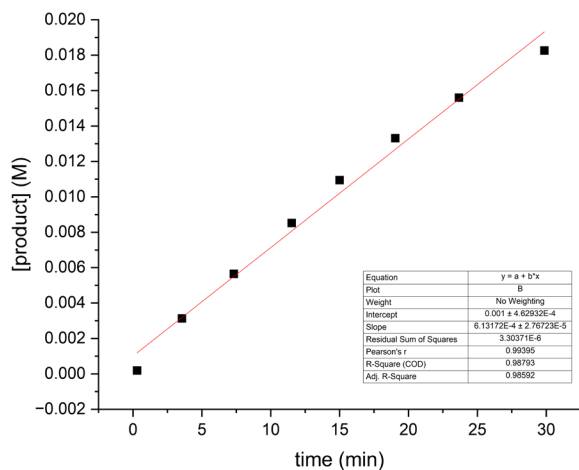
Run 1 and run 2 aliquots diluted to 1 mL



Run 1			Run 2		
time (min)	area (mAU)	[P] (M)	time (min)	area (mAU)	[P] (M)
0.33	13	0.0002	0.37	14	0.0002
3.42	170	0.0027	7.13	349	0.0056
7.37	382	0.0061	14.92	693	0.0110
11.10	503	0.0080	22.28	958	0.0152
14.90	631	0.0100	30.17	1176	0.0187
18.75	806	0.0128	37.45	1378	0.0219
22.77	939	0.0149			
26.20	1024	0.0163			
29.75	1144	0.0182			

A2. 0.25 M 4-fluorobenzonitrile

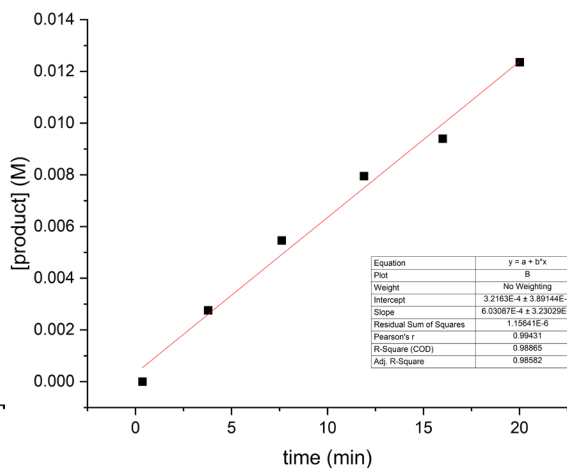
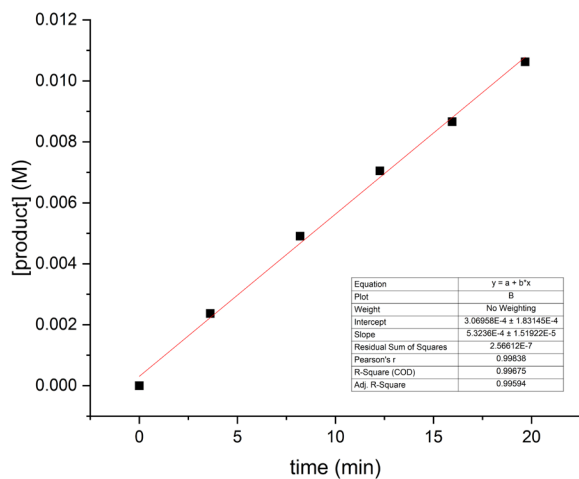
Run 1 and run 2 aliquots diluted to 1 mL



Run 1			Run 2		
time (min)	area (mAU)	[P] (M)	time (min)	area (mAU)	[P] (M)
0.30	12	0.0002	0.25	0	0.0000
3.55	197	0.0031	9.02	407	0.0065
7.32	355	0.0056	18.57	748	0.0119
11.52	536	0.0085	26.90	998	0.0159
15.00	688	0.0109	35.30	1233	0.0196
19.05	837	0.0133			
23.67	981	0.0156			
29.87	1148	0.0183			

A3. 0.1 M 4-fluorobenzonitrile

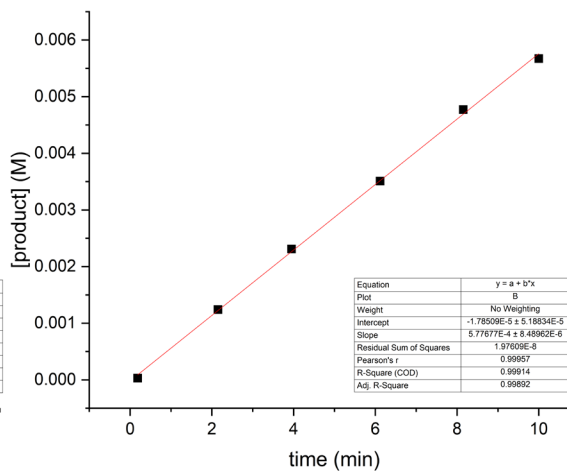
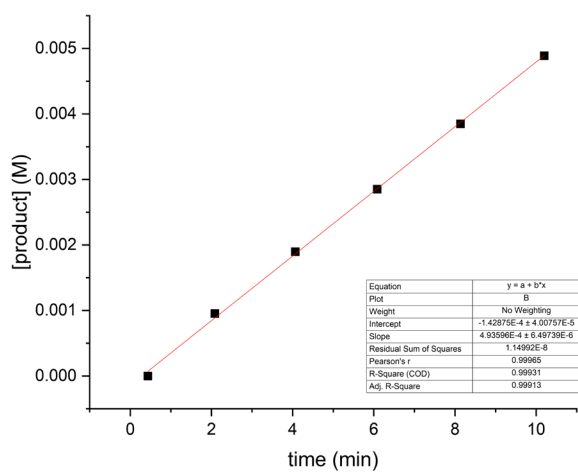
Run 1 and run 2 aliquots diluted to 1 mL



Run 1			Run 2		
time (min)	area (mAU)	[P] (M)	time (min)	area (mAU)	[P] (M)
0.00	0	0.0000	0.37	0	0.0000
3.62	149	0.0024	3.78	260	0.0028
8.20	463	0.0049	7.62	515	0.0055
12.27	665	0.0071	11.90	500	0.0080
15.95	817	0.0087	16.00	886	0.0094
19.67	1002	0.0106	20.02	1165	0.0124

A4. 0.05 M 4-fluorobenzonitrile

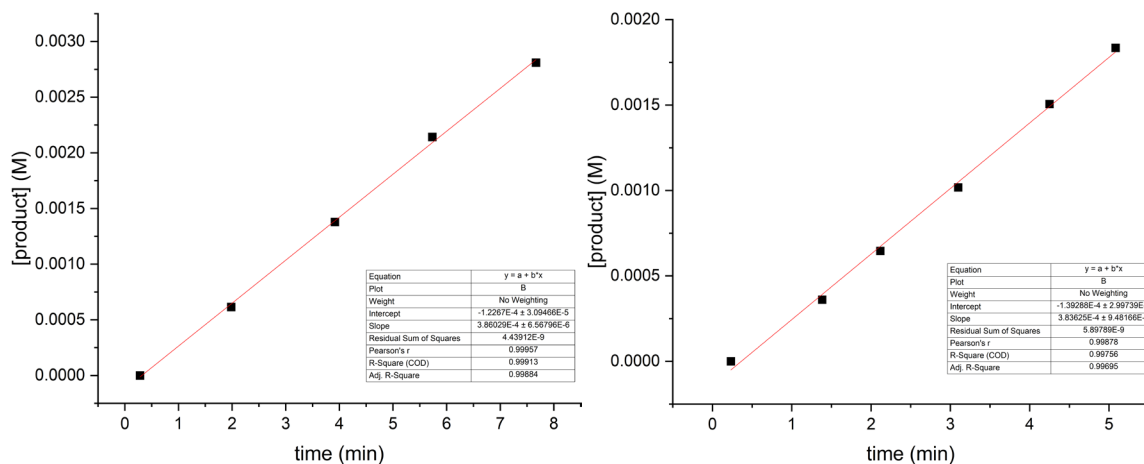
Run 1 and run 2 aliquots diluted to 1 mL



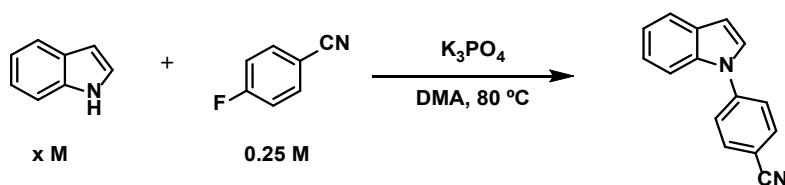
Run 1			Run 2		
time (min)	area (mAU)	[P] (M)	time (min)	area (mAU)	[P] (M)
0.43	0	0.0000	0.18	3	0.0000
2.08	90	0.0010	2.15	117	0.0012
4.07	179	0.0019	3.95	218	0.0023
6.08	269	0.0029	6.12	331	0.0035
8.13	363	0.0038	8.15	450	0.0048
10.20	461	0.0049	10.00	535	0.0057

A5. 0.025 M 4-fluorobenzonitrile

Run 1 and run 2 aliquots diluted to 1 mL



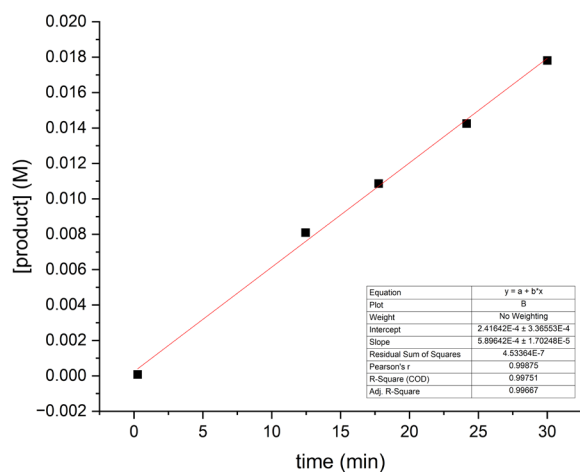
Run 1			Run 2		
time (min)	area (mAU)	[P] (M)	time (min)	area (mAU)	[P] (M)
0.28	0	0.0000	0.23	0	0.0000
1.98	58	0.0006	1.38	34	0.0004
3.92	130	0.0014	2.12	61	0.0006
5.73	202	0.0021	3.10	96	0.0010
7.67	265	0.0028	4.25	142	0.0015
			5.08	173	0.0018

B. Experiments varying indole concentration (Table S3 Data)**B1. 0.25 M indole (see A2 above)**

Run 1 and run 2 aliquots diluted to 1 mL

B2. 0.175 M indole

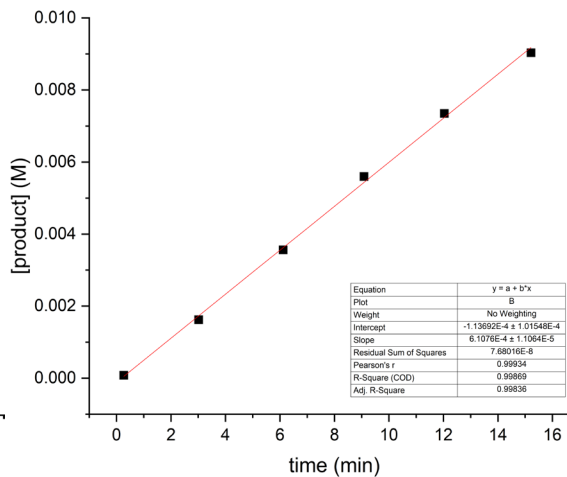
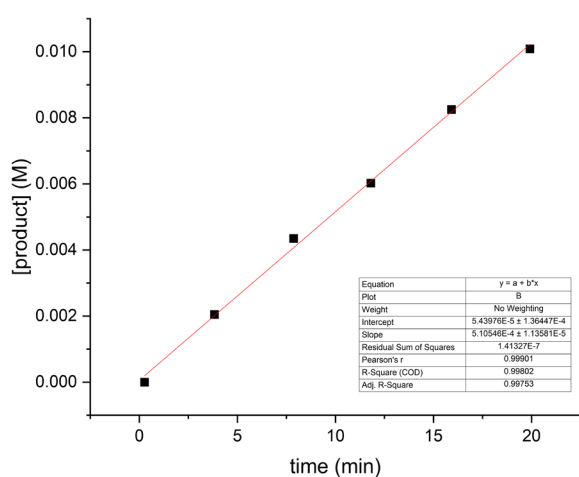
Aliquots diluted to 1 mL



Run 1			Run 2		
time (min)	area (mAU)	[P] (M)	time (min)	area (mAU)	[P] (M)
0.27	5	0.0001	n/a		
12.45	509	0.0081			
17.77	683	0.0109			
24.15	896	0.0143			
30.00	1120	0.0178			

B3. 0.1 M indole

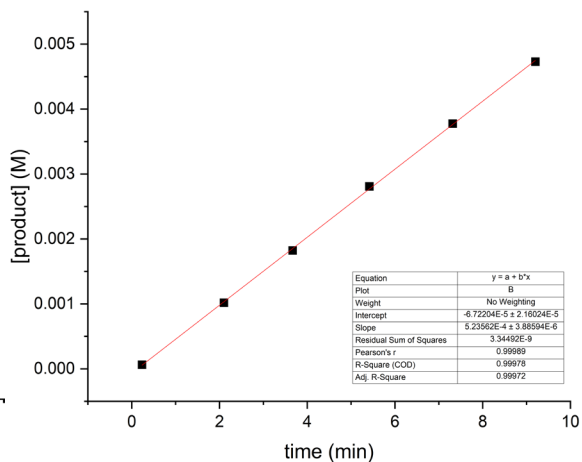
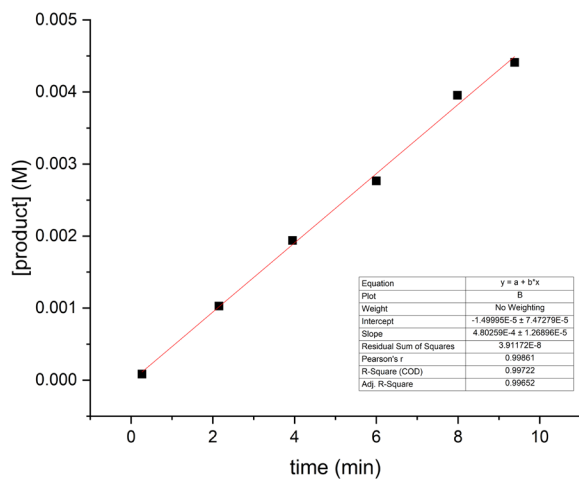
Run 1 and run 2 aliquots diluted to 1 mL



Run 1			Run 2		
time (min)	area (mAU)	[P] (M)	time (min)	area (mAU)	[P] (M)
0.27	0	0.0000	0.27	5	0.0001
3.83	193	0.0020	3.02	102	0.0016
7.87	410	0.0043	6.12	224	0.0036
11.80	568	0.0060	9.08	352	0.0056
15.92	778	0.0083	12.03	462	0.0073
19.92	951	0.0101	15.22	568	0.0090

B4. 0.05 M indole

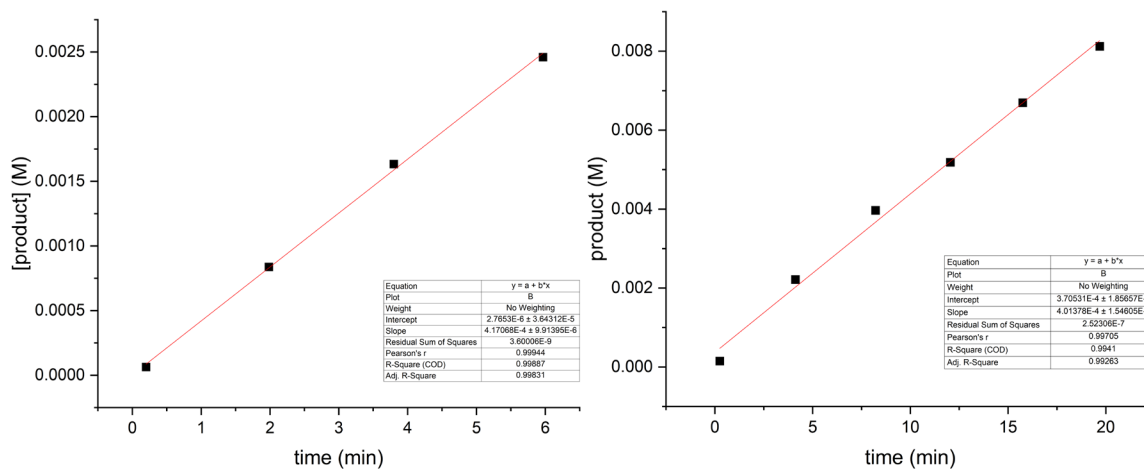
Run 1 and run 2 aliquots diluted to 1 mL



Run 1			Run 2		
time (min)	area (mAU)	[P] (M)	time (min)	area (mAU)	[P] (M)
0.27	8	0.0001	0.23	6	0.0001
2.15	97	0.0010	2.10	96	0.0010
3.95	183	0.0019	3.67	172	0.0018
6.00	261	0.0028	5.42	265	0.0028
7.98	373	0.0040	7.32	356	0.0038
9.38	416	0.0044	9.20	446	0.0047

B5. 0.025 M indole

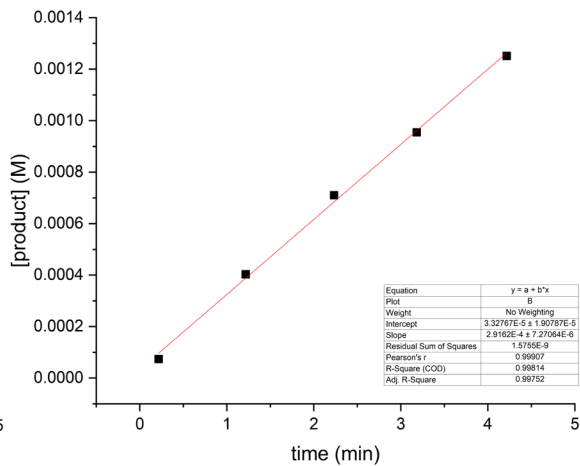
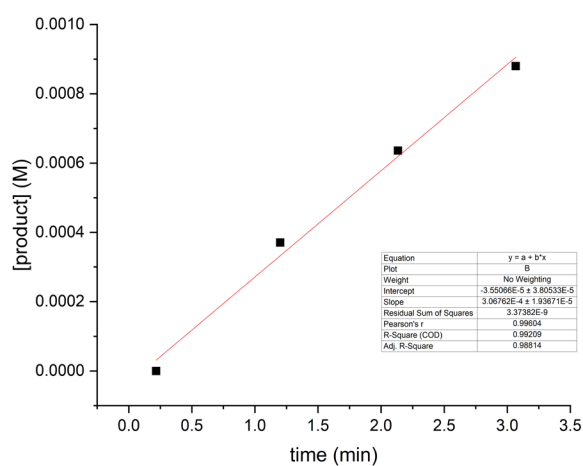
Run 1 and run 2 aliquots diluted to 1 mL



Run 1			Run 2		
time (min)	area (mAU)	[P] (M)	time (min)	area (mAU)	[P] (M)
0.20	6	0.0001	0.25	14	0.0001
1.98	79	0.0008	4.12	209	0.0022
3.80	154	0.0016	8.22	374	0.0040
5.97	232	0.0025	12.05	489	0.0052
			15.75	631	0.0067
			19.68	766	0.0081

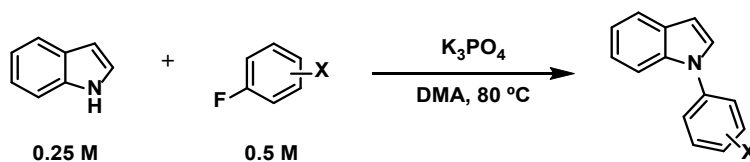
B6. 0.01 M indole

Run 1 and run 2 aliquots diluted to 1 mL



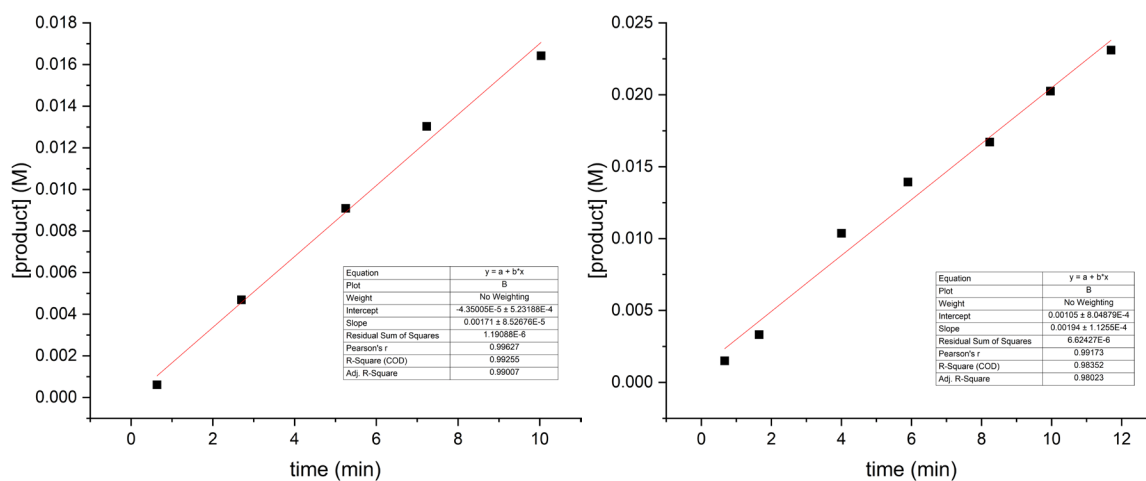
Run 1			Run 2		
time (min)	area (mAU)	[P] (M)	time (min)	area (mAU)	[P] (M)
0.22	0	0.0000	0.22	7	0.0001
1.20	35	0.0004	1.22	38	0.0004
2.13	60	0.0006	2.23	67	0.0007
3.07	83	0.0009	3.18	90	0.0010
			4.22	118	0.0013

C. Experiments for Hammett plot varying aryl fluoride substituent, 0.5 M aryl fluoride (Table S5 Data)



C1. X = -4-NO₂

Run 1 and run 2 aliquots diluted to 1 mL

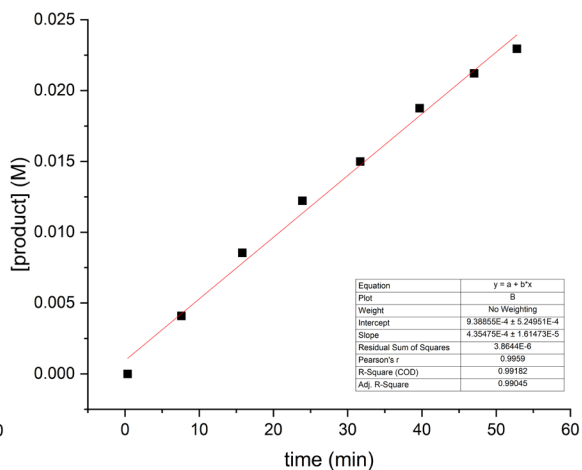
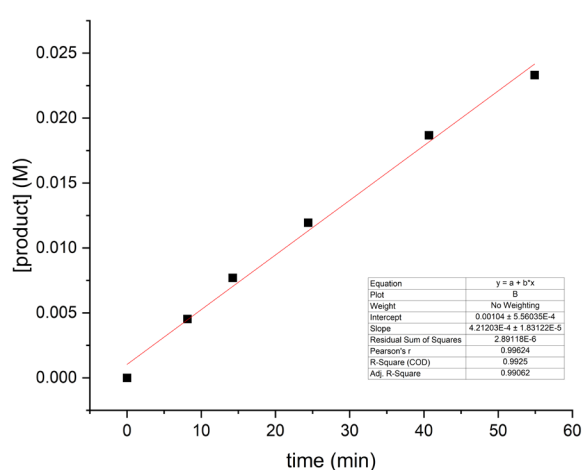


Run 1			Run 2		
time (min)	area (mAU)	[P] (M)	time (min)	area (mAU)	[P] (M)
0.63	25	0.0006	0.67	61	0.0015
2.70	191	0.0047	1.65	135	0.0033
5.25	370	0.0091	4.00	422	0.0104
7.23	530	0.0130	5.90	567	0.0139
10.03	668	0.0164	8.23	680	0.0167
			9.97	824	0.0203
			11.70	940	0.0231

C2. X = -4-CN (see A1 above)

C3. X = -3,5-(Br)₂

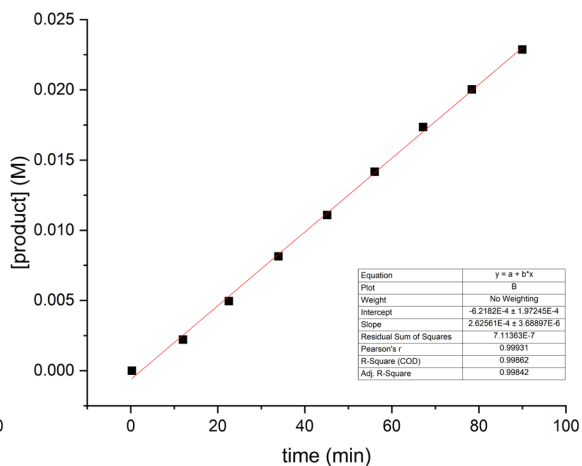
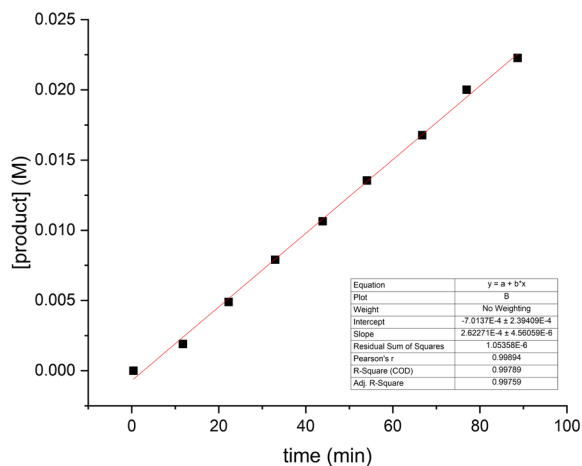
Run 1 and run 2 aliquots diluted to 1 mL



Run 1			Run 2		
time (min)	area (mAU)	[P] (M)	time (min)	area (mAU)	[P] (M)
0.00	0	0.0000	0.35	0	0.0000
8.13	175	0.0045	7.58	158	0.0041
14.23	297	0.0077	15.80	330	0.0085
24.40	461	0.0119	23.90	472	0.0122
40.67	721	0.0187	31.68	579	0.0150
54.90	900	0.0233	39.68	724	0.0188
			47.03	819	0.0212
			52.78	886	0.0230

C4. X = -3- CF₃-4-Br

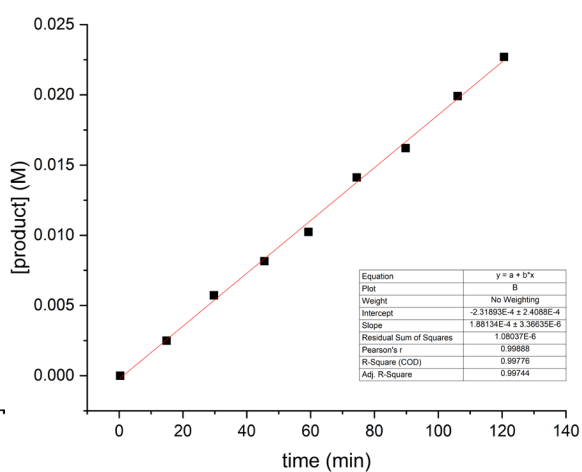
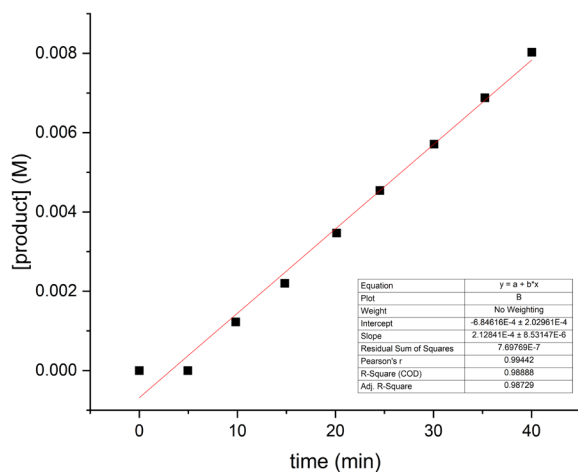
Run 1 and run 2 aliquots diluted to 1 mL



Run 1			Run 2		
time (min)	area (mAU)	[P] (M)	time (min)	area (mAU)	[P] (M)
0.37	0	0.0000	0.25	0	0.0000
11.77	86	0.0019	12.02	100	0.0022
22.27	221	0.0049	22.53	224	0.0050
32.95	357	0.0079	33.93	368	0.0081
43.85	481	0.0106	45.13	501	0.0111
54.03	612	0.0136	56.03	640	0.0142
66.75	758	0.0168	67.17	784	0.0174
76.93	723	0.0200	78.37	905	0.0200
88.68	1006	0.0223	89.98	1033	0.0229

C5. X = -4-CF₃

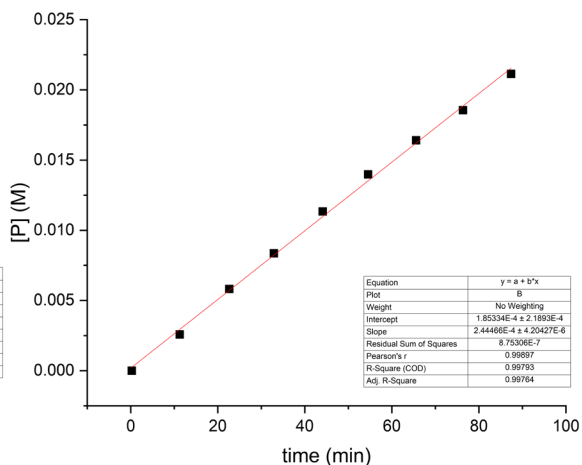
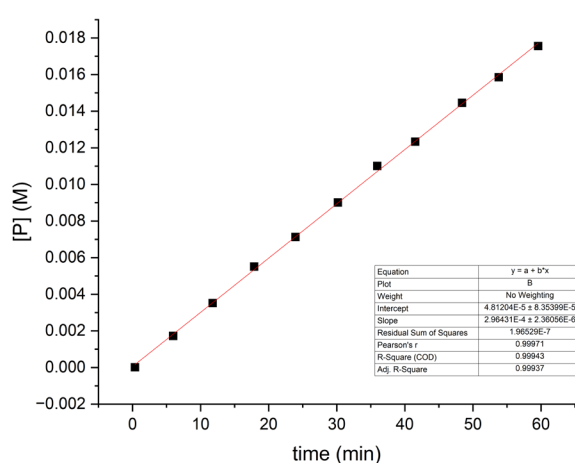
Run 1 and run 2 aliquots diluted to 1 mL



Run 1			Run 2		
time (min)	area (mAU)	[P] (M)	time (min)	area (mAU)	[P] (M)
0.40	0	0.0000	0.32	0	0.0000
4.95	0	0.0000	14.83	128	0.0025
9.83	63	0.0012	29.68	294	0.0057
14.83	113	0.0022	45.52	419	0.0082
20.12	178	0.0035	59.32	526	0.0103
24.53	233	0.0045	74.43	725	0.0141
30.05	293	0.0057	89.75	832	0.0162
35.23	353	0.0069	106.07	1022	0.0199
40.02	412	0.0080	120.60	1165	0.0227

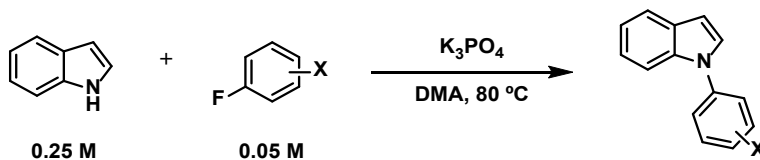
C5. X = -4-COMe

Run 1 and run 2 aliquots diluted to 1 mL



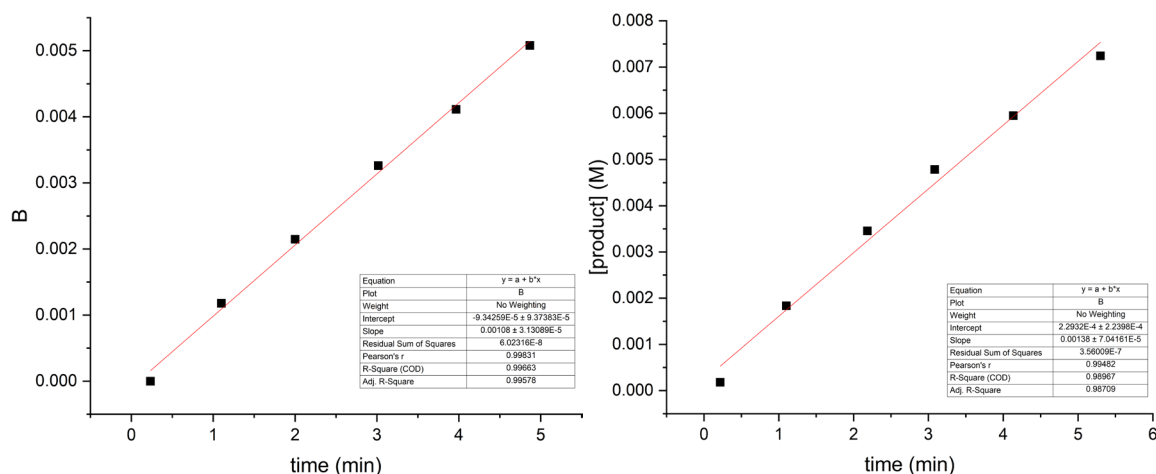
Run 1			Run 2		
time (min)	area (mAU)	[P] (M)	time (min)	area (mAU)	[P] (M)
0.37	1	0.0000	0.22	0	0.0000
5.97	96	0.0017	11.25	144	0.0026
11.78	196	0.0035	22.63	324	0.0058
17.87	307	0.0055	32.88	466	0.0084
23.93	397	0.0071	44.12	632	0.0113
30.17	502	0.0090	54.53	779	0.0140
35.93	613	0.0110	65.57	914	0.0164
41.52	687	0.0123	76.35	1033	0.0186
48.40	805	0.0145	87.38	1177	0.0211
53.78	883	0.0159			
59.58	978	0.0176			

D. Experiments for Hammett plot varying aryl fluoride substituent, 0.05 M aryl fluoride (Table S6 Data)

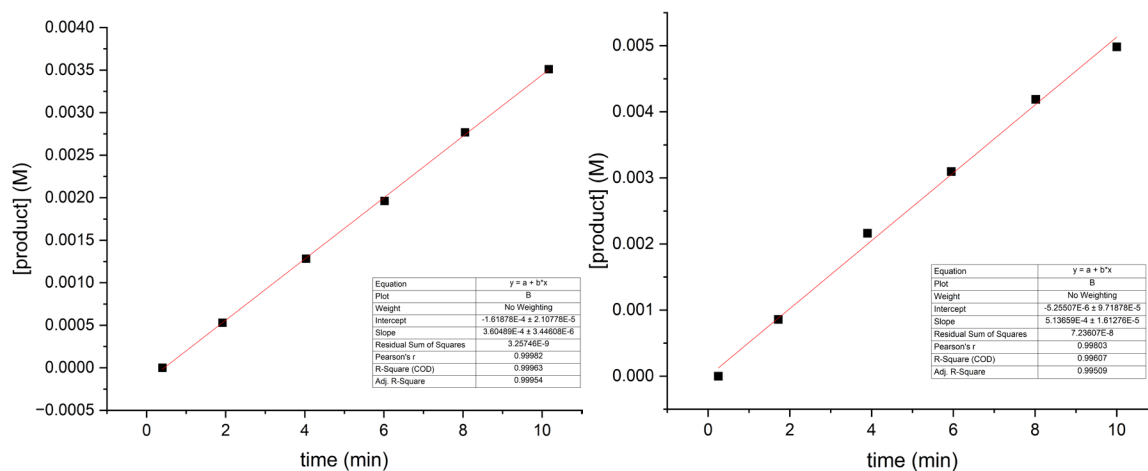


D1. X = -4-NO₂

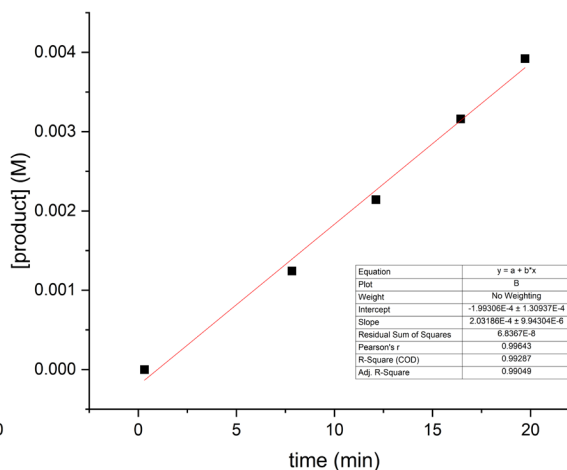
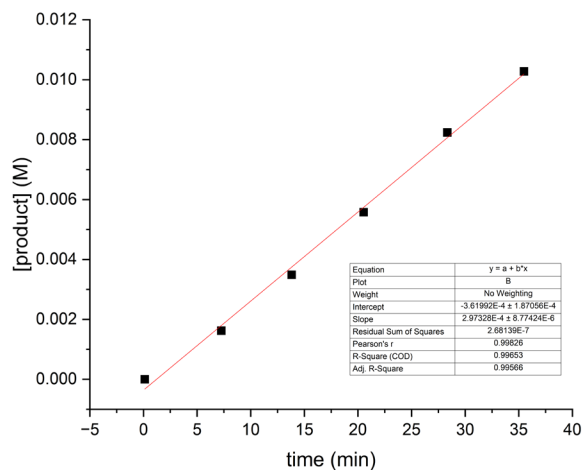
Run 1 and run 2 aliquots diluted to 1 mL, 75 μL aliquots



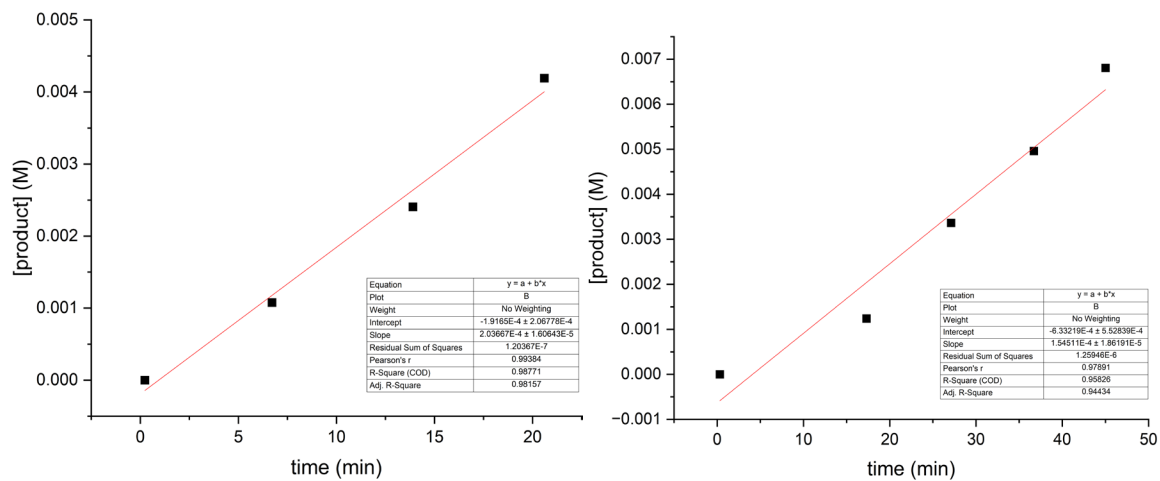
Run 1			Run 2		
time (min)	area (mAU)	[P] (M)	time (min)	area (mAU)	[P] (M)
0.23	0	0.0000	0.22	11	0.0002
1.10	72	0.0012	1.10	112	0.0018
2.00	131	0.0021	2.18	211	0.0035
3.02	199	0.0033	3.08	292	0.0048
3.97	251	0.0041	4.13	363	0.0059
4.87	310	0.0051	5.30	442	0.0072

D2. X = -4-CNRun 1 and run 2 aliquots diluted to 1 mL, 75 μ L aliquots

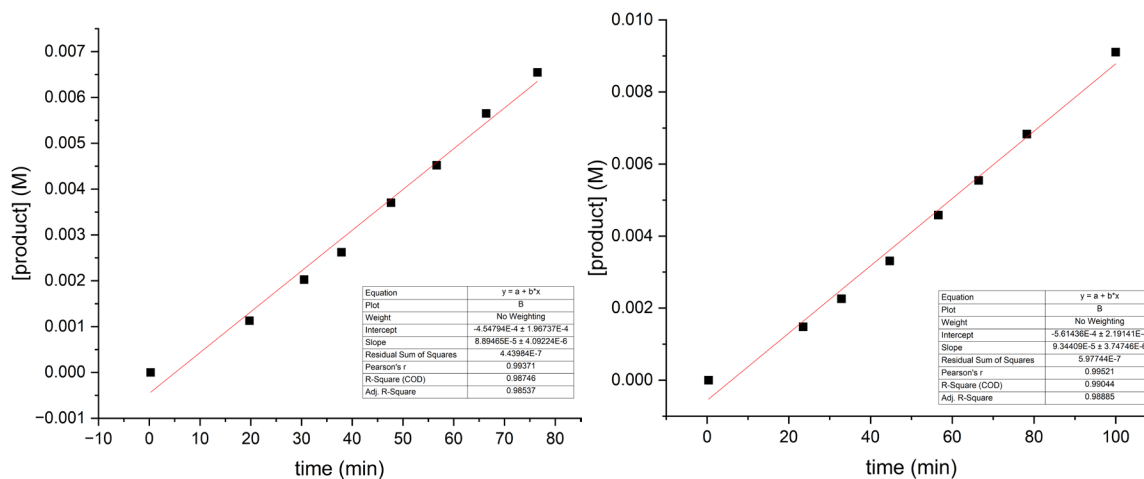
Run 1			Run 2		
time (min)	area (mAU)	[P] (M)	time (min)	area (mAU)	[P] (M)
0.40	0	0.0000	0.25	0	0.0000
1.92	50	0.0005	1.72	81	0.0009
4.03	121	0.0013	3.90	204	0.0022
6.02	185	0.0020	5.95	292	0.0031
8.05	261	0.0028	8.02	395	0.0042
10.17	331	0.0035	10.00	470	0.0050

D3. X = -3,5-(Br)₂Run 1 and run 2 aliquots diluted to 1 mL, 75 μ L aliquots

Run 1			Run 2		
time (min)	area (mAU)	[P] (M)	time (min)	area (mAU)	[P] (M)
0.12	0	0.0000	0.32	0	0.0000
7.25	94	0.0016	7.83	72	0.0012
13.82	202	0.0035	12.12	124	0.0021
20.53	323	0.0056	16.43	183	0.0032
28.33	477	0.0082	19.72	227	0.0039
35.48	595	0.0103			

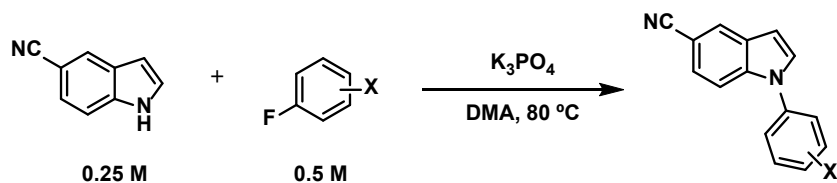
D4. X = -3- CF₃-4-BrRun 1 and run 2 aliquots diluted to 1 mL, 75 μ L aliquots

Run 1			Run 2		
time (min)	area (mAU)	[P] (M)	time (min)	area (mAU)	[P] (M)
0.23	0	0.0000	0.30	0	0.0000
6.72	73	0.0011	17.30	56	0.0012
13.90	163	0.0024	27.12	228	0.0034
20.60	284	0.0042	36.70	336	0.0050
			45.02	461	0.0068

D5. X = -4-CF₃Run 1 and run 2 aliquots diluted to 1 mL, 75 μ L aliquots

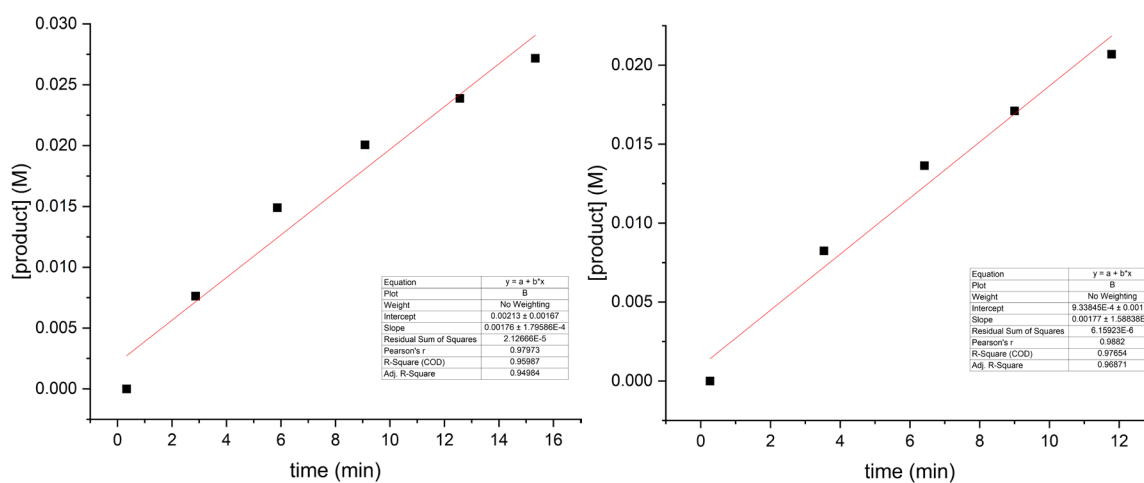
Run 1			Run 2		
time (min)	area (mAU)	[P] (M)	time (min)	area (mAU)	[P] (M)
0.25	0	0.0000	0.37	0	0.0000
19.73	87	0.0011	23.48	114	0.0015
30.50	156	0.0020	32.88	174	0.0023
37.88	202	0.0026	44.68	255	0.0033
47.63	285	0.0037	56.57	353	0.0046
56.63	348	0.0045	66.43	427	0.0055
66.38	435	0.0057	78.23	526	0.0068
76.50	504	0.0065	99.97	701	0.0091

E. Experiments for Hammett plot varying aryl fluoride substituent, using 5-cyanoindole (Table S7 Data).

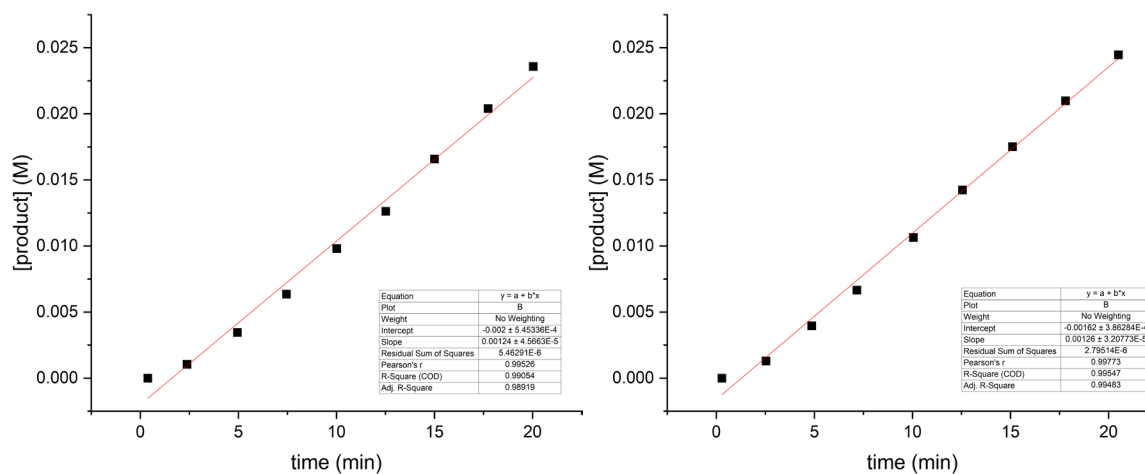


E1. X = -4-CN

Run 1 and run 2 aliquots diluted to 1 mL

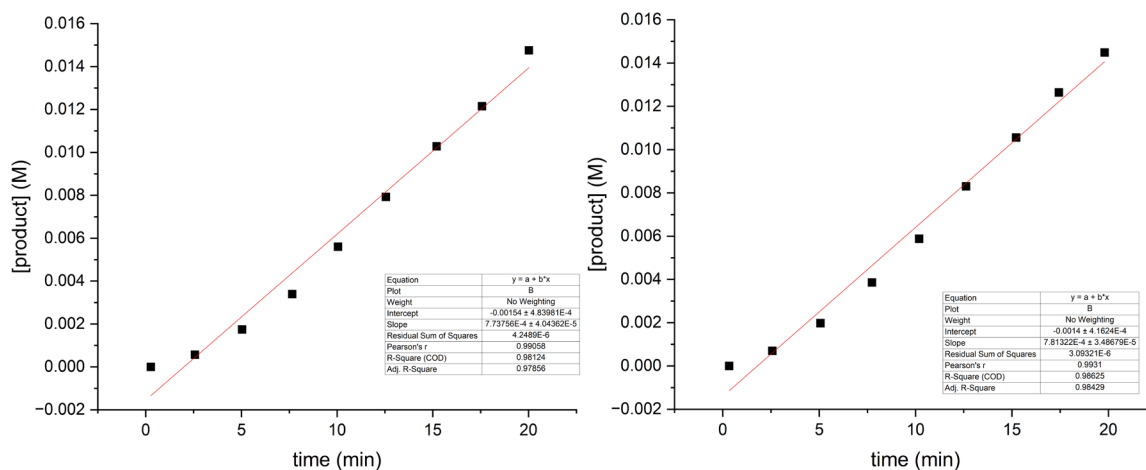


Run 1			Run 2		
time (min)	area (mAU)	[P] (M)	time (min)	area (mAU)	[P] (M)
0.33	0	0.0000	0.27	0	0.0000
2.87	591	0.0076	3.53	639	0.0082
5.87	1155	0.0149	6.42	1057	0.0136
9.08	1555	0.0201	9.00	1326	0.0171
12.57	1851	0.0239	11.78	1604	0.0207
15.33	2106	0.0272			

E2. X = -3,5-(Br)₂

Run 1 and run 2 aliquots diluted to 1 mL

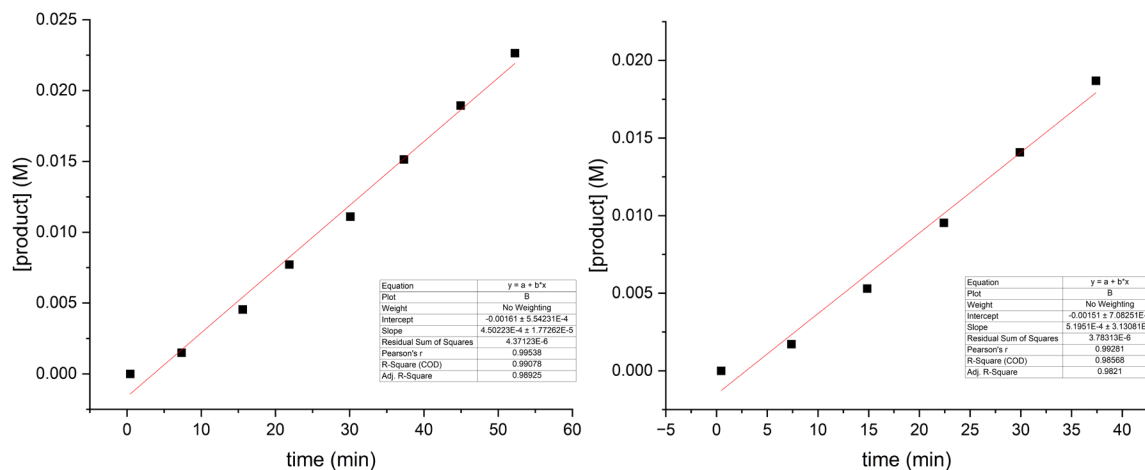
Run 1			Run 2		
time (min)	area (mAU)	[P] (M)	time (min)	area (mAU)	[P] (M)
0.38	0	0.0000	0.28	0	0.0000
2.38	88	0.0010	2.53	109	0.0013
4.95	290	0.0035	4.87	332	0.0040
7.45	533	0.0064	7.17	559	0.0067
10.02	822	0.0098	10.05	893	0.0106
12.52	1059	0.0126	12.55	1194	0.0142
15.00	1391	0.0166	15.10	1469	0.0175
17.73	1711	0.0204	17.80	1760	0.0210
20.03	1978	0.0236	20.50	2052	0.0245

E3. X = -3-CF₃-4-BrRun 1 and run 2 aliquots diluted to 1 mL, Run 1 aliquots = 75 μ L

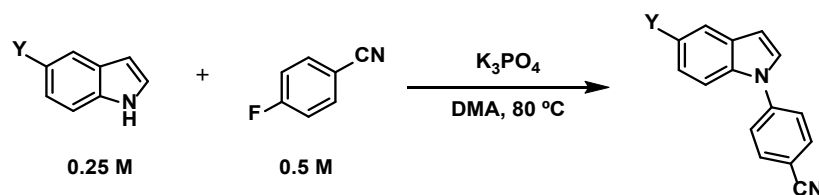
Run 1			Run 2		
time (min)	area (mAU)	[P] (M)	time (min)	area (mAU)	[P] (M)
0.27	0	0.0000	0.33	0	0.0000
2.57	57	0.0006	2.57	47	0.0007
5.03	176	0.0017	5.07	133	0.0020
7.65	342	0.0034	7.73	259	0.0039
10.05	565	0.0056	10.18	395	0.0059
12.55	799	0.0079	12.62	558	0.0083
15.20	1036	0.0103	15.22	709	0.0106
17.57	1224	0.0122	17.43	849	0.0126
20.02	991	0.0148	19.80	973	0.0145

E4. X = -4-CF₃

Run 1 and run 2 aliquots diluted to 1 mL

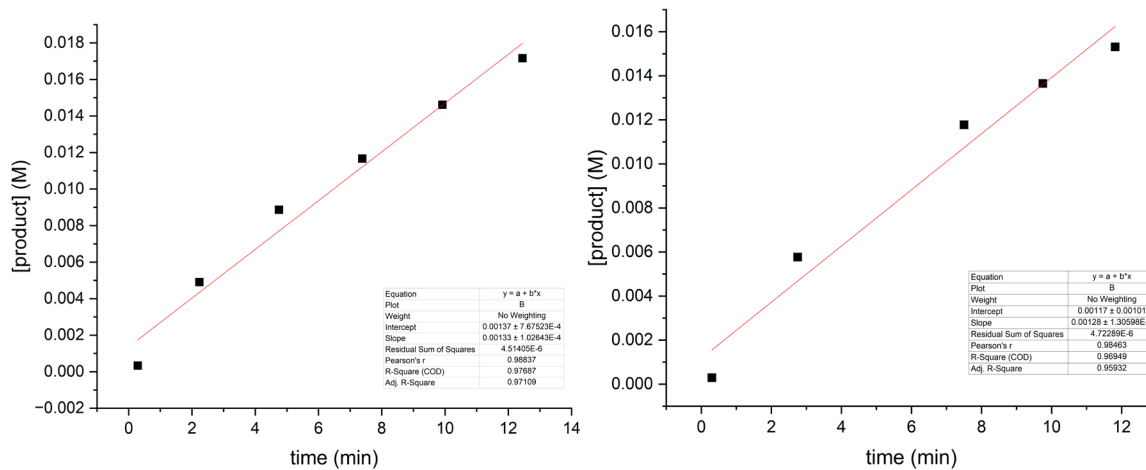


Run 1			Run 2		
time (min)	area (mAU)	[P] (M)	time (min)	area (mAU)	[P] (M)
0.43	0	0.0000	0.37	0	0.0000
7.35	115	0.0015	6.92	109	0.0014
15.58	350	0.0045	16.72	286	0.0037
21.87	594	0.0077	24.07	426	0.0055
30.08	855	0.0111	29.83	556	0.0072
37.30	1165	0.0151	37.37	809	0.0105
44.93	1458	0.0189	45.88	1109	0.0144
52.25	1743	0.0226	52.93	1413	0.0184
61.00	1929	0.0251	59.87	1650	0.0214

F. Experiments for Hammett plot varying indole substituent, using 4-fluorobenzonitrile (Table S8 Data).**F1. Y = -4-CN (see E1 above)**

F2. Y = -4-Br

Run 1 and run 2 aliquots diluted to 1 mL

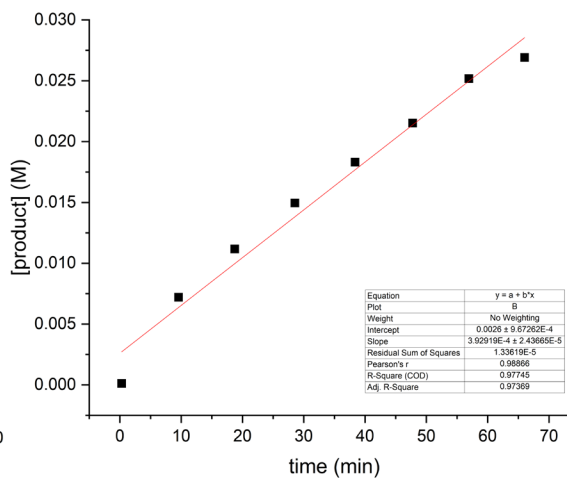
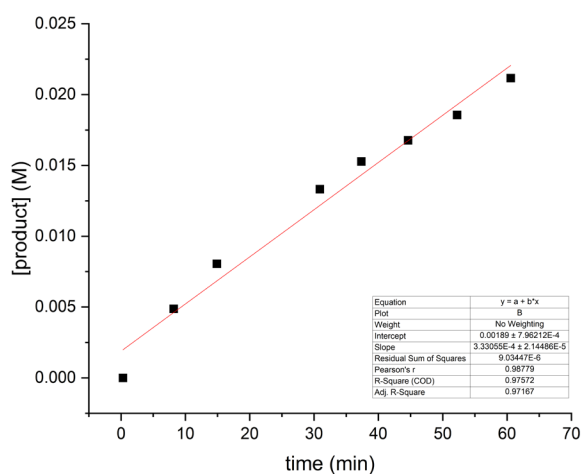


Run 1			Run 2		
time (min)	area (mAU)	[P] (M)	time (min)	area (mAU)	[P] (M)
0.28	16	0.0003	0.30	14	0.0003
2.23	233	0.0049	2.75	274	0.0058
4.75	421	0.0089	7.50	559	0.0118
7.38	554	0.0117	9.75	648	0.0137
9.92	694	0.0146	11.82	727	0.0153
12.45	815	0.0172			

F3. Y = -H (see A1 above)

F4. Y = -4-Me

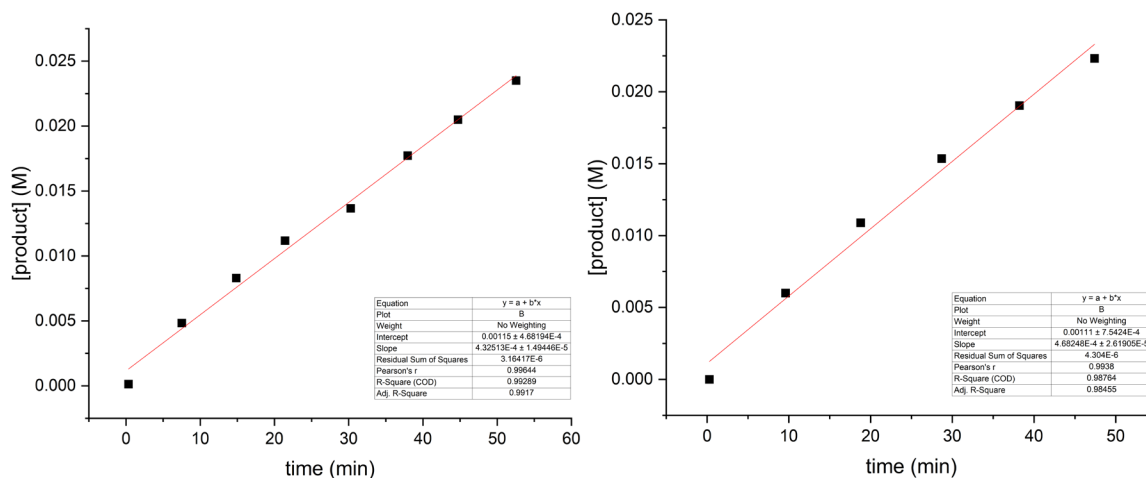
Run 1 and run 2 aliquots diluted to 1 mL



Run 1			Run 2		
time (min)	area (mAU)	[P] (M)	time (min)	area (mAU)	[P] (M)
0.30	0	0.0000	0.28	6	0.0001
8.18	245	0.0049	9.57	362	0.0072
14.88	405	0.0081	18.73	562	0.0112
30.90	670	0.0133	28.53	752	0.0150
37.35	768	0.0153	38.37	921	0.0183
44.60	843	0.0168	47.75	1082	0.0215
52.23	933	0.0186	56.92	1266	0.0252
60.57	1064	0.0212	66.02	1353	0.0269

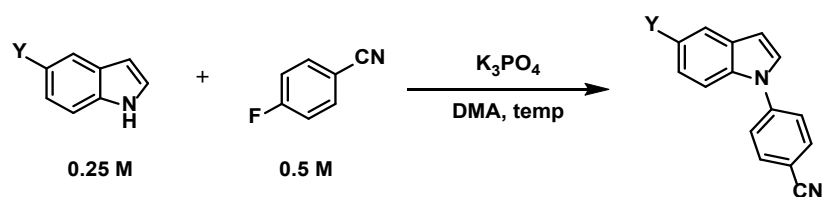
F5. Y = -4-OMe

Run 1 and run 2 aliquots diluted to 1 mL

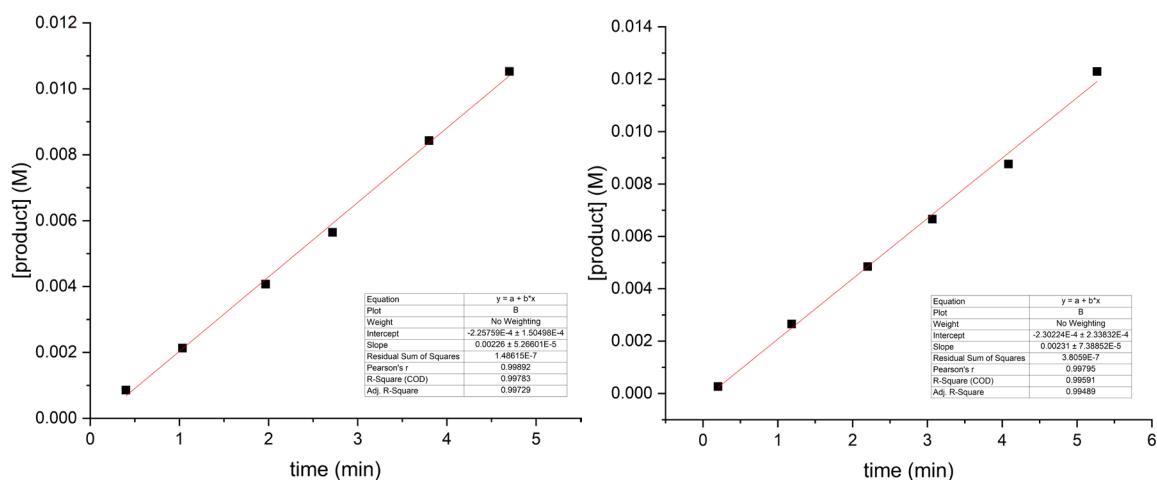


Run 1			Run 2*		
time (min)	area (mAU)	[P] (M)	time (min)	area (mAU)	[P] (M)
0.33	6	0.0001	0.28	0	0.0000
7.52	220	0.0048	9.60	273	0.0060
14.85	378	0.0083	18.78	744	0.0109
21.42	509	0.0112	28.70	699	0.0154
30.27	622	0.0137	38.22	867	0.0190
37.93	807	0.0177	47.40	1016	0.0223
44.72	933	0.0205			
52.55	1070	0.0235			

*data points 1 and 3 used 0.075 mL aliquot

G. Experiments for Eyring plot (Table S10 Data).**G1. T = 100 °C**

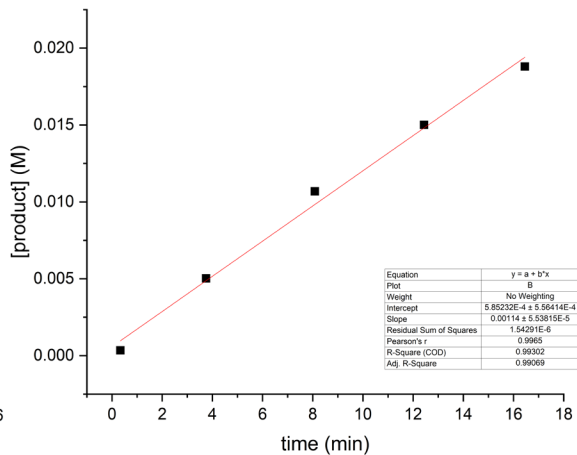
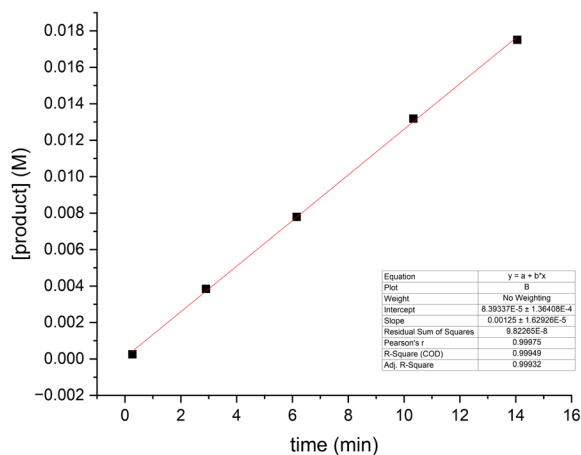
Run 1 and run 2 aliquots diluted to 1 mL



Run 1			Run 2		
time (min)	area (mAU)	[P] (M)	time (min)	area (mAU)	[P] (M)
0.40	54	0.0009	0.20	17	0.0003
1.03	134	0.0021	1.18	167	0.0027
1.97	256	0.0041	2.20	305	0.0049
2.72	355	0.0056	3.07	419	0.0067
3.80	530	0.0084	4.08	551	0.0088
4.70	662	0.0105	5.27	773	0.0123

G2. T = 90 °C

Run 1 and run 2 aliquots diluted to 1 mL

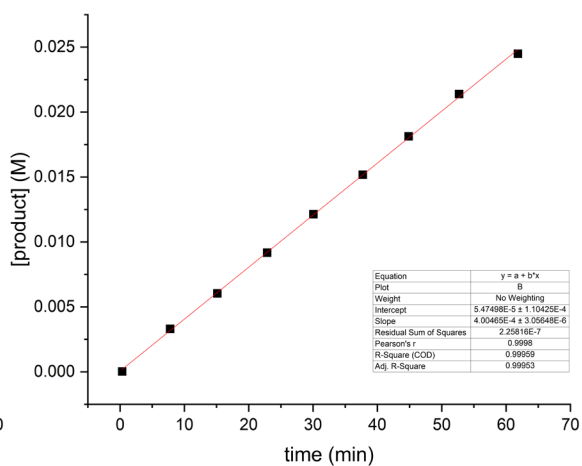
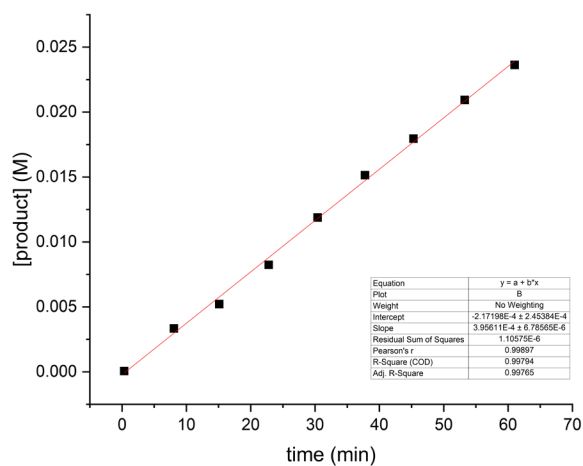


Run 1			Run 2		
time (min)	area (mAU)	[P] (M)	time (min)	area (mAU)	[P] (M)
0.27	16	0.0003	0.33	22	0.0003
2.90	242	0.0038	3.75	316	0.0050
6.15	490	0.0078	8.08	672	0.0107
10.33	829	0.0132	12.43	944	0.0150
14.05	1101	0.0175	16.45	1182	0.0188

G3. T = 80 °C (see A1 above)

G4. T = 70 °C

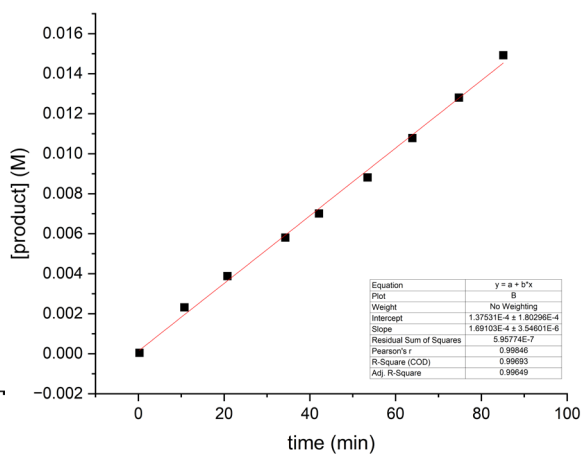
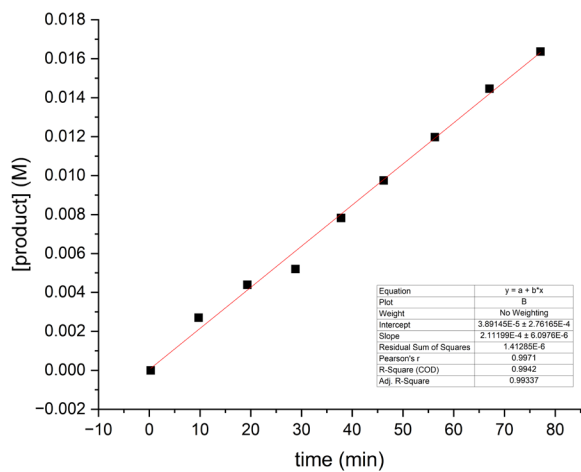
Run 1 and run 2 aliquots diluted to 1 mL



Run 1			Run 2		
time (min)	area (mAU)	[P] (M)	time (min)	area (mAU)	[P] (M)
0.33	4	0.0001	0.33	2	0.0000
8.05	210	0.0033	7.78	208	0.0033
15.10	328	0.0052	15.12	380	0.0060
22.78	518	0.0082	22.85	577	0.0092
30.38	747	0.0119	30.05	763	0.0121
37.75	952	0.0151	37.72	954	0.0152
45.28	1129	0.0180	44.85	1140	0.0181
53.25	1316	0.0209	52.68	1345	0.0214
61.02	1486	0.0236	61.83	1540	0.0245

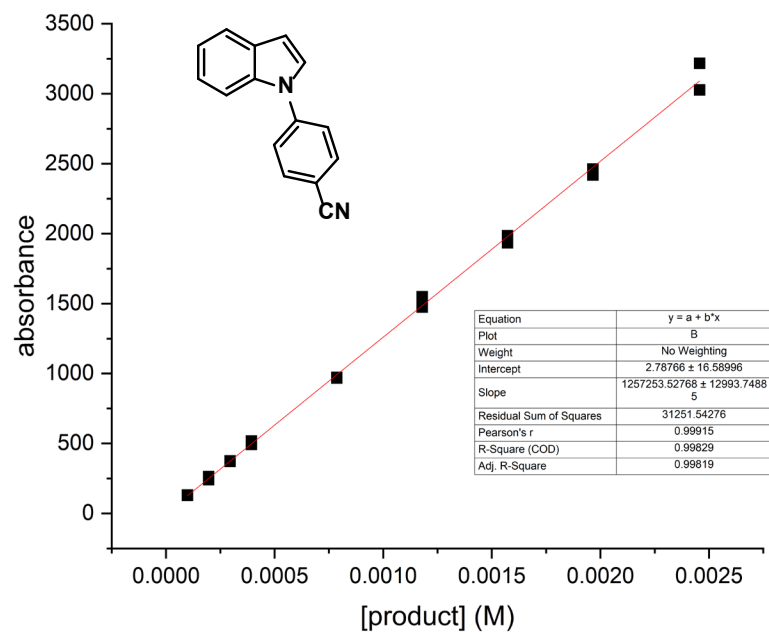
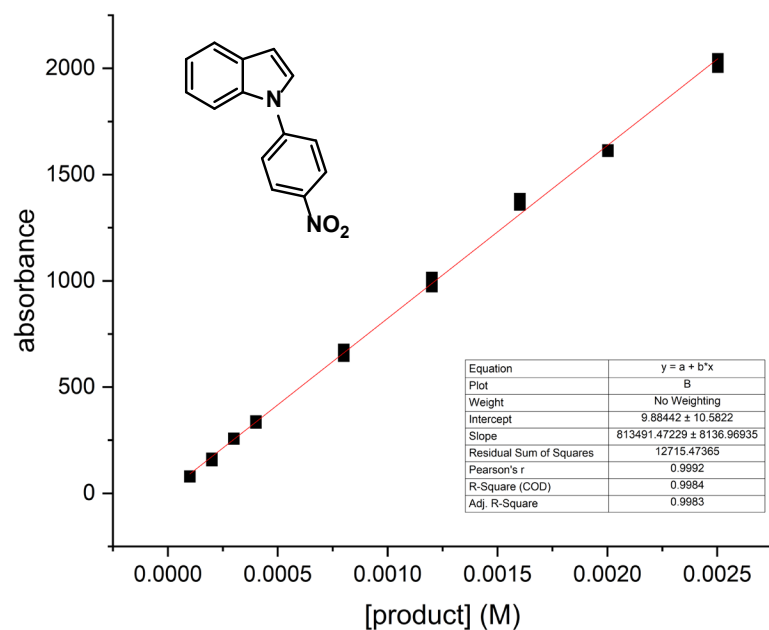
G5. T = 60 °C

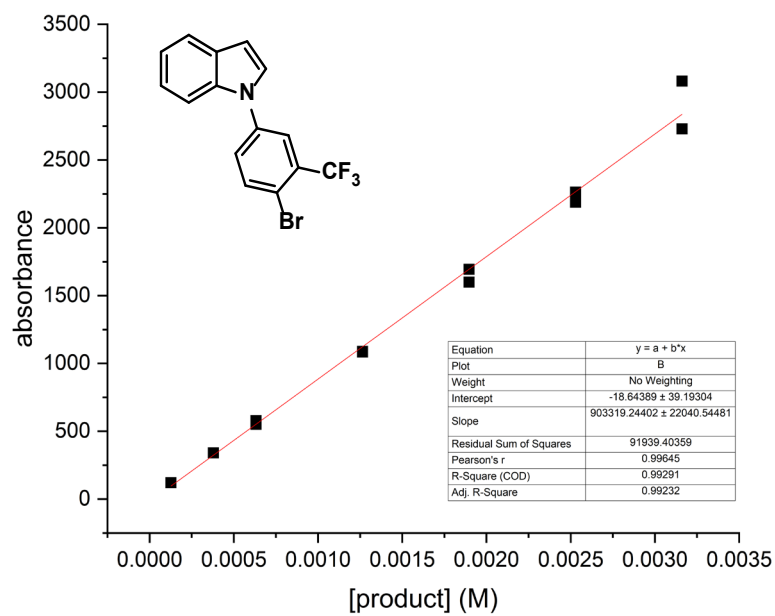
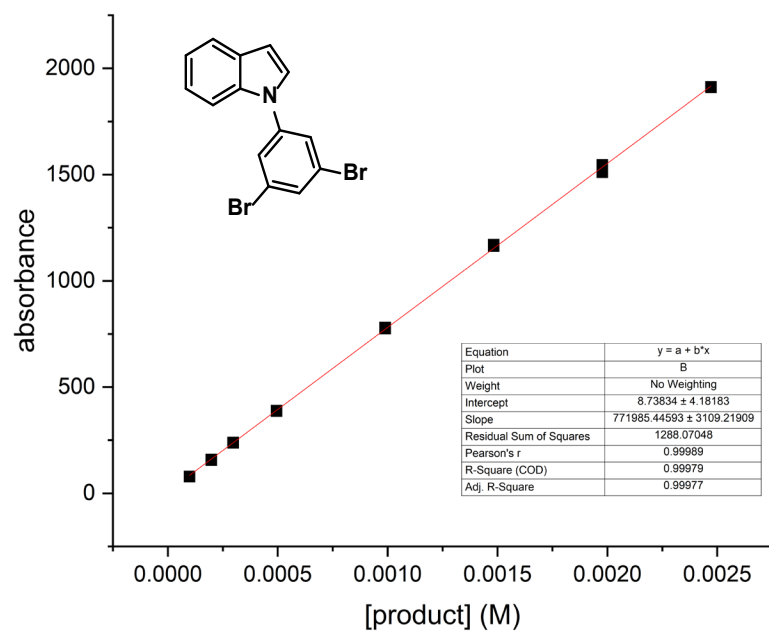
Run 1 and run 2 aliquots diluted to 1 mL

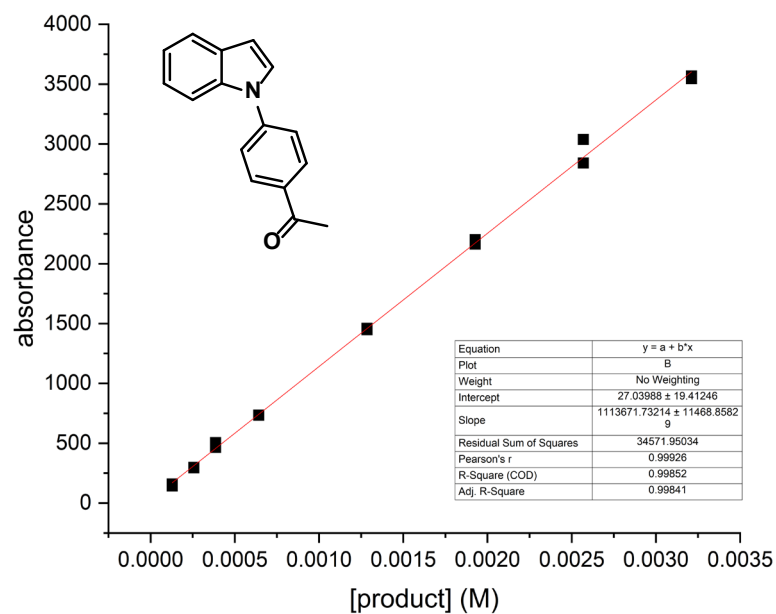
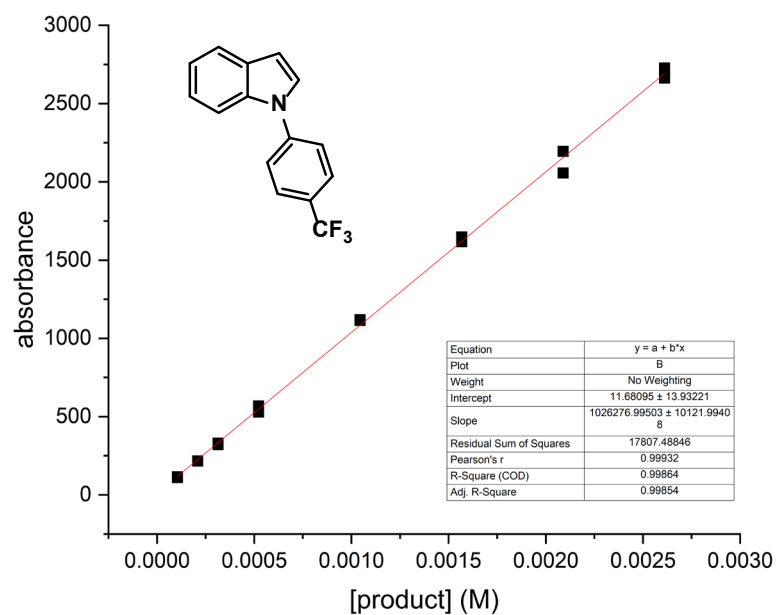


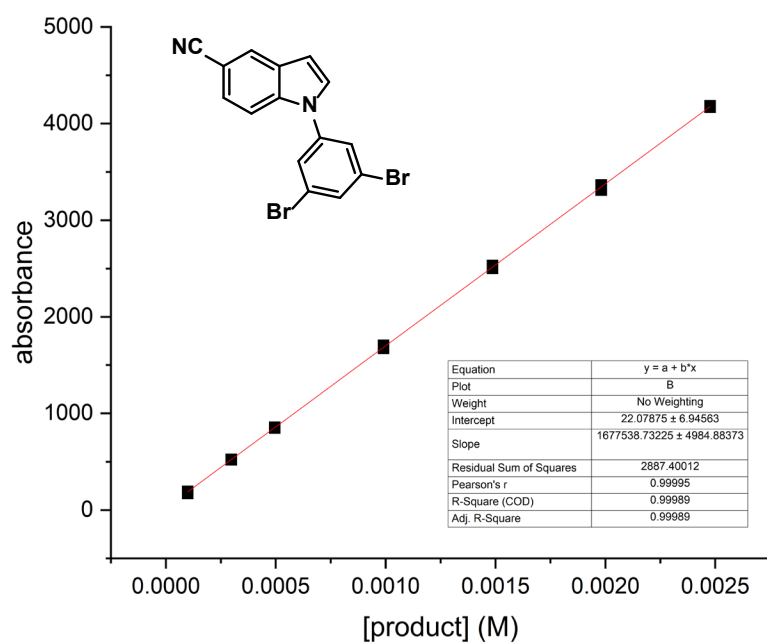
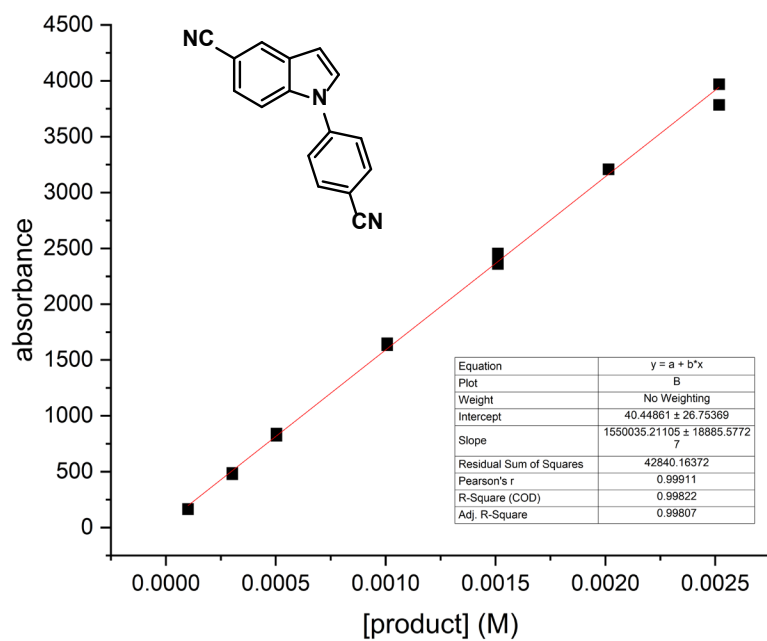
Run 1			Run 2		
time (min)	area (mAU)	[P] (M)	time (min)	area (mAU)	[P] (M)
0.28	0	0.0000	0.25	3	0.0000
9.72	170	0.0027	10.73	146	0.0023
19.32	276	0.0044	20.75	244	0.0039
28.78	327	0.0052	34.25	365	0.0058
37.78	492	0.0078	42.13	441	0.0070
46.20	613	0.0098	53.45	554	0.0088
56.28	753	0.0120	63.90	678	0.0108
67.03	909	0.0145	74.75	805	0.0128
77.08	1029	0.0164	85.12	938	0.0149

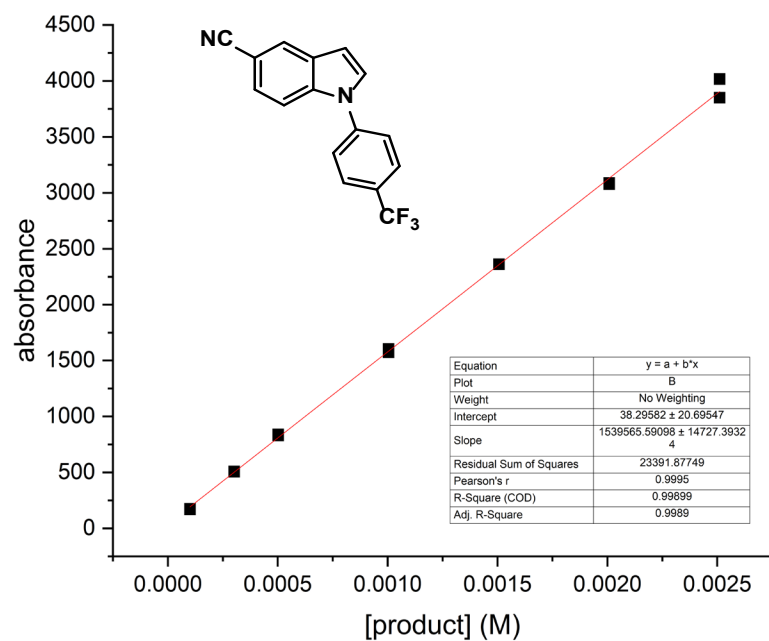
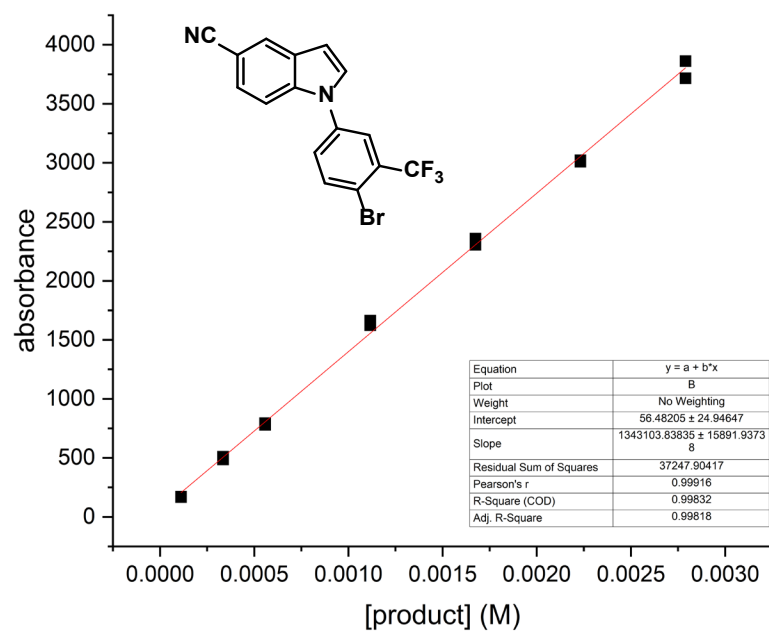
H. Plots for Determination of Response Factors

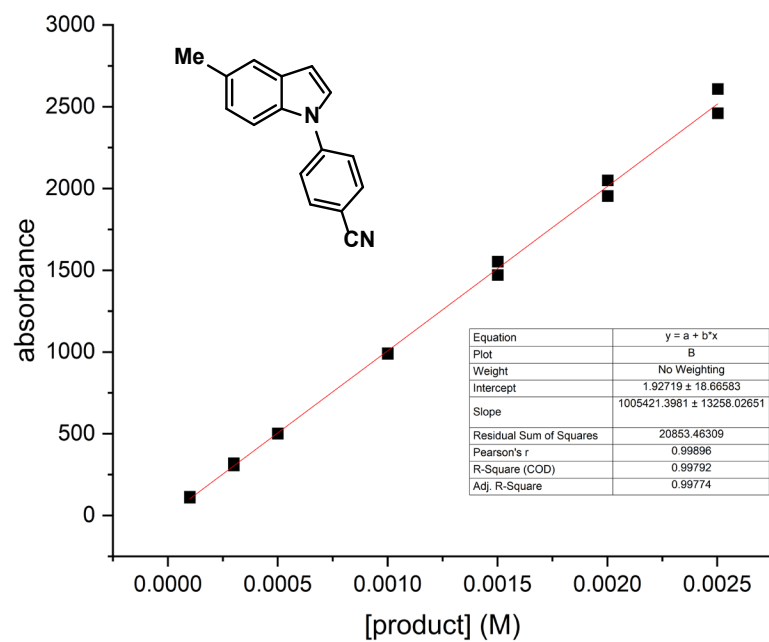
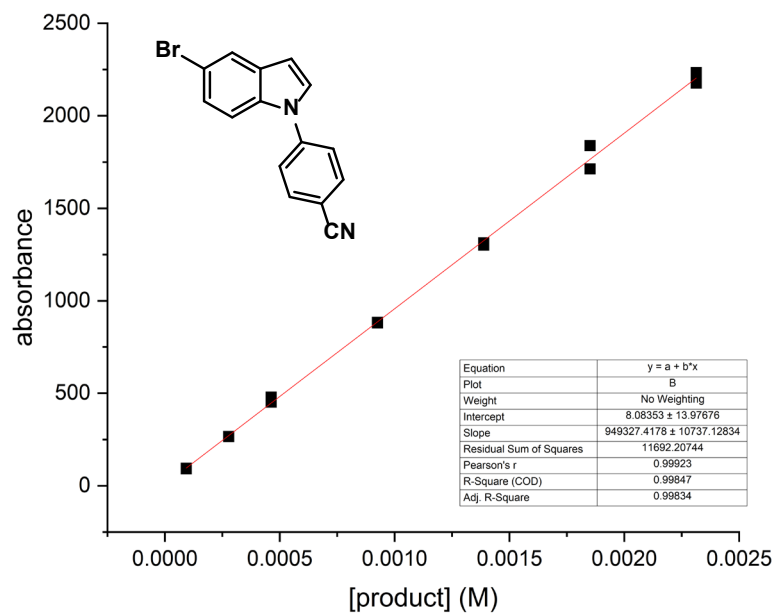


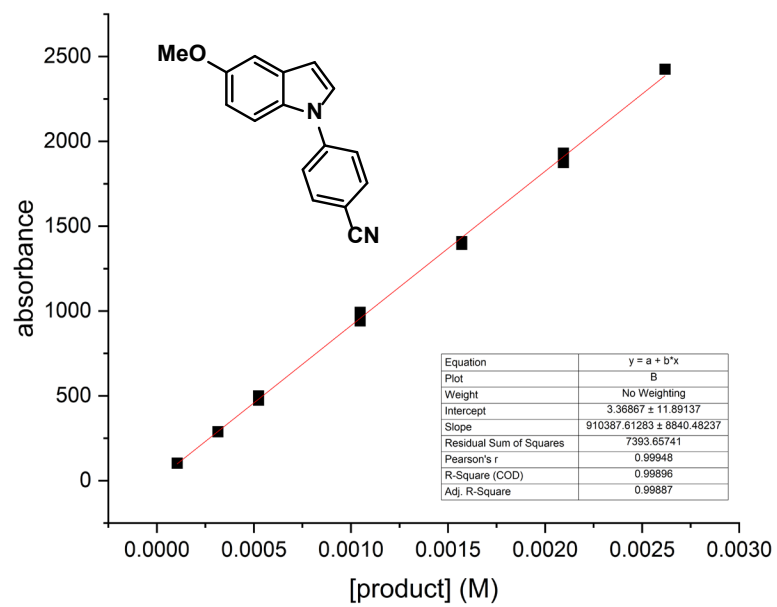




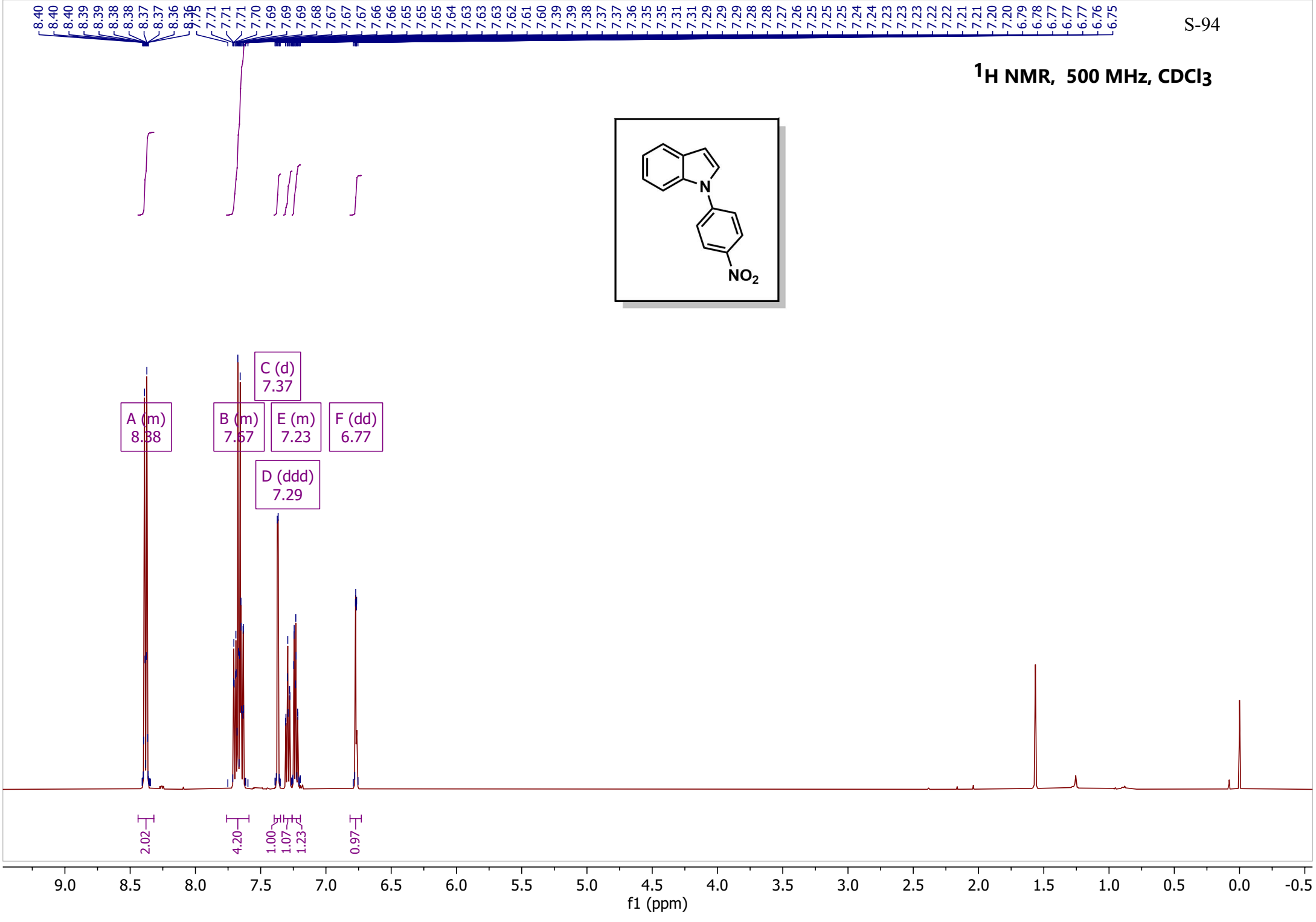
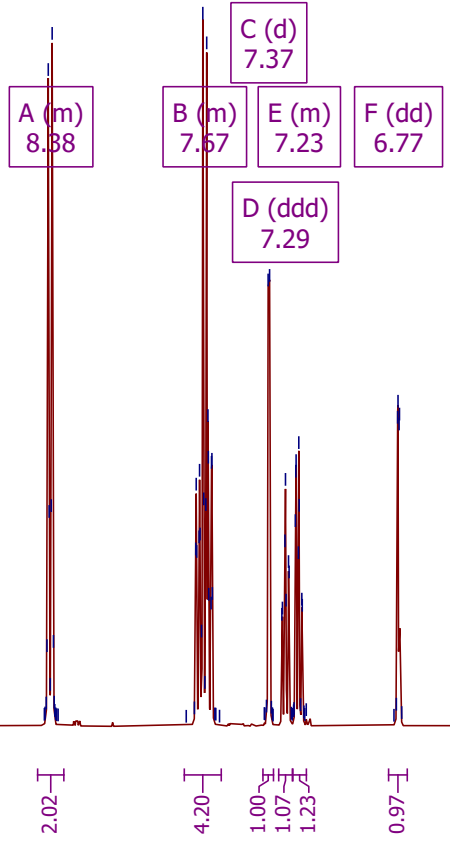
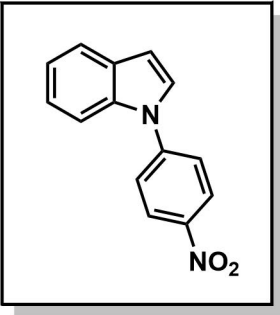




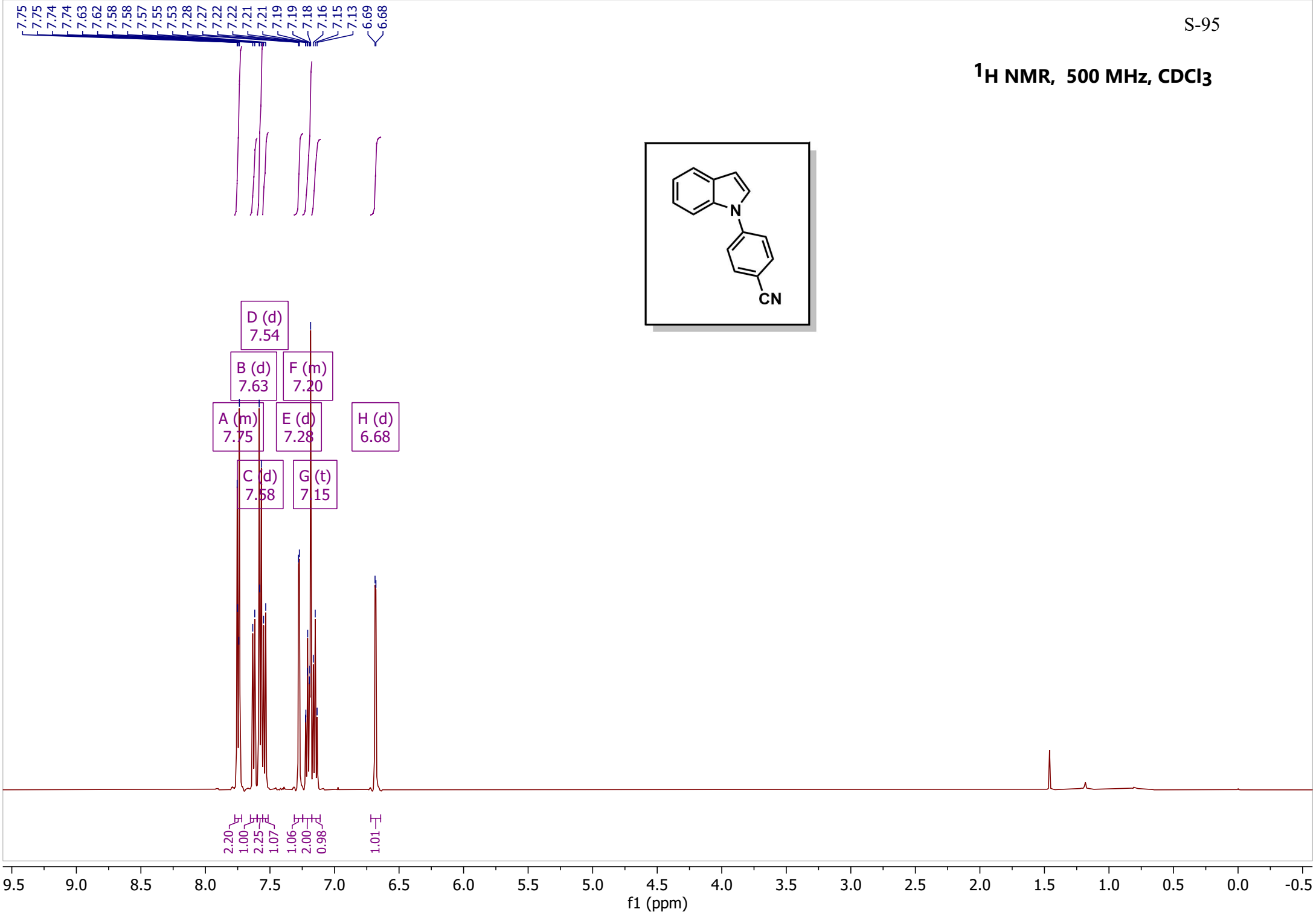
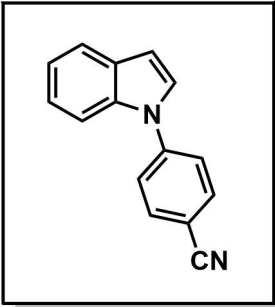




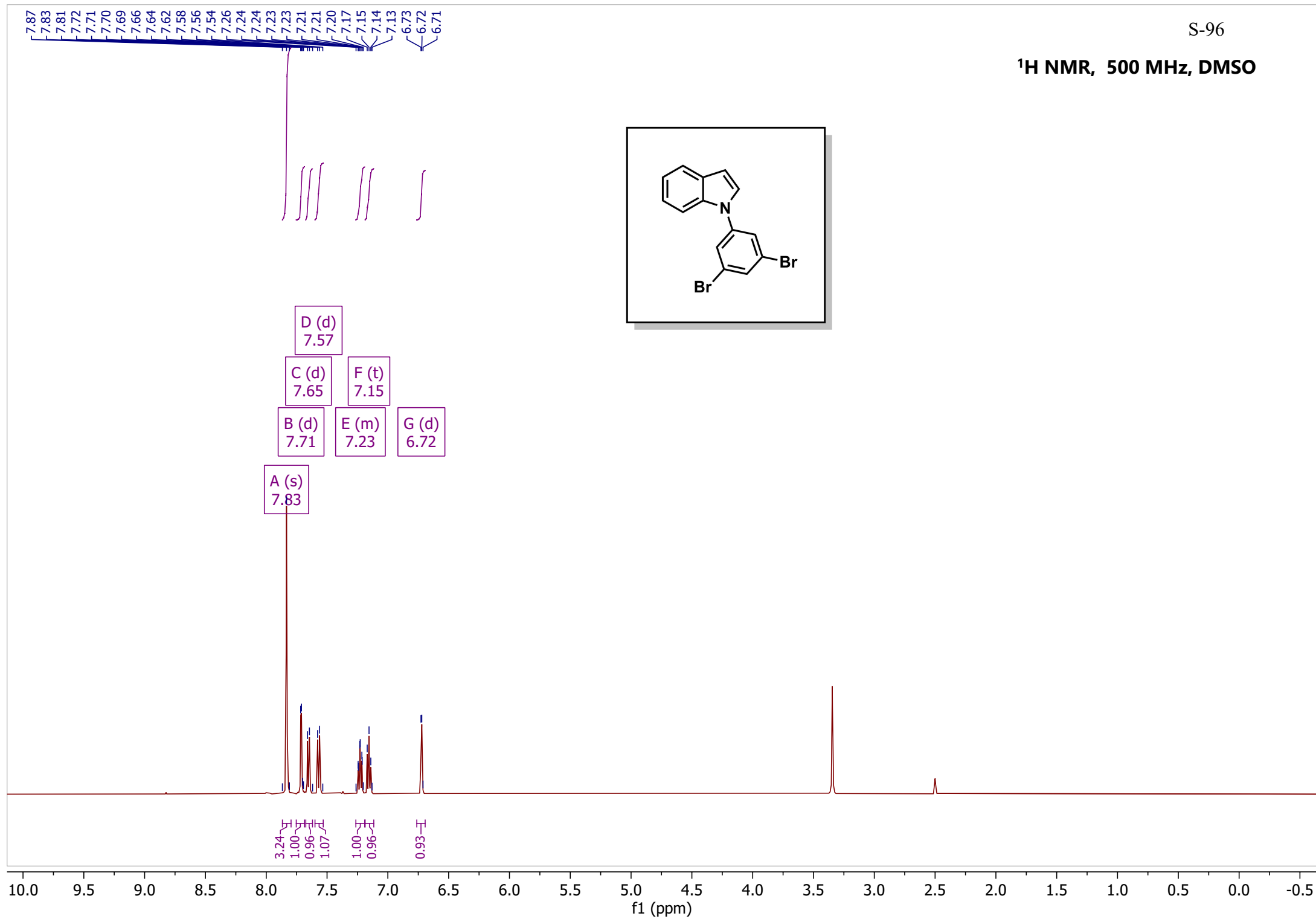
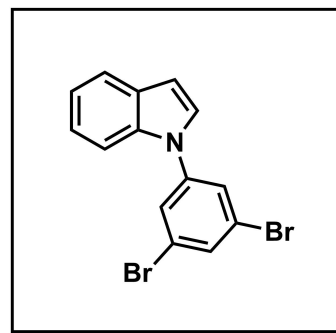
¹H NMR, 500 MHz, CDCl₃



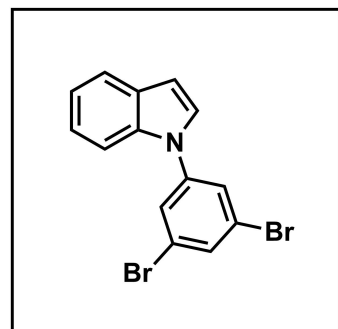
¹H NMR, 500 MHz, CDCl₃



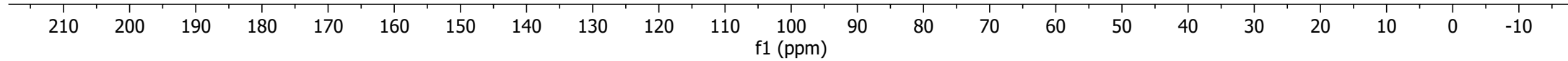
S-96

¹H NMR, 500 MHz, DMSO

S-97

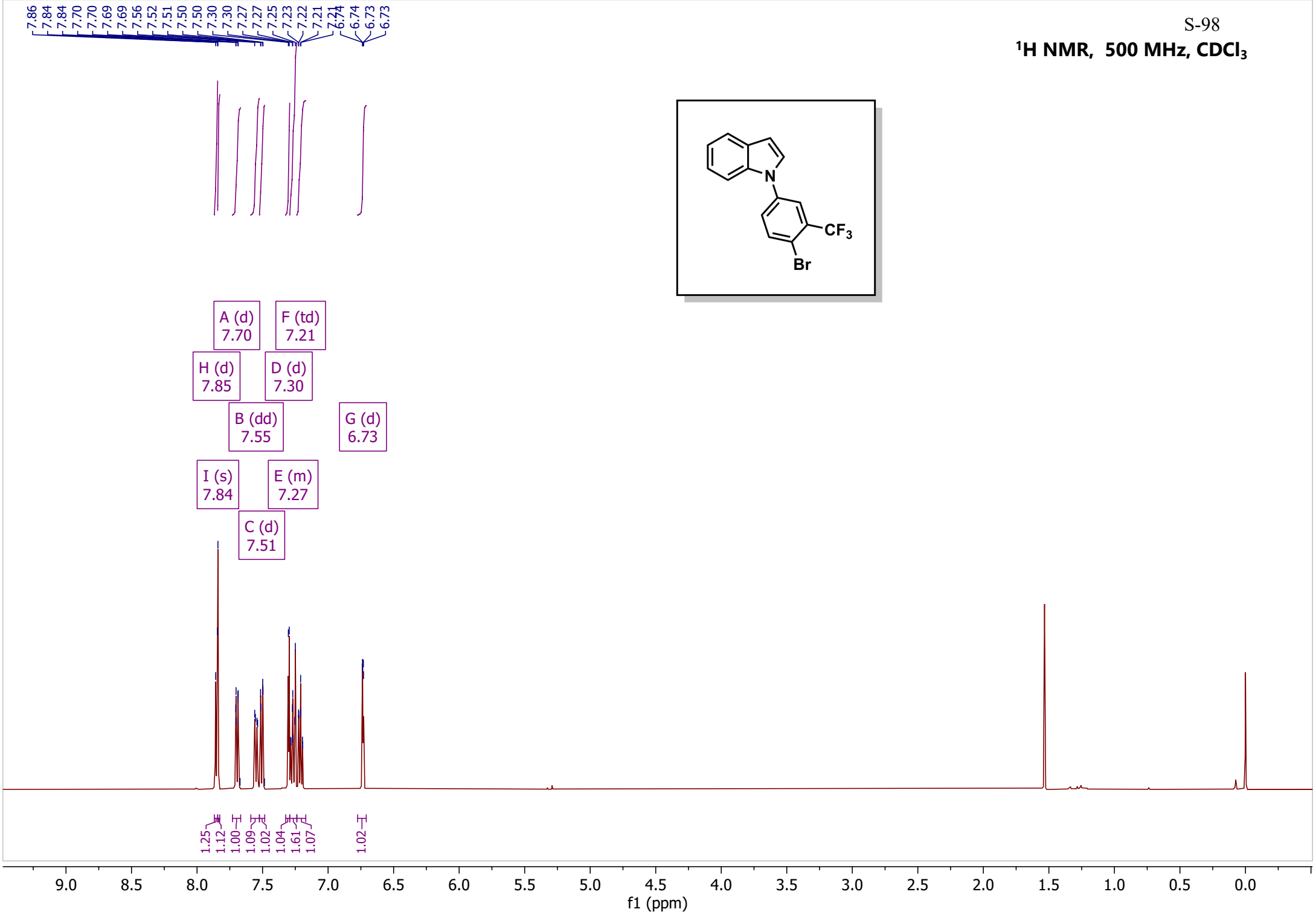
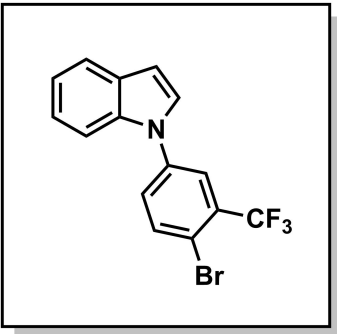
 $^{13}\text{C}\{^1\text{H}\}$ NMR, 500 MHz, DMSO

141.93
135.24
131.58
129.85
128.93
125.92
123.69
123.34
121.60
121.39
110.77
105.19

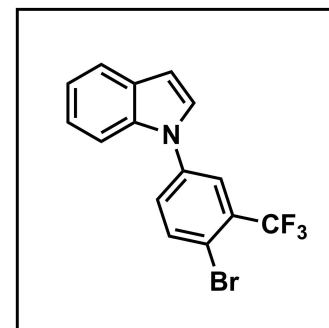


S-98

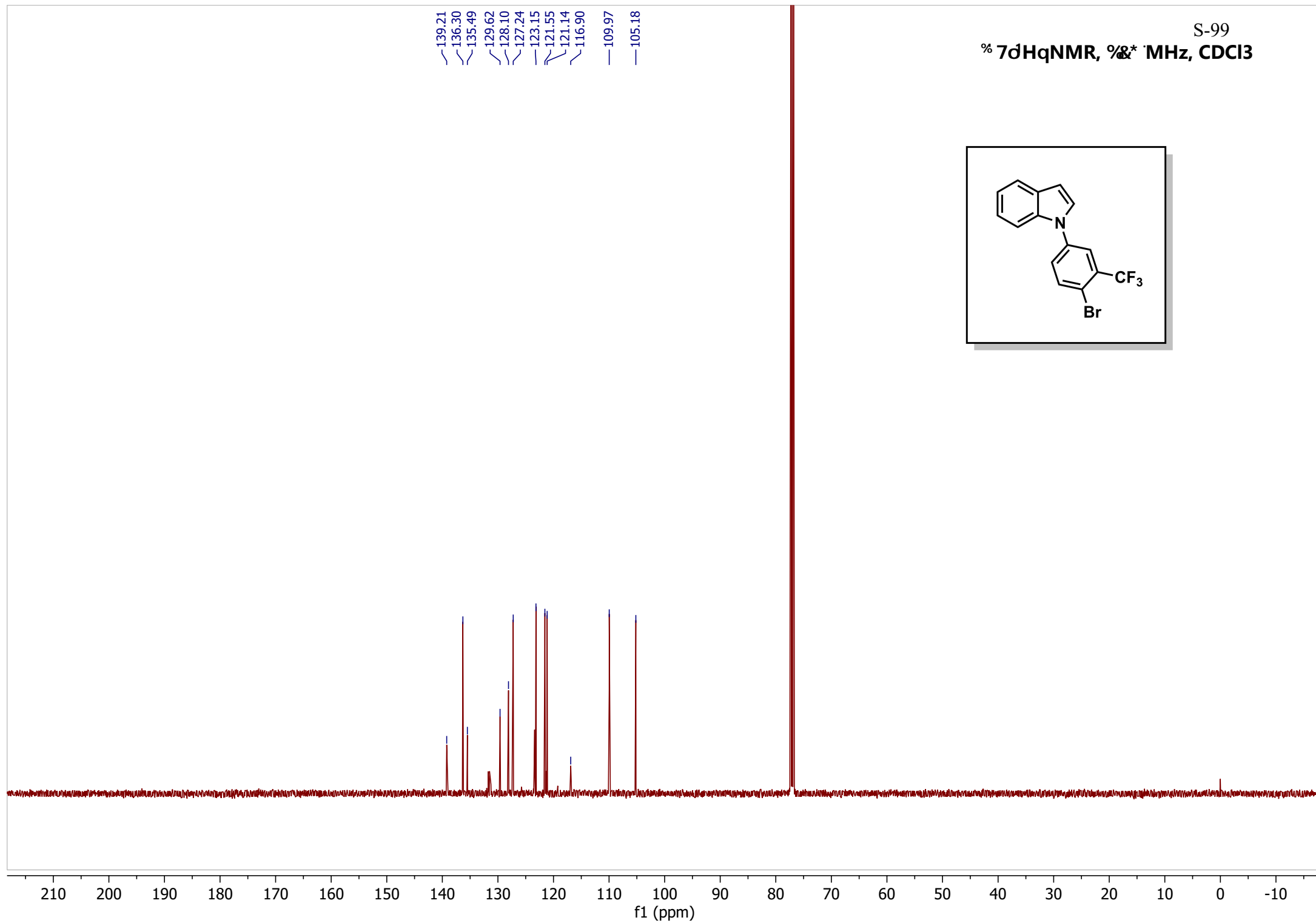
¹H NMR, 500 MHz, CDCl₃



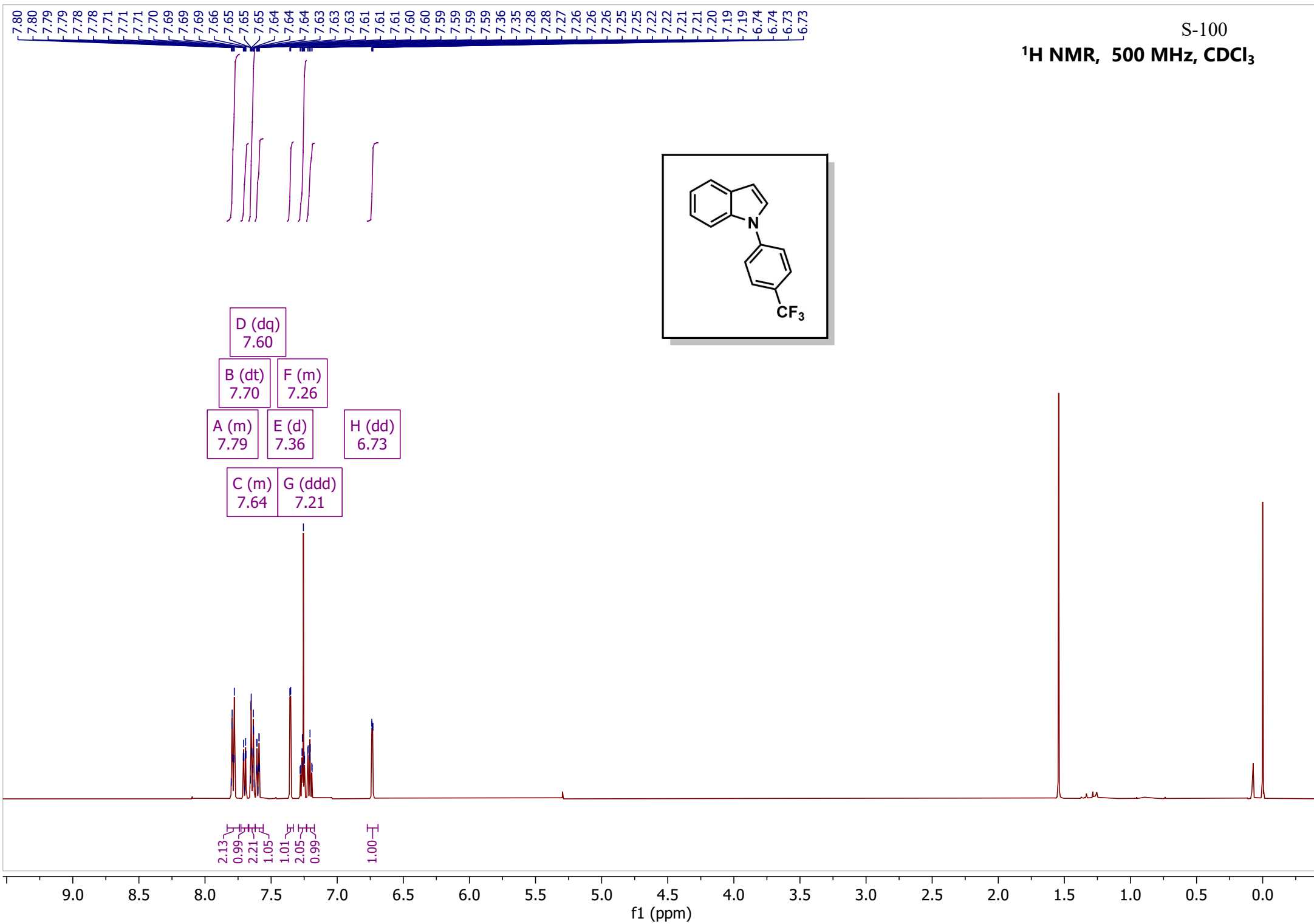
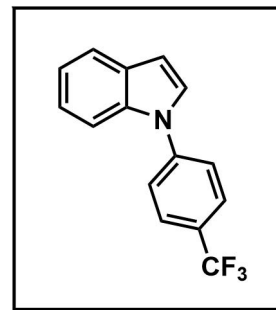
S-99

 ^{13}C NMR, 101 MHz, CDCl₃

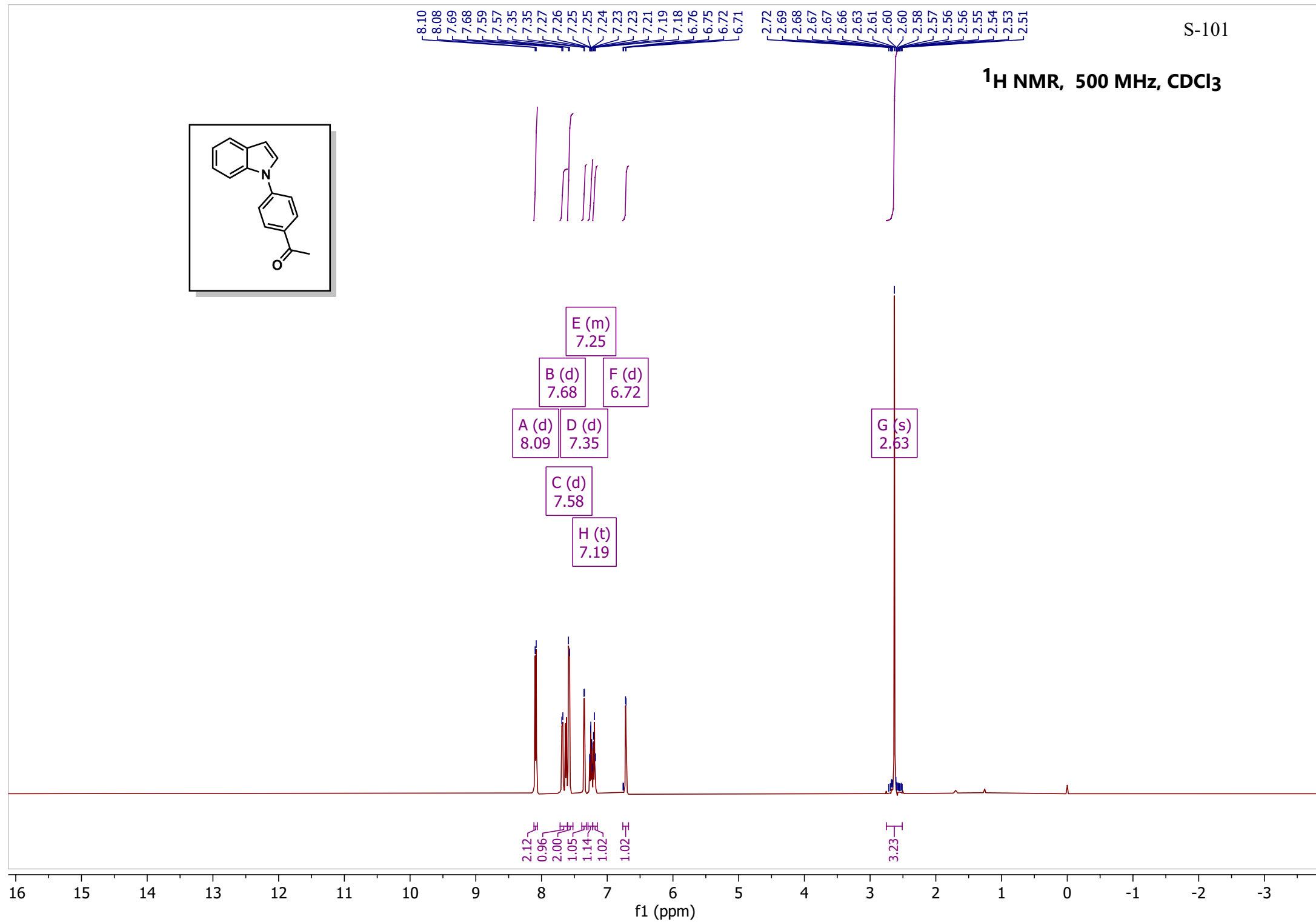
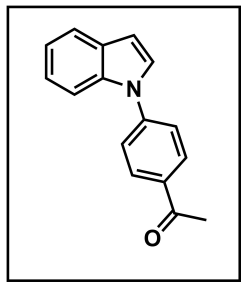
139.21
136.30
135.49
129.62
128.10
127.24
123.15
121.55
121.14
116.90
109.97
105.18



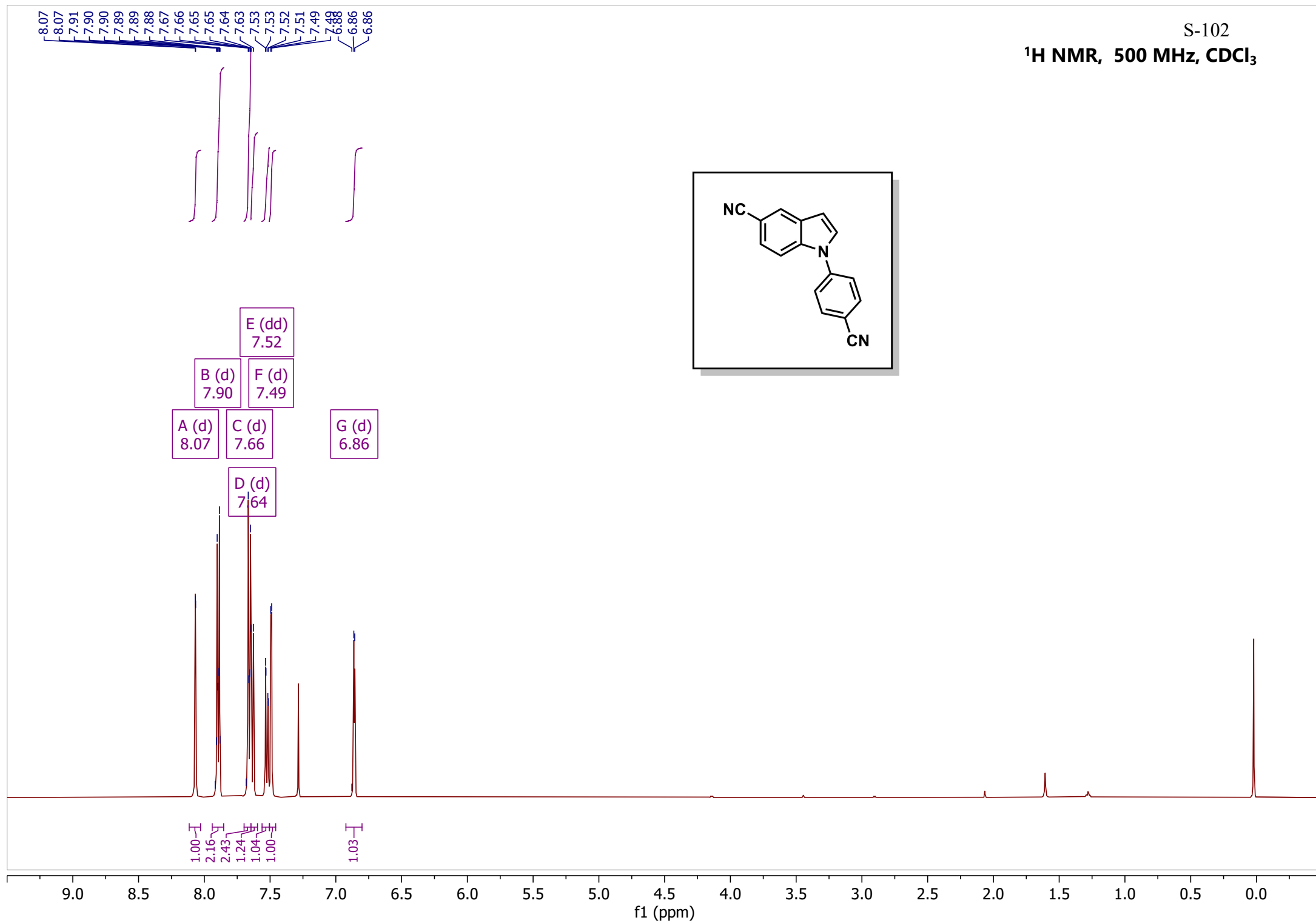
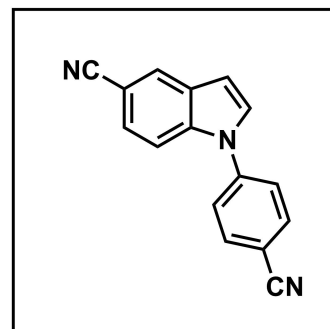
S-100

¹H NMR, 500 MHz, CDCl₃

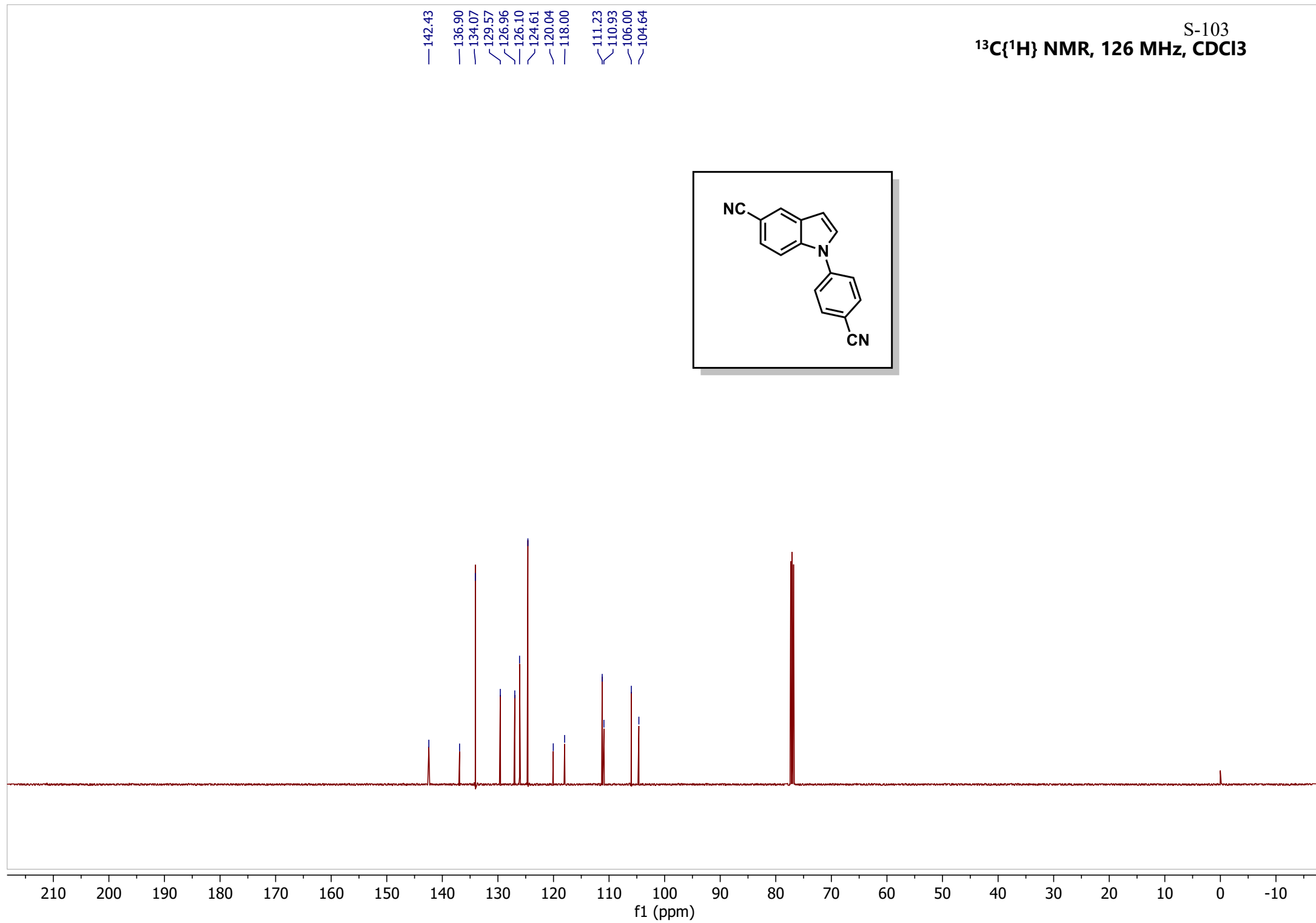
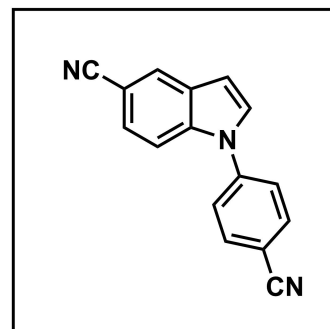
S-101

¹H NMR, 500 MHz, CDCl₃

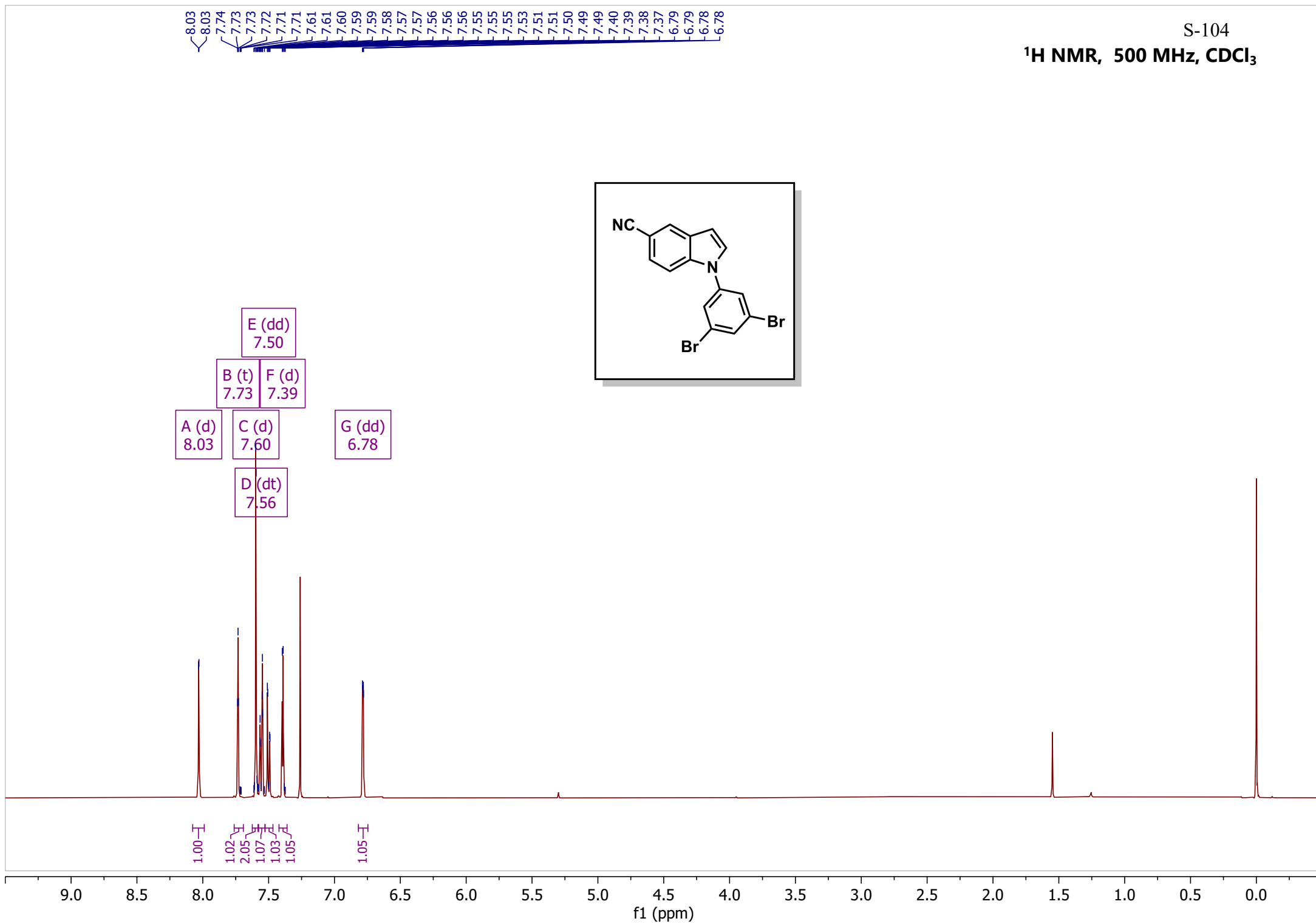
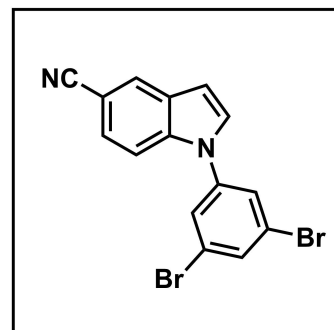
S-102

 ^1H NMR, 500 MHz, CDCl_3 

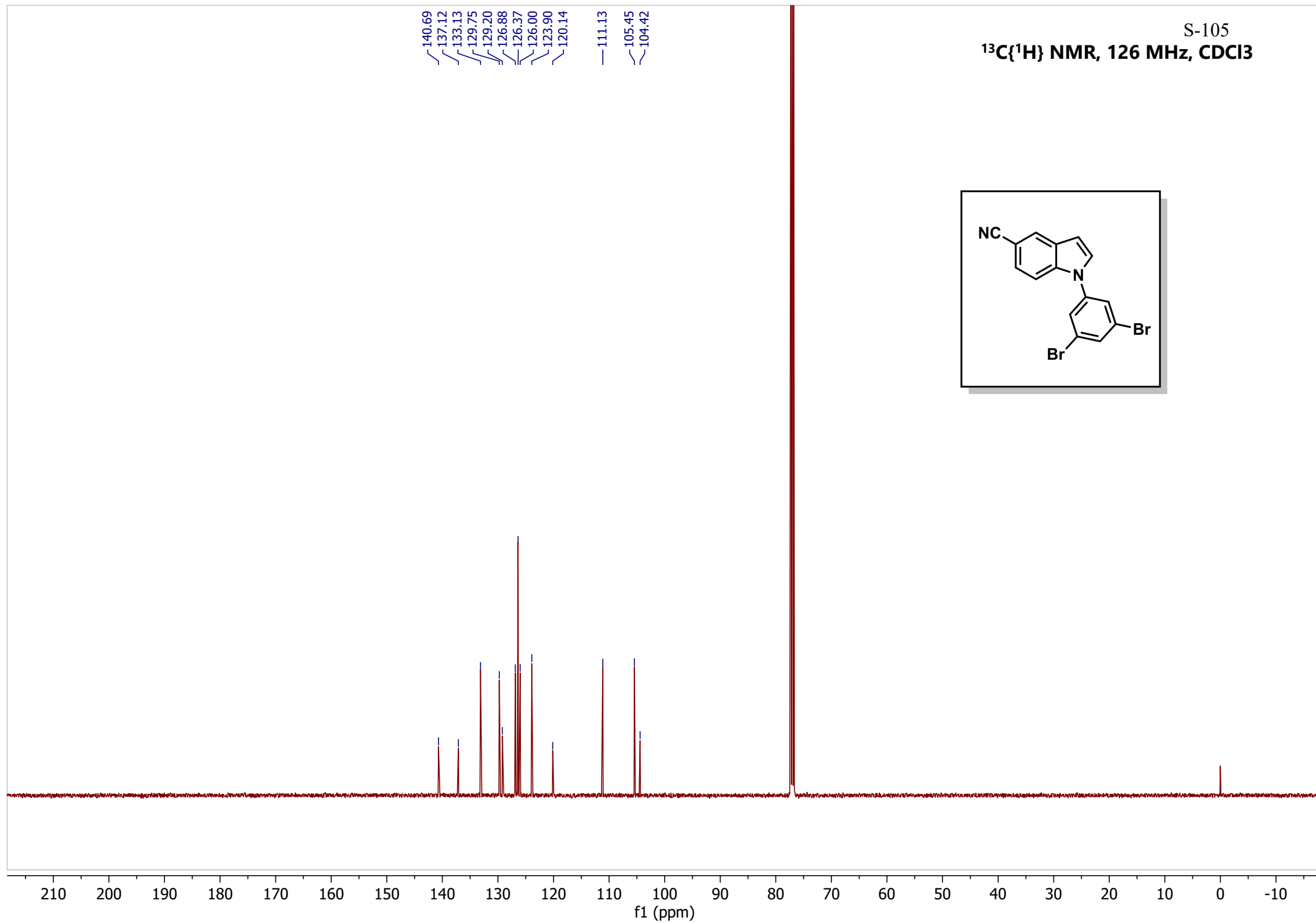
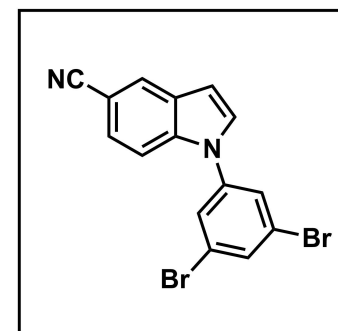
S-103

 $^{13}\text{C}\{^1\text{H}\}$ NMR, 126 MHz, CDCl_3 

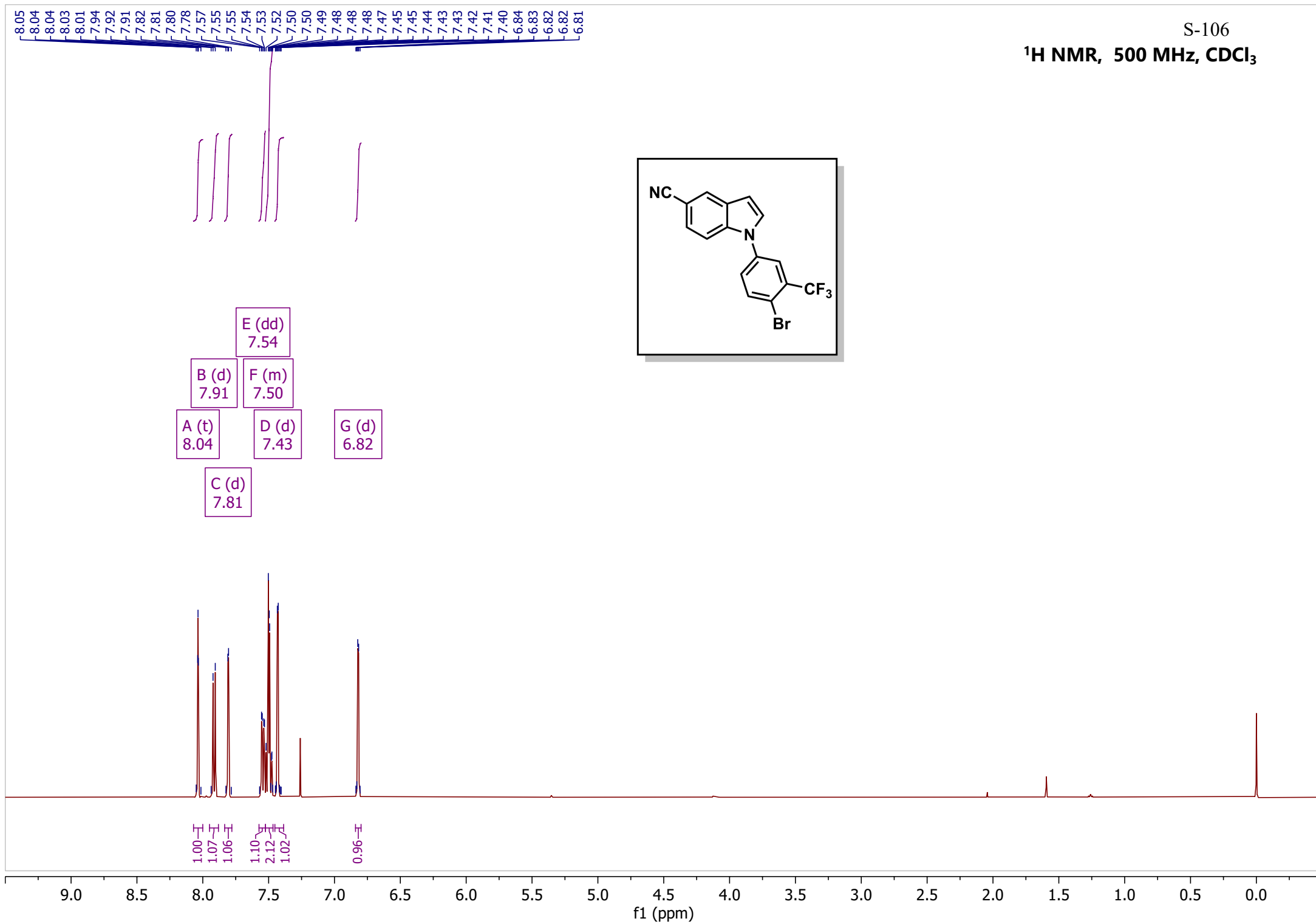
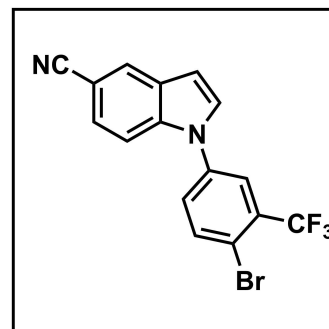
S-104

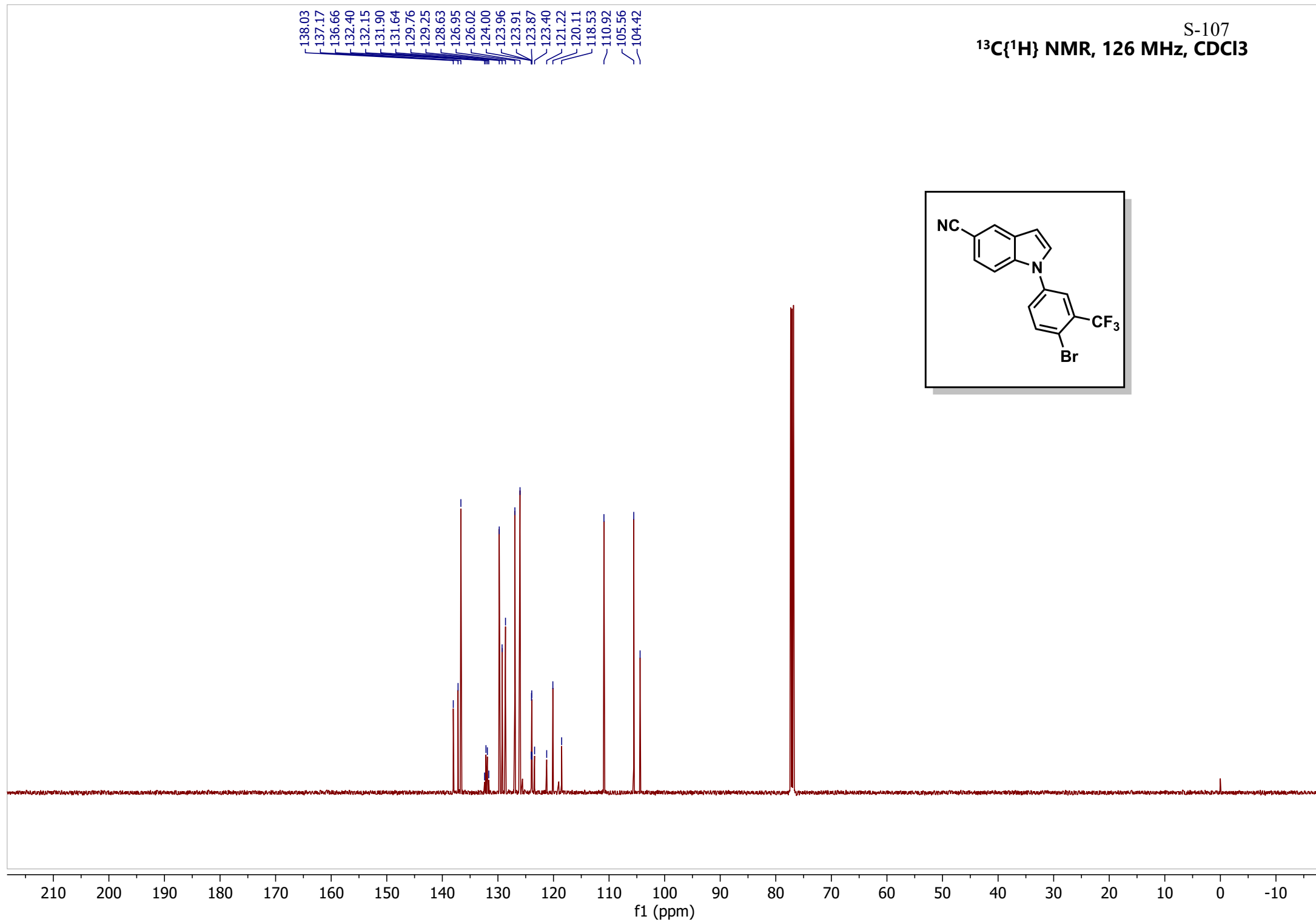
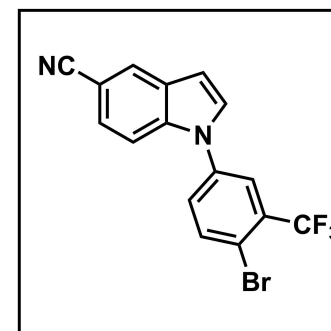
¹H NMR, 500 MHz, CDCl₃

S-105

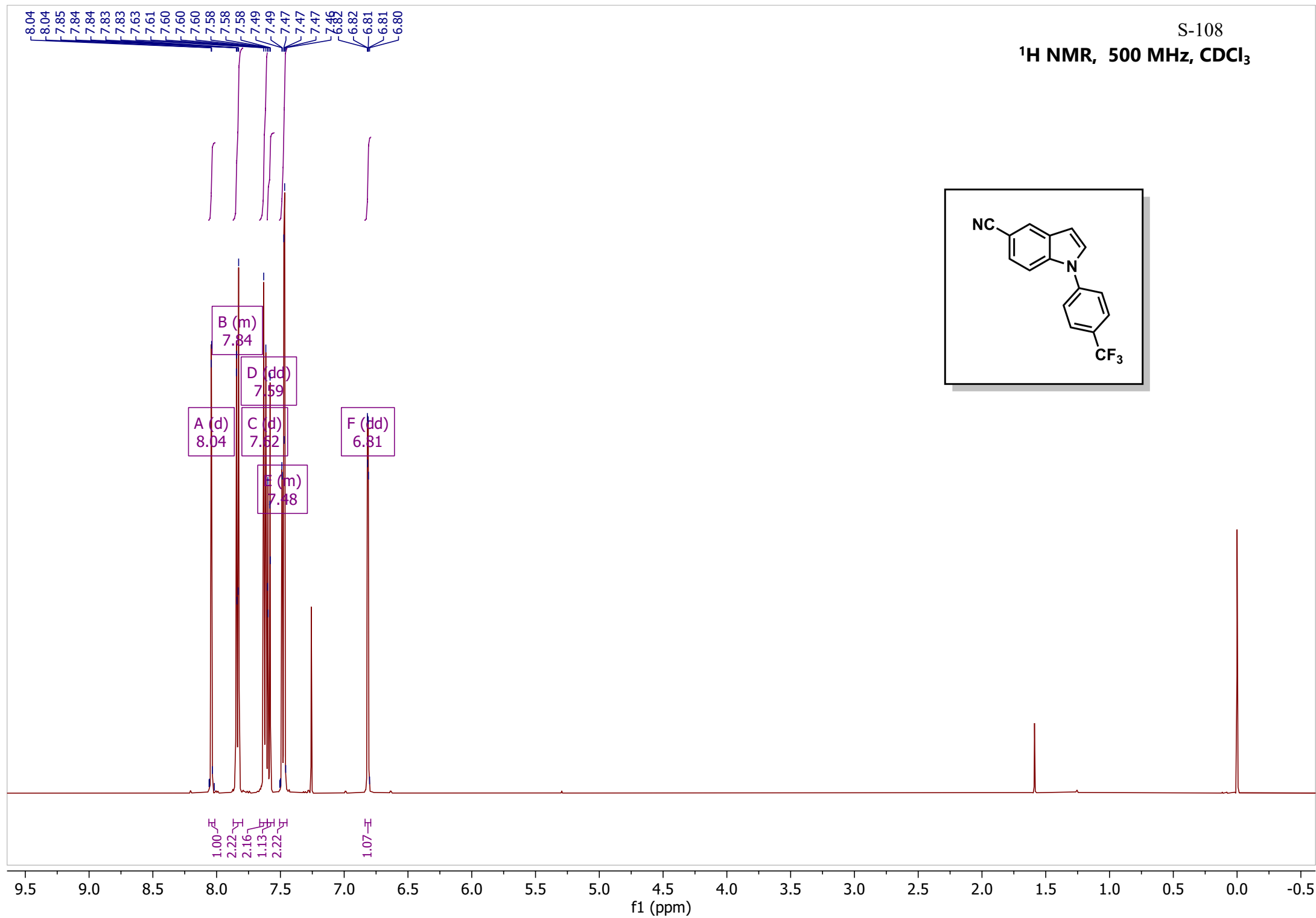
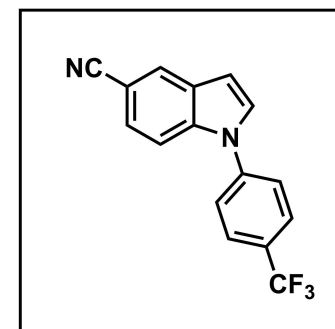
 $^{13}\text{C}\{^1\text{H}\}$ NMR, 126 MHz, CDCl_3 

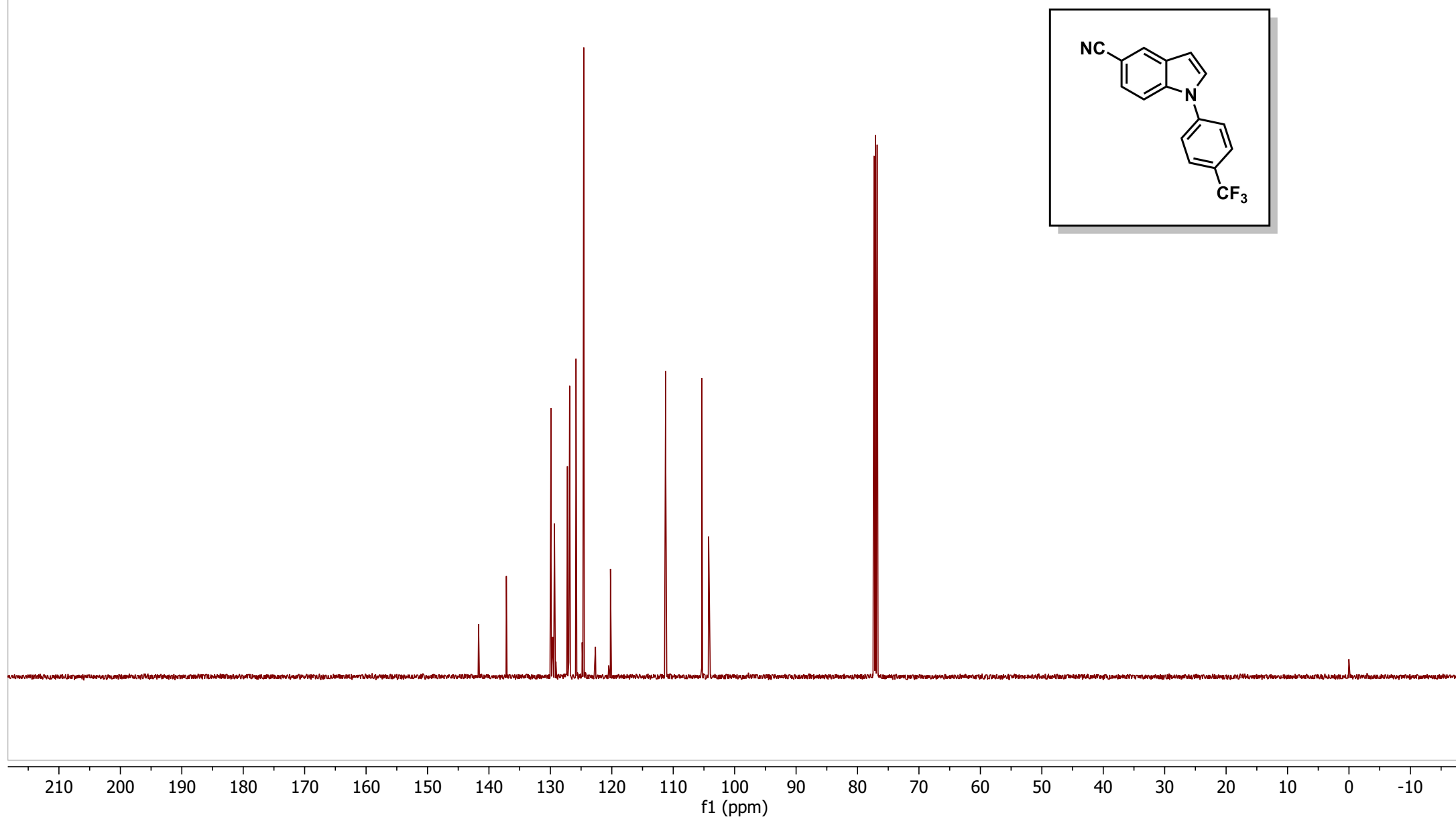
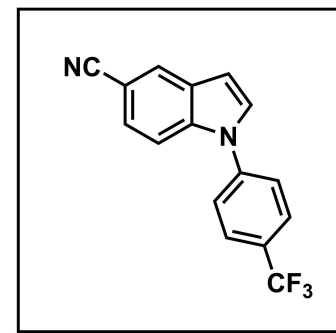
S-106

¹H NMR, 500 MHz, CDCl₃

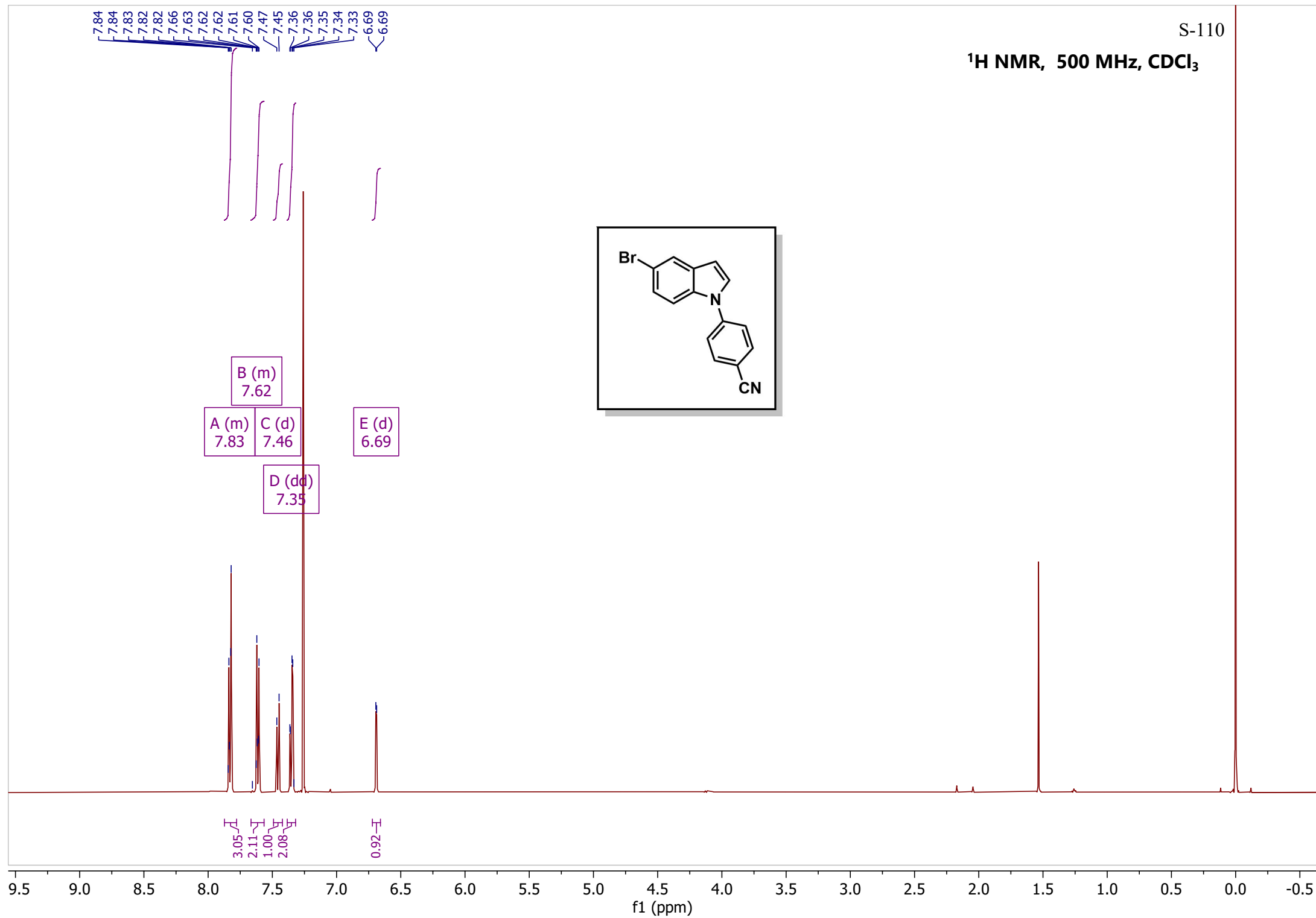
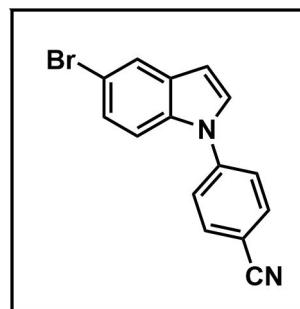


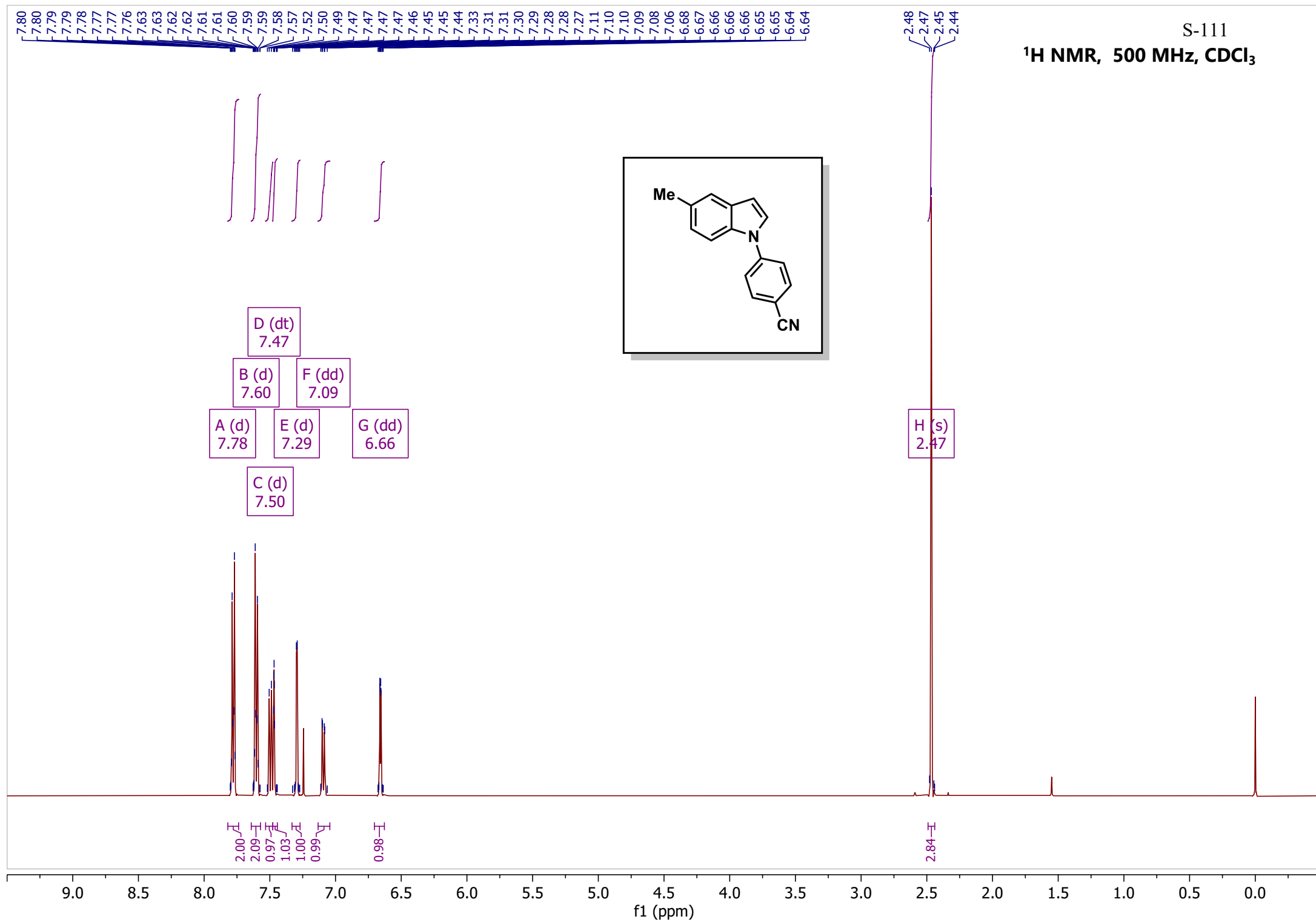
S-108

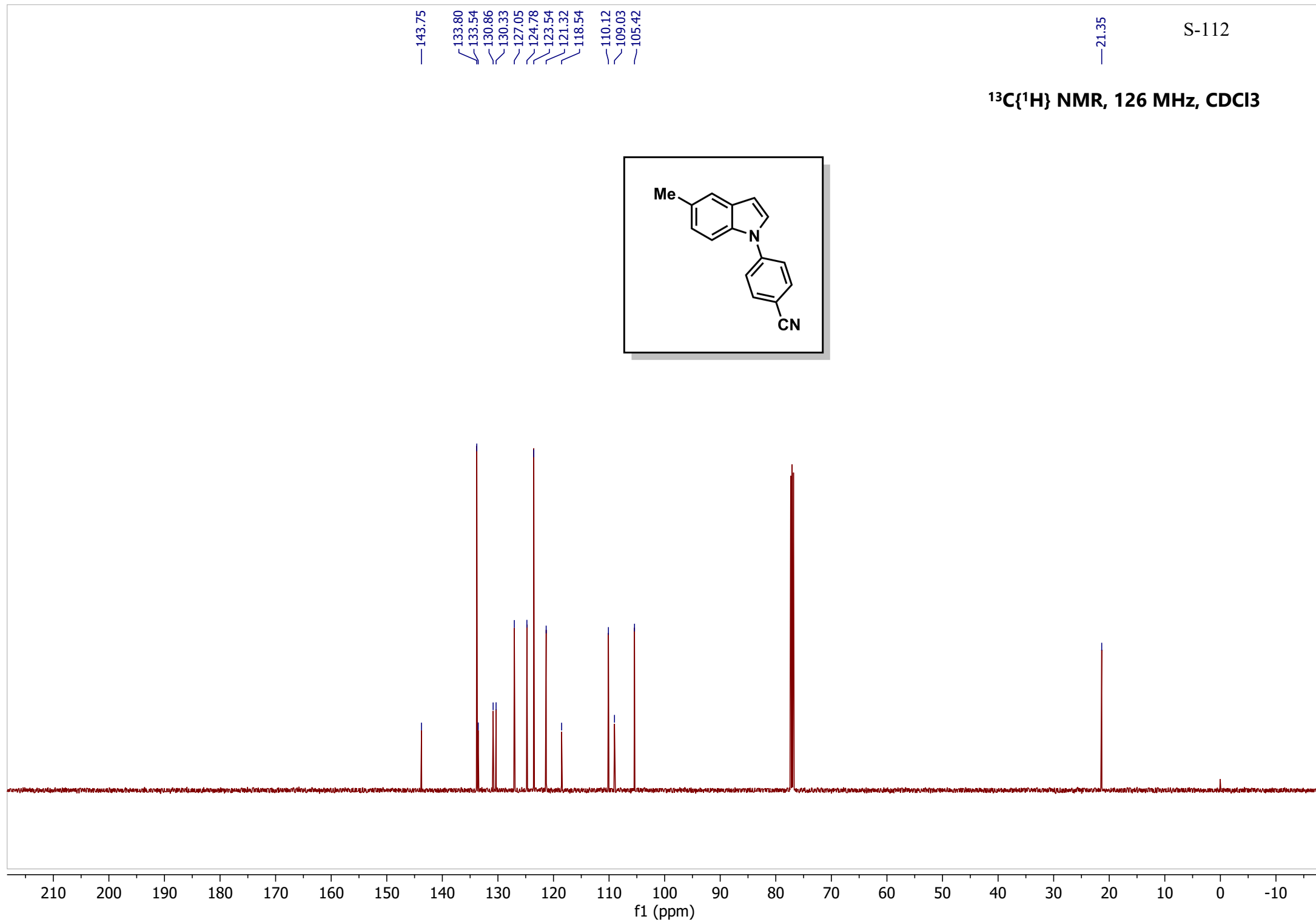
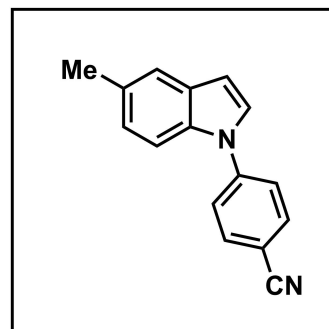
¹H NMR, 500 MHz, CDCl₃



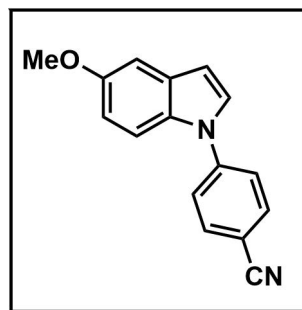
S-110

¹H NMR, 500 MHz, CDCl₃



$^{13}\text{C}\{^1\text{H}\}$ NMR, 126 MHz, CDCl_3 

S-113



B (m)	E (d)	G (dd)
7.62	7.14	6.67
A (m)	D (d)	F (dd)
7.80	7.32	6.92
C (m)		
7.51		

H (s)
3.88

7.81
7.81
7.80
7.79
7.63
7.63
7.63
7.62
7.61
7.52
7.52
7.50
7.50
7.50
7.33
7.32
7.14
7.14
6.93
6.91
6.91
6.68
6.67
6.67

3.90
3.88
3.87

2.00
2.06
1.02
0.99
0.97
1.04
0.98

3.09

f1 (ppm)